



INTERNATIONAL UNIVERSITY LIAISON INDONESIA

BACHELOR'S THESIS

PREDICTION OF AIRCRAFT CRASH LANDING SITE FROM
ADS-B DATA USING MONTE CARLO METHOD

By

Ezra Favian

11201701006

Presented to the Faculty of Engineering
In Partial Fulfilment Of the Requirements for the Degree of

SARJANA TEKNIK

In

AVIATION ENGINEERING

FACULTY OF ENGINEERING

BSD City 15345

Indonesia

August 2021

APPROVAL PAGE

PREDICTION OF AIRCRAFT CRASH LANDING SITE FROM ADS-B DATA USING MONTE CARLO METHOD

EZRA FAVIAN

11201701006

Presented to the Faculty of Engineering

In Partial Fulfillment of the Requirements for the Degree of

SARJANA TEKNIK

In

AVIATION ENGINEERING

FACULTY OF ENGINEERING

Triwanto Simanjuntak, Ph.D.

Thesis Advisor

Date

Tutun Nugraha, BAsC, MASc, Ph.D.

Vice Rector of Academic Affairs

Date

EXAMINERS APPROVAL PAGE

Dr. Eng. Ressa Octavianty

Examiner 1

Date

Dr. Ir. Erie Sandhita, MsAe, DEA

Examiner 2

Date

Triwanto Simanjuntak, Ph.D.

Examiner 3

Date

STATEMENT BY THE AUTHOR

I hereby declare that this thesis entitled PREDICTION OF AIRCRAFT CRASH LANDING SITE FROM ADS-B DATA USING MONTE CARLO METHOD is my own work and to the best of my knowledge. I put my best attempt, discipline, knowledge, and time into completing this thesis. It contains no material previously published or written by another person, or material which to a substantial extent has been accepted for the award of any other degree or diploma at any educational institution, except where due acknowledgment is made in the thesis.

Ezra Favian
Student

Date

ABSTRACT

PREDICTION OF AIRCRAFT CRASH LANDING SITE FROM ADS-B DATA USING MONTE CARLO METHOD

by

Ezra Favian

Triwanto Simanjuntak, Ph.D., Advisor

In this thesis, the author examines the prediction of the location of the plane crash using the last recorded historical ADS-B data, considering the uncertainty of the initial state, the atmosphere referring to ICAO standards, and wind speed. This numerical computation uses Newton's second law, ballistic motion, and Monte Carlo propagation theory. Identifying the best potential plane crash sites is a problem for investigators to find CVR and FDR, especially when looking for plane crash sites. In addition, this research explores how the uncertainty of the final state influences the coverage of potential crash sites. The study results will be presented in the form of a statistical Joint Density Function (JDF), which shows the most significant probability in predicting a plane crash. This study shows that with this method, the potential location of the crashed plane can be predicted. For the best potential of the crash site area, a high value of ADS-B Quality Indicator in Navigation Uncertainty in Position and Navigation Uncertainty in velocity is needed. Additionally, ADS-B variable records must be complete, such as wind direction, position and initial state of aircraft.

Keyword: *Monte Carlo, ADS-B, Quality Indicator, Aircraft Accident*

ACKNOWLEDGEMENTS

Praise and gratitude I pray to the presence of God have given patience and strength to me in the process of writing this thesis with the title "PREDICTION OF AIRCRAFT CRASH LANDING SITE FROM ADS-B DATA USING MONTE CARLO METHOD."

I realize that there are many obstacles in the process of this thesis. However, thanks to God's blessings and assistance from various parties, these obstacles can be overcome. On this happy occasion, I do not forget to thank all those who have provided guidance and advice in writing this paper, especially to:

- I respect and thank Triwanto Simanjuntak, Ph.D., for being the adviser and giving me an excellent opportunity to work on the thesis with him. I will never forget all of his effort, time, dedication, support, and guidance. He is the best, even though by guiding many students, I feel he put his efforts, ideas, and time into this thesis and provided advice in academic and non-academic fields;
- I appreciate the advice and support. I have received from my loving parents and family, who have constantly supported and prayed for me during this thesis;
- I am grateful to my friends, namely Aghadhia Firaz Uno Kusuma, Prana Paramartha Rao, Raihan Syauqi, Jordan Yap Hong Yong, Faisal Tri Mulyawan, who have always provided advice and support for this thesis;
- I thank my employees and partners at Primajasa and Dini Hari Angkringan, who have always supported this thesis;
- I want to express my gratitude to all of the readers who took the time to read my thesis. Hopefully, the advantages and information gained through this thesis will be beneficial;
- Last but not least, I want to thank me for believing in me, for doing all this hard work, for having no days off, for never quitting, for always being a giver and trying to give more than I receive, for just being me all time.

Contents

Approval Page	i
EXAMINERS APPROVAL PAGE	ii
Statement by The Author	iii
Abstract	iv
Acknowledgements	v
Contents	vii
List of Figures	xi
List of Tables	xv
1 Introduction	1
1.1 Background	1
1.2 Problem Statement	3
1.3 Research Purpose	4
1.4 Research Scope	4
1.5 Thesis Organization	5
2 Literature Review	8
2.1 Overview	8
2.2 ADS-B (Automatic Dependent Surveillance - Broadcast)	9
2.2.1 History of ADS-B	10
2.2.2 Flow of ADS-B System	12
2.2.3 ADS-B Message Structure	13

	Downlink Format	14
	Capability Field	14
	Aircraft Address	15
	Data Segment	15
	Parity Field	16
2.3	ADS-B Quality Indicators	16
2.3.1	ADS-B Quality Indicators Version 0	16
2.3.2	ADS-B Quality Indicators Version 1	17
2.3.3	ADS-B Quality Indicators Version 2	17
2.3.4	Navigation Uncertainty Category (NUC)	17
2.3.5	Navigation Accuracy Category (NAC)	21
2.3.6	Surveillance / Source Level Integrity(SIL)	22
2.3.7	Navigation Integrity Level	23
2.3.8	System Design Assurance(SDA)	26
2.3.9	Geometric Vertical Accuracy(GVA)	26
2.4	Capability differences between the ADS-B Quality Indicator	27
2.5	ADS-B data received by ATC	28
2.5.1	Time	29
2.5.2	Hex Code and Call Sign	30
2.5.3	Position from Latitude and Longitude(Geographical Coordinates)	30
2.5.4	Altitude	32
2.5.5	Velocity	35
2.5.6	Track	36
2.5.7	Squawk	38
2.6	Multilateration	38
2.7	Regulation ADS-B from ICAO	39
2.8	Aircraft Performance	40
2.8.1	coordinates system	41
	The body coordinates systems	42
2.8.2	Flight-path angle	42
2.8.3	Heading angle	43
2.8.4	Coefficient Lift	44

2.8.5	Coefficient Drag	46
2.8.6	The Atmosphere	47
2.8.7	Gravitation	52
2.9	Monte Carlo Simulation	55
2.9.1	Normal Distribution	56
2.9.2	Error Propagation Using Monte Carlo Simulation	57
2.10	Joint Density Function	58
3	Research Methodology	61
3.1	Overview	61
3.2	Initial state	62
3.2.1	ADS-B Data	63
3.2.2	Convert geodetic coordinates to cartesian coordinates	64
3.3	Calculation Development	65
3.3.1	Analytical approach - one dimensional	65
3.3.2	Numerical approach - three dimensional	68
3.4	Final state	70
3.4.1	Cartesian Coordinates systems	70
3.4.2	Time to hit ground	71
4	Results and Discussions	72
4.1	Introduction	72
4.2	Simulation without uncertainty	73
4.2.1	Simulation without uncertainty case 1	74
4.2.2	Simulation without uncertainty case 2	76
4.2.3	Simulation without uncertainty case 3	79
4.2.4	Simulation without uncertainty case 4	81
4.2.5	Simulation without uncertainty case 5	84
4.3	Simulation with uncertainty	87
4.3.1	Simulation with uncertainty	87
4.4	Simulation 11 cases with uncertainty	90
4.4.1	Simulation with uncertainty case 1	92
4.4.2	Simulation with uncertainty case 2	94
4.4.3	Simulation with uncertainty case 3	96

4.4.4	Simulation with uncertainty case 4	98
4.4.5	Simulation with uncertainty case 5	99
4.4.6	Simulation with uncertainty case 6	101
4.4.7	Simulation with uncertainty case 7	103
4.4.8	Simulation with uncertainty case 8	105
4.4.9	Simulation with uncertainty case 9	108
4.4.10	Simulation with uncertainty case 10	109
4.4.11	Simulation with uncertainty case 11	111
5	Summary, Conclusion, Recommendation	114
5.1	Conclusion	114
5.2	Recommendation	116
	References	118
	Appendices	121
	Turnitin Report	136
	Curriculum Vitae	155

List of Figures

1.1	The location of aircraft crash site from Lion Air JT610.	2
1.2	Schematic: Prediction of aircraft crash landing site.	3
1.3	Outline of literature review.	6
1.4	Outline of research methodology.	7
2.1	Evolution of ADS-B	11
2.2	Flow of ADS-B System	13
2.3	NUCp Parameters	18
2.4	NUCp Parameters	19
2.5	Airborne position with GNSS height (Type Code = 20 - 22)	20
2.6	Vertical and Horizontal of radius of containment for NIC	25
2.7	Coordinated Universal Time (UTC) in Indonesia	30
2.8	Meaning of coordinates	31
2.9	Parameter of latitude and longitude	31
2.10	Longitudes in degree	32
2.11	Definition of altimeter setting	34
2.12	The parameter of geoid	35
2.13	Reference of true north and magnetic north	37
2.14	Track are determined by reference to true north on flight plan	37
2.15	MLAT process to determine aircraft location	39
2.16	Three-Dimensional Cartesian Coordinate (ECEF)	41
2.17	Body coordinates systems of aircraft	42
2.18	Definition of flight-path angle	43
2.19	Definition of heading angle	44
2.20	Airfoil of Boeing 737 MIDSPAN AIRFOIL (b737c-il). Source: (Tools, 27 May 2021).	44

2.21	Schematic of lift coefficient variation with angle of attack for an airfoil Boeing 737 MIDSPAN AIRFOIL (b737c-il). Source: (Tools, 27 May 2021).	45
2.22	Layers of Earth's atmosphere.	48
2.23	International Standard Atmosphere for temperature effect of geopotential altitude	50
2.24	International Standard Atmosphere for pressure effect of geopotential altitude	51
2.25	International Standard Atmosphere for density effect of geopotential altitude	52
2.26	Gravity acceleration effect of geometric altitude	54
2.27	Example of distribution function (Kreyszig, 2009)	57
2.28	Example of normal distribution (Kreyszig, 2009)	57
2.29	Step of Monte Carlo Simulation	58
2.30	Example of plot difference between histogram and Probability Density Function (PDF)	59
2.31	Example of Joint Density Function (JDF) source: (blog on science, 2020)	60
3.1	Reserach Framework	61
3.2	The last location of Lion Air (PK-LQP) (<i>Aircraft Accident Investigation Report PT. Lion Mentari Airlines Boeing 737-8 (MAX); PK-LQP</i> , 2019)	64
3.3	Free Body Diagram	65
3.4	Frontal area of Boeing 737-800	67
3.5	Free body diagram of three dimensioanl	68
4.1	Illustration 3D of simulation.	72
4.2	Result of simulation 1.	74
4.3	Result of simulation 1 at displacement x-axis on time.	75
4.4	Result of simulation 1 at displacement y-axis on time.	75
4.5	Result of simulation 1 at displacement z-axis on time.	76
4.6	Result of simulation 2.	77
4.7	Result of simulation 2 at displacement x-axis on time.	77

4.8	Result of simulation 2 at displacement y-axis on time.	78
4.9	Result of simulation 2 at displacement z-axis on time.	78
4.10	Result of simulation 3.	79
4.11	Result of simulation 3 at displacement x-axis on time.	80
4.12	Result of simulation 3 at displacement y-axis on time.	80
4.13	Result of simulation 3 at displacement z-axis on time.	81
4.14	Result of simulation 4.	82
4.15	Result of simulation 4 at displacement x-axis on time.	82
4.16	Result of simulation 4 at displacement y-axis on time.	83
4.17	Result of simulation 4 at displacement z-axis on time.	83
4.18	Result of simulation 5.	84
4.19	Result of simulation 5 at displacement x-axis on time.	85
4.20	Result of simulation 5 at displacement y-axis on time.	85
4.21	Result of simulation 5 at displacement z-axis on time.	86
4.22	Illustration with uncertainty of ADS-B Quality Indicators of score 8 in NUCp and $V_w = 0$	87
4.23	Result of 10 000 point crash site	88
4.24	Result of 10 000 point crash site	89
4.25	Joint Density Function (JDF) for prediction of aircraft crash site. .	89
4.26	Parameters of uncertainties for position	91
4.27	Parameters of uncertainties for velocity	92
4.28	Result: crash site of simulation with uncertainty 1 in 2D.	93
4.29	Joint Density Function (JDF) for simulation with uncertainty 1. . .	93
4.30	Result: crash site of simulation with uncertainty 2 in 2D.	95
4.31	Joint Density Function (JDF) for simulation with uncertainty 2. . .	95
4.32	Result: crash site of simulation with uncertainty 3 in 2D.	96
4.33	Joint Density Function (JDF) for simulation with uncertainty 3. . .	97
4.34	Result: crash site of simulation with uncertainty 4 in 2D.	98
4.35	Joint Density Function (JDF) for simulation with uncertainty 4. . .	99
4.36	Result: crash site of simulation with uncertainty 5 in 2D.	100
4.37	Joint Density Function (JDF) for simulation with uncertainty 5. . .	101
4.38	Result: crash site of simulation with uncertainty 6 in 2D.	102
4.39	Joint Density Function (JDF) for simulation with uncertainty 6. . .	102

4.40	Result: crash site of simulation with uncertainty 7 in 2D.	104
4.41	Joint Density Function (JDF) for simulation with uncertainty 7. . .	105
4.42	Result: crash site of simulation with uncertainty 8 in 2D.	106
4.43	Joint Density Function (JDF) for simulation with uncertainty 8. . .	107
4.44	Result: crash site of simulation with uncertainty 9 in 2D.	108
4.45	Joint Density Function (JDF) for simulation with uncertainty 9. . .	109
4.46	Result: crash site of simulation with uncertainty 10 in 2D.	110
4.47	Joint Density Function (JDF) for simulation with uncertainty 10. .	111
4.48	Result: crash site of simulation with uncertainty 11 in 2D.	112
4.49	Joint Density Function (JDF) for simulation with uncertainty 11. .	113

List of Tables

1.1	Aircraft accident in Indonesia	1
2.1	five main parts of ADS-B Message Structure	13
2.2	ADS-B Message Structure	14
2.3	The definition of Capability Field	15
2.4	The definition of Data Segment	16
2.5	Airborne position with barometric altitude (Type Code = 9 - 18) .	19
2.6	Airborne position with GNSS height (Type Code = 20 - 22)	20
2.7	Surface position (Type Code = 5 - 8)	20
2.8	NUCv figure of merit	21
2.9	NACp values	22
2.10	NACv values	22
2.11	Values for Surveillance Integrity Level	23
2.12	Values for Source Integrity Level	23
2.13	SIL supplement bit to define unit	23
2.14	Values of NIC for Version 1	25
2.15	Values of NICbaro for Version 2	26
2.16	Values of SDA in version 2	26
2.17	Values of GVA in version 2	27
2.18	Summarized differences	28
2.19	Parameters of ADS-B data	29
2.20	Values of parameter constant	33
2.21	Temperature gradient λ at certain altitude	49
3.1	The last recorded ADS-B of Lion Air JT610 (<i>Aircraft Accident Investigation Report PT. Lion Mentari Airlines Boeing 737-8 (MAX); PK-LQP, 2019</i>)	63

4.1	Simulation without uncertainty.	74
4.2	Result of simulation 1.	76
4.3	Result of simulation 2.	79
4.4	Result of simulation 3.	81
4.5	Result of simulation 4.	84
4.6	Result of simulation 5.	86
4.7	Initial state of Simulation with uncertainty	91
4.8	Score 9 of NUCp	92
4.9	Score 9 of NUCp	94
4.10	Score 4 of NUCv	94
4.11	Score 6 of NUCp	98
4.12	Score 4 of NUCv	98
4.13	Score 6 of NUCp	100
4.14	Score 2 of NUCv	100
4.15	Score 1 of NUCp	103
4.16	Score 1 of NUCv	103
4.17	Score 6 of NUCp	106
4.18	Score 2 of NUCv	106
5.1	Simulation without uncertainty.	115
5.2	Final state with uncertainty.	116

List of Abbreviations

ADS-B	A utomatic D ependent S urveillance - B roadcast
NUC	N avigation U ncertainty C ategory
NUC	N avigation A ccuracy C ategory
SIL	S ource L evel I ntegrity
SIL	S urveillance L evel I ntegrity
SDA	S ystem D esign A ssurance
GVA	G eometric V ertical A ccuracy
ATC	A ir T raffic C ontrol
ICAO	I nternational C ivil A viation O rganization
GNSS	G lobal N avigation S atellite S ystems
UTC	C oordinated U niversal T ime
ECEF	E arth C entered E arth F ixed
IRP	I nternational R eference P ole
JDF	J oint D ensity F unction
GPS	G lobal P ositioning S ystem
VPL	V ertical P rotection L imit
HPL	H orizontal P rotection L imit
GMT	G reenwich M ean T ime
ISA	I nternational S tandard A tmosphere
MSL	M ean S ea L evel

Dedicated to my parents

CHAPTER 1

INTRODUCTION

1.1 Background

Aircraft are built by a method that is defined in detail which is used to balance many requirements. To produce an aircraft that is strong, economical, and can carry an adequate payload while being reliable enough to fly safely over the life of the aircraft. National airworthiness authorities regulate the design of aircraft, but aircraft accidents still happen. Airplane accidents are important events for the aviation sector that require urgent investigation to find out or analyze their causes. Even though it was accidental, a plane crash occurred. In Indonesia, aviation accidents continue to occur, claiming many lives and making aircraft debris challenging to find and disappear. From 2010 to 2021, there were eight aircraft accidents in Indonesia.

No	Date	Aircraft	Location
1	April 13, 2010	Merpati Nusantara Airlines	Rendani airport
2	May 7, 2011	Merpati Nusantara Airlines	Utarom, West Papua
3	September 29, 2011	Nusantara Buana	Langkat, North Sumatra
4	May 9, 2012	Sukhoi Superjet 100	Salak mountain
5	December 28, 2014	AirAsia Indonesia	Java Sea
6	August 16, 2015	Trigana Air Service	Oksibil, Papua
7	October 29, 2018	Lion Air JT610	Karawang Sea
8	January 9, 2021	Sriwijaya Air SJ182	Kepulauan Seribu

TABLE 1.1: Aircraft accident in Indonesia

If an aircraft accident, the performance of Search and Rescue (SAR) is needed

to quickly find the aircraft wreckage, Cockpit Voice Recorder (CVR) and Flight Data Recorder (FDR), to support the search for these components requires an accurate data and evaluation for the crash site.

This research is to determine the prediction of the crash location of the aircraft from the last ADS-B data using Monte Carlo Method. Automatic Dependent Surveillance-Broadcast (ADS-B) is a system in which an aircraft's accurate position is broadcast via a digital data connection by onboard electronic equipment. The ADS-B data must be used by nearby aircraft and air traffic control to display the aircraft's position and altitude on a display screen without radar. An ADS-B-equipped aircraft uses a satellite system to detect its position and then broadcasts that location, along with identity, altitude, speed, and other data, via instant message. A dedicated ADS-B base station collects transmissions for accurate aircraft monitoring and provides air traffic management with information. ADS-B was published in September 2000 to provide better tracking compared to radar-based tracking. In Indonesia, it became mandatory to complete ADS-B for each airspace by 2015, and all categories of carriers must have ADS-B equipment by 2017.

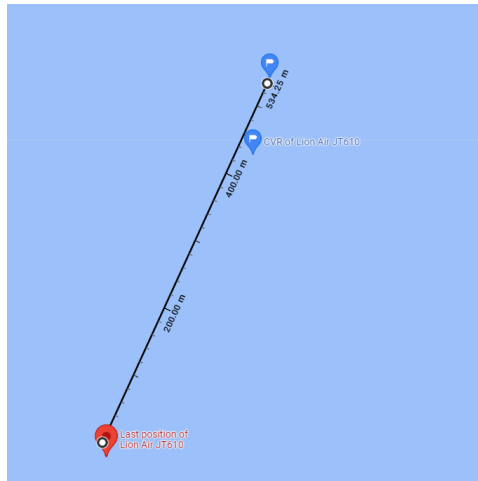


FIGURE 1.1: The location of aircraft cras site from Lion Air JT610.

The last report's location of aircraft cannot be the best prediction. It has several considerations, such as analyzing the effect of degrees of freedom on the location of the plane crash, the cartesian coordinate system, and considering atmospheric parameters on earth such as gravity, temperature, density, pressure, and wind. Besides that, it is also necessary to analyze the uncertainty of the last state of

the aircraft. In general, trajectory analysis seeks to understand the behavior of an unpowered or accidental aircraft falling to the ground and being affected by gravity, drag, and the Earth's atmosphere (Greaves, 2012). It is to estimate where the search area will be and determine the potential location of the crash area.

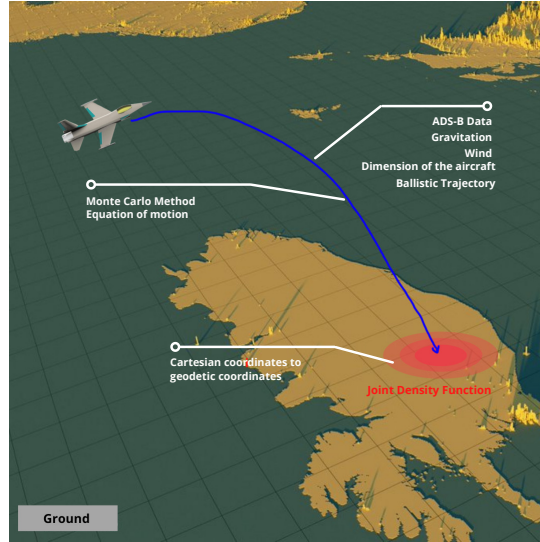


FIGURE 1.2: Schematic: Prediction of aircraft crash landing site.

1.2 Problem Statement

The problem statement in this thesis will take into account:

- Wind speed and wind direction are disturbances to the falling aircraft, which will determine the possible position of the crash site due to the changing wind direction and wind speed; not only that, each region has different pressure, direction, and wind speed;
- Ordinary Differential Equation (ODE) examines the effect of the initial state on time. The assumptions used in this study are to consider wind speed and direction, which were previously ignored, and the presence of wind speed and direction. The ballistic trajectory can be determined by integrating time steps, which are then considered drag coefficients;

- Initial state where the uncertainty factor in position and velocity. Initial state, which is integrated and accurate by ADS-B Quality Indicator. The initial state will determine the prediction of the location of the plane crash.

1.3 Research Purpose

The study's primary purpose is as follows:

- To predict the location of the aircraft crash site using the Monte Carlo Method;
- Explore how the uncertainty of the final state influence the coverage of the potential crash site;
- To provide the statistical likelihood of the aircraft crash site.

1.4 Research Scope

The scope of this research describes the area to explored work and establishes the following conditions for the research to develop:

- The data record of a flight that is needed in this research is ADS-B. The author will explain the system of ADS-B in the aviation industry. However, first, understand the function and use of the ADS-B system;
- The last ADS-B transmitted data referred to in this research is the initial state of the aircraft, such as the parameters of the initial state of the velocity and location of the aircraft;
- The notion of development to support the analysis in this research is aircraft performance. Aircraft performance considers the effect of the angle of an aircraft on the ground on the earth and the effects of the earth's atmosphere such as density, pressure, temperature, and wind which refers to the International Standard Atmosphere (ISA) and gravity acceleration;

- The theory used in this research is Newton's second law, which is expressed as a system of Ordinary Differential Equations (ODEs) that examines the impact of starting circumstances on time. The assumptions employed in this study were to consider the wind speed and direction, which were previously neglected, and the presence of wind speed and direction. The ballistic trajectory may be determined via time-step integration (Crider, 2015), which is then considered the drag coefficient. The midair aircraft explosion causing debris is not considered;
- Use parameters NUCp and NUCv of ADS-B Quality Indicators to give the uncertainty of the final states of the aircraft;
- The development of calculations from Newton's second law will produce one value when on the ground of the earth, and the role of the Monte Carlo simulation will double the point value on the ground of the earth to produce a probability which becomes a parameter of the area of the plane crash.

1.5 Thesis Organization

In this study, the authors divide into five chapters. Described in the following:

- In the first chapter, the author will explain the general introduction of this thesis, explaining the problems that exist in the aviation industry, especially for the research and Search and Rescue (SAR) team when dealing with a plane crash. Then, variable parameters or assumptions are used in calculating a case and explaining the purpose of this study;
- The author will explain the literature review explaining the ADS-B system in the aviation industry in the second chapter. The aircraft performance related to research is like the atmosphere on the earth that affects the movement of the aircraft. Finally, explain the Monte Carlo method theory, where this theory will generate probabilities and reduce the search space for aircraft locations;

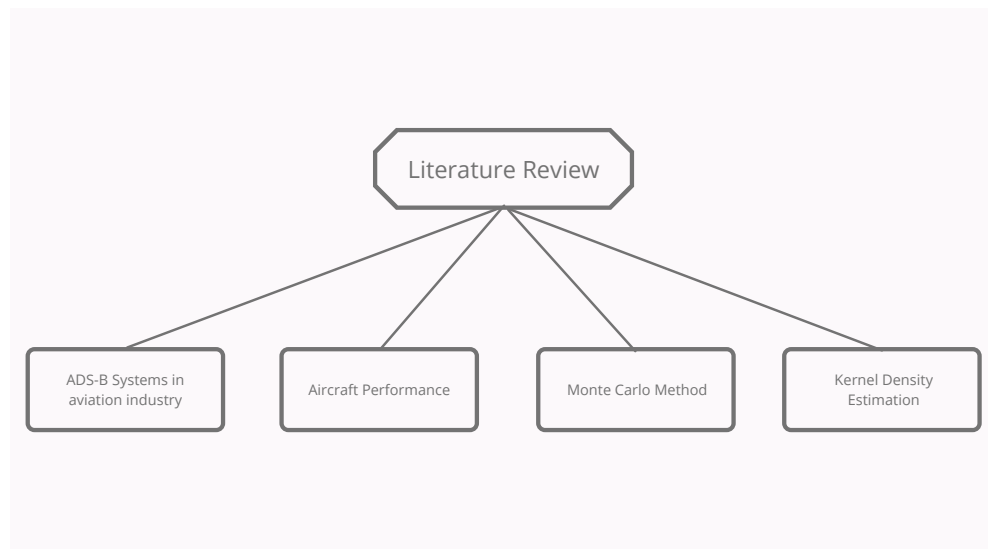


FIGURE 1.3: Outline of literature review.

- In the third chapter, the author will explain the research methodology in this study. The research methodology section will explain in detail the research framework, where there are input steps: as the initial condition of the ADS-B aircraft, the parameters contained in the aircraft characteristics, and the earth's atmosphere. Calculation steps: using basic science Newton's second law theory was developed using Ordinary Differential Equation (ODEs) and determined the probability using the theory of the Monte Carlo method. Output step: final condition, which will produce the time to hit ground and coordinates on the ground that will be considered as the final condition where the plane crashed;

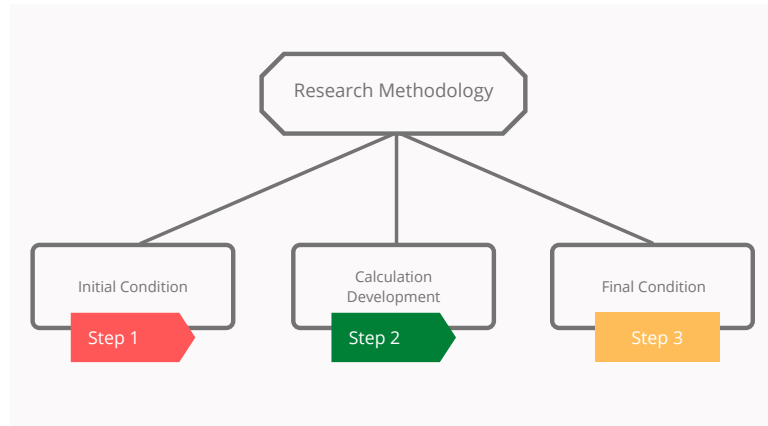


FIGURE 1.4: Outline of research methodology.

- The fourth chapter will show the research results by showing simulations with different initial conditions. In this fourth chapter, the direction of this research will be more precise with category prediction divided into two, namely the first, the coordinates of the location of the aircraft in the form of a Cartesian coordinate system and the second, the travel time of the aircraft during the initial condition to the final condition. The estimation will be shown in the form of a Kernel Density or Joint Density Function (JDF) plot;
- In chapter five, researchers will analyze the results of the simulation described in chapter 4. The results of the simulation will be explained and compared to obtain conclusions from the required data.

CHAPTER 2

LITERATURE REVIEW

2.1 Overview

ADS-B (Automatic Dependent Surveillance-Broadcast) has become a vital component of next-generation air traffic surveillance technology. Every aircraft equipped with an ADS-B device transmits plain text signals once or twice per second to other aircraft and ground station controllers. ADS-B's fundamentals include how it operates, its history, definition, type, and the message format of a single ADS-B message. MLAT is another surveillance technique that aids in tracking airplanes by ATM (Air Traffic Management). The basic understanding of ADS-B is essential to understand in order to support the development of this thesis. Then understand the parameters generated by ADS-B by checking by the ADS-B Quality Indicator. ADS-B has undergone an update to have a different capability and understands each of these differences. ADS-B transmits a data message to the ground station after that to ATC (Air Traffic Control) and will be managed

Understanding aircraft performance is also a consideration. In this thesis, the definition of aircraft performance is the performance related to the fall of the aircraft, which impacts the coordinates or the location of the aircraft falling on the ground. Earth's variables affect when the plane falls, and the first is The atmosphere is the layer around the Earth filled with various gases pressed against it by gravity. The Troposphere, Stratosphere, Mesosphere, and Thermosphere are the four vertically split sections of the atmosphere. The International Standard Atmosphere (ISA), often known as the ICAO Standard Atmosphere, is a guideline against which the actual atmosphere at any given moment may be compared. The ISA has based the following values of pressure, density, and temperature at mean sea level, each decreasing with an increase in height, which refers to the International Standard Atmosphere with standard sea level at 1013.25 hPa at 15° and

density sea level $1,225 \text{ kg/m}^2$. In addition to the Earth's atmosphere, that affects the fall of the plane is a drag. Drag is a term used in aerodynamics to describe forces that resist an object's relative velocity in the air. Drag always opposes an object's motion and is countered by propulsion in an aircraft. The freedom of movement of a rigid body (such as an aircraft) in three-dimensional space is referred to as six degrees of freedom (6DoF) (Ruijgrok, 2009). The body may move forward and backwards, up and down, left and right, and rotate along three perpendicular axes.

Following consideration and analysis, this study will employ the Monte Carlo technique theory, which employs a numerical approach in three-dimensional computations. The idea for Monte Carlo error propagation is to select at random from a known initial condition. The beginning circumstances utilized in this final project include ADS-B data, such as the aircraft's changing speed and initial position. These computations are then placed into a table to be one point away from a random beginning state but with the standard deviation specified. To acquire a more exact probability, repeat this technique as many times as necessary. The standard deviation and mean may be used to calculate the number of points. The central value is the mean of the sample replies, while the standard deviation represents uncertainty after finding the uncertainty of the crash site points. The crash site points will be plotted using the theory of Kernel Density estimation.

2.2 ADS-B (Automatic Dependent Surveillance - Broadcast)

ADS-B is a surveillance method that relies on aircraft or airport vehicles transmitting their location, velocity, and direction, and other data extracted from onboard devices via satellite. This signal (ADS-B out) may be recorded on the ground (ADS-B out) or onboard other aircraft for monitoring purposes to improve airborne traffic situational perception, spacing, and separation. It is reliant because it depends on onboard monitoring devices to supply information to third parties. Suddenly, the data is broadcast without interrogation or a two-way deal, and the source has no idea about who gets the data. A locally optimized combination of available technology, such as airport Multilateration, Surface Movement Radars,

ADS-B, and automated airport operations, is used at airports. It may require a suitable view of surveillance data in the form of a moving map in flight decks and surface vehicles. Transponders connected to the related avionics systems allow the "ADS-B Out" functionality onboard (GNSS, pressure altimeters.). Many aircraft still have ADS-B Extended Squitter capabilities as part of the Mode S system. The "ADS-B In" capability necessitates the use of a receiver, a processing machine (traffic computer), and a graphical user interface (GUI) (often called Cockpit Display of Traffic Information - CDTI). The "ADS-B in" device could be inserted into the Forward Field of View. The regulatory authorities must certify and approve the practical usage of ADS-B before it can be used. EASA AMC 20-24 for ADS-B in Non-Radar Airspace or CS-ACNS for "ADS-B down" are the appropriate certification records (Martin Strohmeier & Martinovic, May 2014).

2.2.1 History of ADS-B

ADS-B has evolution up to 3 times, namely ADS-B Version 0 (DO-260), ADS-B Version 1 (DO-260 A), ADS-B Version 2 (DO-260 B). The first type, DO-260 (ADS-B Version 0), published in September 2000, has only the Navigation Uncertainty Category Quality Indicator for Position (NUCp) and the Navigation Uncertainty Category for Speed (Nov). In April 2003, the second issue, namely DO-260 A (ADS-B Version 1), was amended 2 in December 2006. DO-260 A (ADS-B Version 1) has parameters for Navigation Accuracy Category for Velocity (NACv), Navigation Accuracy Category for Position (NACp), Navigation Integrity Category (NIC), Navigation Integrity Category for Barometric (NICbaro), Surveillance / Source Level Integrity (SIL). The newest is DO-260 B (ADS-B Version 2) Publish in December 2009. DO-260 B (ADS-B Version 2) has parameters Geometric Vertical Accuracy (GVA), Navigation Integrity Category (NIC), Surveillance / Source Level Integrity (SIL), Navigation Accuracy Category (NAC), Navigation Uncertainty Category (NUC), System Design Assurance (SDA). Meaning of Name: DO = Document; 260 = Number are assigned sequentially; A = Alphabetical letters is for the consecutive changes in specification of system; Change 1 = in this case includes editorial changes, clarifications and corrections.

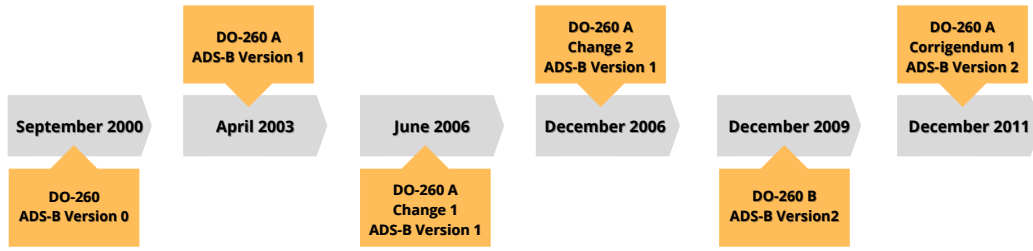


FIGURE 2.1: Evolution of ADS-B

For flight safety and efficiency in Indonesia, air traffic services must give relevant recommendations and information. In 2015, a Ministerial Regulation was issued. The Civil Aviation Safety Regulation (CASR) Part 92, which addresses the general regulations of flight operations, is the subject of this regulation.”Aircraft carrying ADS-B transmission equipment for operational purposes in Indonesian airspace must fulfill the criteria in FAA TSO-C116b or other standards acceptable to the Directorate General of Civil Aviation,” according to CASR Part 91, Section 91,226. Then there was Ministerial Regulation Number 48 of 2017, which dealt with CASR Part 171, or Aeronautical Telecommunication Service Providers. Part 171015 of the CASR specifies a collection of surveillance facilities, which include Movement Radar (SMR), Secondary Surveillance Radar (SSR), Primary Surveillance Radar (PSR) Multi-Mission Surveillance Radar (MMSR), Multilateration (MLAT), ADS- B, ADS-Contract, Surface, Precision App-approach Radar (PAR), Air Trac Control Automation, Advanced Surface Movement Guidance and Control System (ASMGCS), and Automatic Identification System (AIS). Subsequently, Ministerial Regulation No. 89 of 2017 replaced Ministerial Regulation No. 94 of 2015. The ministerial decree stipulates that all transport aircraft must be equipped with ADSB equipment before January 1, 2020. Not only that but also It also stipulates that by January 1, 2030, all category aircraft must have ADS-B equipment. Concerning ADS-B equipment, it must meet the minimum requirements stated in DO-260 (ADS-B Version 0), DO-260A (ADS-B Version 1), or DO-260B (ADS-B Version 2).

2.2.2 Flow of ADS-B System

ADS-B system flow is divided into three categories, namely space, air, land. In space, there is a satellite device (GNSS, GPS). Satellites in outer space will transmit aircraft data signals using GPS or GNSS. The United States owns and operates the Global Positioning System (GPS). The official US Department of Defense name for GPS is NAVSTAR. Global Navigation Satellite System (GNSS) is a generic name for a group of artificial satellites that send position and timing data from their high orbits. Galileo is the European Union's global GNSS (Strohmeier, 2016). The workings of the satellite only send data signals to the air category, namely aircraft. In the air system, ADS-B IN, ADS-B OUT, and Mode-s are used. Aircraft equipped with ADS-B IN, ADS-B OUT, and Mode-s systems. Aircraft in the air receive signal data from GNSS or aircraft GPS data via ADS-B IN, after which ADS-B OUT transmits aircraft data to the earth station. Earth station consisting of ADS-B Ground Station, MLAT, and ATC. How it works, MLAT will read the data signal via the s-mode plane. Then the earth station operation from the ADS-B and MLAT ground stations sends data to the ATC so that the ATC will process the aircraft data as a management procedure. An aircraft not equipped with ADS-B but with a transponder can still transmit its position to ground radar and nearby aircraft. If nearby aircraft are equipped with ADS-B, non-ADS-B aircraft will be considered potential traffic with the assistance of TCAS.

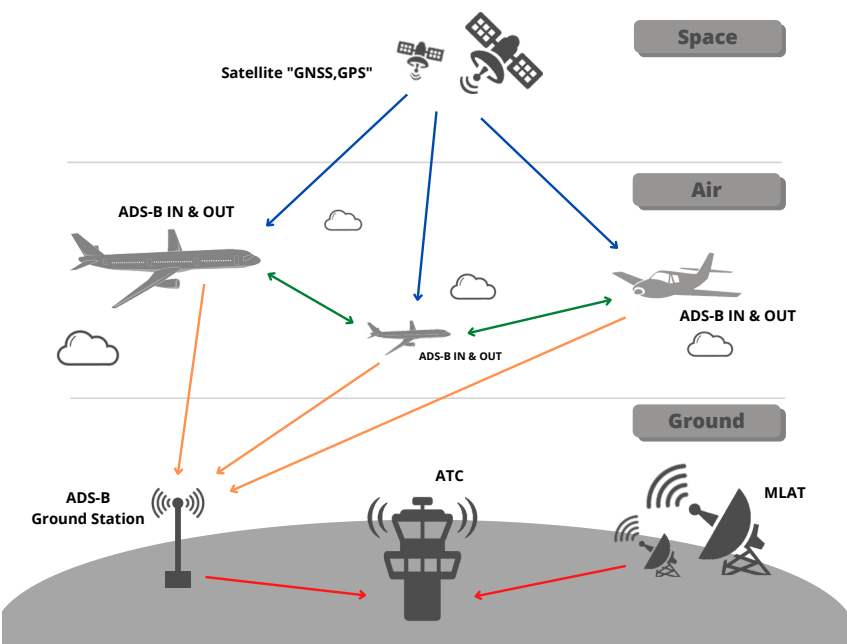


FIGURE 2.2: Flow of ADS-B System

2.2.3 ADS-B Message Structure

ADS-B is a satellite-based surveillance technology that stands for Automatic Dependent Surveillance-Broadcast. The S Extended Squitter (1090 MHz) Mode transmits parameters such as location, velocity, and identity (Sun, 2021). Currently, ADS-B is mandatory for aircraft. In this section, part of the ADS-B system is the Message Structure. ADS-B Message Structure has a frame that is 112 bits long and consists of 5 main parts: Downlink Format (DF), Capability Field (CF), Aircraft Address (AA), Data Segment, Parity Field (PI).

DF(5)	CA(3)	AA(24)	DATA(56)	PI(24)
-------	-------	--------	----------	--------

TABLE 2.1: five main parts of ADS-B Message Structure

Bit	No. bit	Abbreviation	Information
1-5	5	DF	Downlink Format
6-8	3	CA	Transponder Capability
9-32	24	ICAO	ICAO aircraft address
(33-37)	(5)	(TC)	(Type Code)
33-38	56	ME	Message, extended Squitter
88-112	24	PI	Parity/Interrogator ID

TABLE 2.2: ADS-B Message Structure

Downlink Format

Downlink format has 5 bits long. There are several types of downlinks, namely format 17 downlink, 18 format downlink, 19 format downlink, 20 format downlink. Each ADS-B Message must start with downlink 17 only. Downlink 18 is only used by TIS-B messages. Downlink Format 17 (DF = 17) is used by the ADS-B Extended Squitter transmitted by a Mode S transponder. Downlink Format 18 (DF = 18) is used by non-transponder-based ADS-B transmitting subsystems and TIS-B transmitting equipment. An ADS-B / TIS-B Receiving Subsystem will recognize that the Message originated from equipment that cannot be probed if DF = 18 is used instead of DF = 17.

Capability Field

Capability Fields ranging from bit 6 to bit 8 (3 bits long) and transponder-based Mode-S will report on the ADS-B transmission system's capabilities. The capability values are from 0 to 7. The definitions of these values are as follows:

CA	Definition
0	Level 1 transponder
1-3	Reserved
4	Level 2 transponder with ability to set CA to 7 on-ground
5	Level 2 transponder, with ability to set CA to 7 airborne
6	Level 2 transponder, with ability to set CA to 7, either on-ground or airborne
7	Signifies the downlink request value is 0, or the flight status is 2,3,4,5 either airborne or on the ground

TABLE 2.3: The definition of Capability Field

Aircraft Address

The sender (originating aircraft) is identified in each ADS-B message using the Mode S transponder code assigned by ICAO regulations. The ICAO address, or hex code, is another description for the Mode S transponder code. The ICAO address ranges from 9 to 32 bits (or 3 to 8 in hexadecimal positions) in binary. Each aircraft's Mode S transponder is given an ICAO address. An example of an ICAO address is 0X8A030B (Hex Code). This Hex code identifies as an SJ-182 Sriwijaya Air with the registration of PK-CLC.

Data Segment

To figure out what information is in an ADS-B message. The message code type will indicate the message's content. Bits 33 to 37 are used to store type codes (or the first 5 bits of the data segment). The relationship between each Type of Code and the data in the data segment is displayed.

Type Code	Data Frame
1-4	Aircraft Identification
5-8	Surface Position
9-18	Airborne position(w/baro altitude)
19	Airborne velocities
20-22	Airborne position(w/GNSS height)
23-27	Reserved
28	Aircraft Status
29	Target state and status information
31	Aircraft operation status

TABLE 2.4: The definition of Data Segment

Parity Field

The parity or identity field consists of bits 89 through bits 112 (24 bits long). The last bit part of the ADS-B message structure will validate the message or examine its content.

2.3 ADS-B Quality Indicators

ADS-B is operational across Australia, Canada, East Asia, and portions of Europe. In ICAO Circular 326, the standards for quality indicators are laid forth. ADS-B Quality indicators are used to verify that ADS-B communications meet the required accuracy and integrity levels (Tesi & Pleninger, 2017).

2.3.1 ADS-B Quality Indicators Version 0

The criteria for the degree of accuracy and integrity of data in the report are represented by one parameter. The location is NUCp, while the velocity is NUCv. The NUCp parameter is dependent on other factors, as shown in table 3. They are HPL (Horizontal Protection Limit) and /v (Vertical Protection Limit) (95 percent containment radius). The radius of a circle in the horizontal plane (plane equivalent to the WGS-84 ellipsoid) with its center in the aircraft's actual position is HPL.

It denotes a radius in which the given location has a high likelihood of being true. The accuracy is defined as a location region in which 95 percent of the specified places are located.

2.3.2 ADS-B Quality Indicators Version 1

The accuracy and integrity parameters are divided in this version. NAC (NACP, NACV), NIC, and SIL are the newly defined parameters. There is a dependency on VPL in version 1. (vertical protection limit). It is valid for the NIC and SIL parameters. The SIL must be set to 0 if VPL cannot be established. For the parameter NIC, a similar dependency was specified. Though the VPL cannot be determined, we cannot use values larger than 8, even if the available data might provide a more precise indication in the horizontal plane (SC-186, 2006).

2.3.3 ADS-B Quality Indicators Version 2

The following quality parameters are available in version 2: NIC and SIL with SIL-SUPP to denote accuracy, NAC (NACP, NACV) to denote integrity. The risk of system failure is determined by SDA, the quality of altitude information is determined by NIC_{BARO} , and GVA determines the vertical position accuracy (Do, 2009).

2.3.4 Navigation Uncertainty Category (NUC)

Navigation Uncertainty Category, where accuracy and integrity are both combined into a single quality indicator. GNSS calculates HPL, and in theory, containment is 100 % limiting in the horizontal plane. It helps determine the separation between the two aircraft and the HFOM, with the 95 % position specifying that the pilots' separation should be more careful. In HFOM, it divides into the vertical and horizontal radius of containment. The hold radius, usually denoted as R_c , is the statistical radius. There is a 95 % chance that the aircraft will be within the radius of its original stated position in flight and only available in DO-260. NUC has divided into two: Navigation Uncertainty Category for Position (NUCp) and Navigation Uncertainty Category for Velocity (NUCv). NUCp made up Horizontal Protection Level (Integrity) and Horizontal Figure of Merit (Accuracy) then both of

them has type code 0-9 (where HPL and RC get more accurate as values increase.), Type code 22 - 22 Airborne position with GNSS height, Code 5-8 surface position, 6,7,8,9 the NUCp values (the higher NUCp values than more accurate the position report. NUCp values (the higher NUCp values , the more accurate the position report. NUCv is Indicate. the uncertainty of horizontal and vertical speed, Type code 19 (it means airborne velocity message and divided two parameters horizontal vertical error 95 %, vertical velocity error 95% and has a values 0-4 the higher values then more accurate the velocity report. For example, ATC got the data values nine information HPL <80 and Rc <40 it means the data accurately.

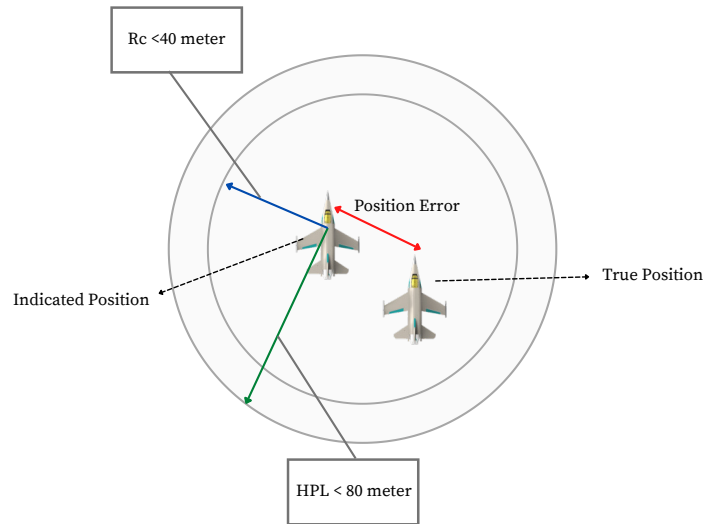


FIGURE 2.3: NUCp Parameters

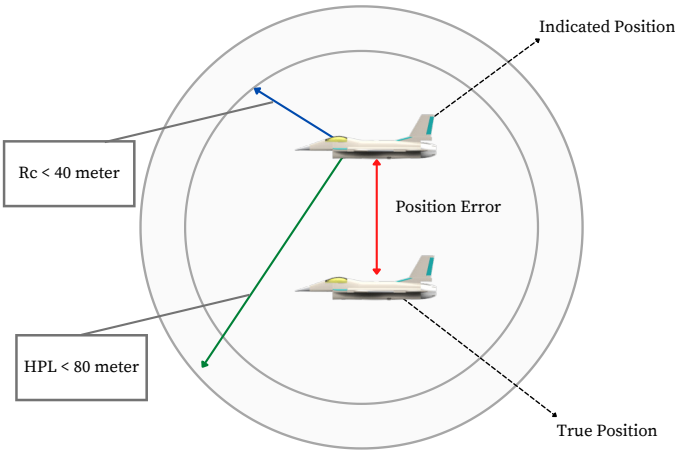


FIGURE 2.4: NUCp Parameters

NUCp	HPL	Rc Horizontal
0	> 35 020	> 24 610
1	<35 020	< 24 610
2	< 20 410	< 10 170
3	< 4683	< 2897
4	< 2132	< 1164
5	< 1087	< 570
6	< 635	< 420
7	< 225	< 119
8	< 105	< 50
9	< 80	< 40

TABLE 2.5: Airborne position with barometric altitude (Type Code = 9 - 18)

PREDICTION OF AIRCRAFT CRASH LANDING SITE FROM ADS-B DATA USING
MONTE CARLO METHOD

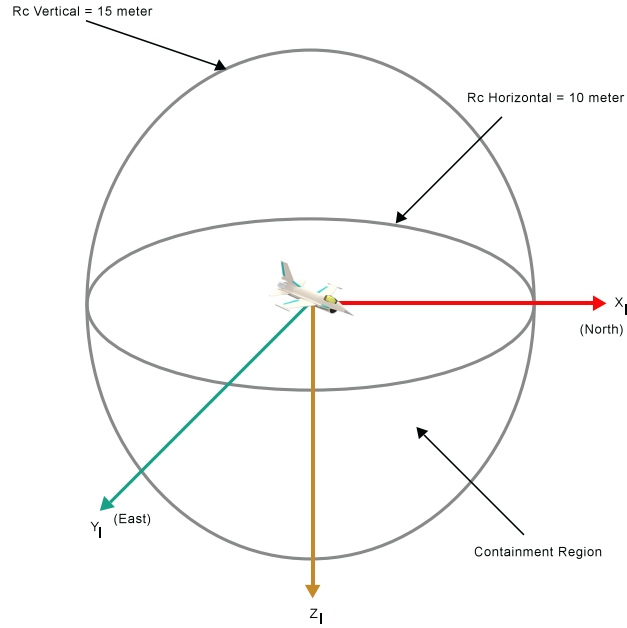


FIGURE 2.5: Airborne position with GNSS height (Type Code = 20 - 22)

NUCp	HPL	Rc Horizontal(m)	Rc Vertical (m)
0	> 25	> 10	>15
8	< 25	< 10	<15
9	< 8	< 4	<6

TABLE 2.6: Airborne position with GNSS height (Type Code = 20 - 22)

NUCp	HPL(m)	RCu (m)
6	> 165	> 92
7	< 165	< 93
8	< 30	< 11
9	< 8	< 5

TABLE 2.7: Surface position (Type Code = 5 - 8)

NUCv	HVE 95% (m/s)	VVE 95% (m/s)
0	Unknown	Unknown
1	< 10	< 14
2	< 4	< 5
3	< 1.5	< 2.5
4	< 1	< 1.5

TABLE 2.8: NUCv figure of merit

2.3.5 Navigation Accuracy Category (NAC)

The Navigation Accuracy Category for Position (NACp) and the Navigation Accuracy Category for Velocity (NACV) are the two components of the Navigation Accuracy Category (NACv). Estimated Position Uncertainty (EPU) and Vertical Estimated Position Uncertainty (VEPU), both of which have a high 95 percent accuracy, are the two factors NACp concentrates. NACp will determine that the position report data is acceptable or not. The values of NACp from 0 until 15, values 0 - 11 its figure, and the values 12 until 15 is reserved for future purpose. The values from NACp mean that the higher the reported value, the higher the accuracy that is obtained. The Horizontal Figure of Merit (HFOMr) and Vertical Figure of Merit (VFOMr) are used to assess the accuracy group for velocity (VFOMr). It was previously known as NUCv in ADS-B Version 0. The values are the same as in DO-260, so they have been renamed.

NACp	95% HFOM and VFOM (m)
0	> 18 410
1	< 18 410
2	< 7210
3	< 3822
4	< 1851
5	< 925
6	< 424
7	< 180
8	< 90
9	< 31 and VEPu < 42
10	< 10 and VEPu < 15
11	< 3 and VEPu < 5
12-15	Reserved

TABLE 2.9: NACp values

NACv	HFOMr 95%(m/s)	VFOMr 95%(m/s)
0	Unknown	Unknown
1	< 10	< 14
2	< 3.5	< 4
3	< 1	< 1.2
4	< 0.5	< 0.8

TABLE 2.10: NACv values

2.3.6 Surveillance / Source Level Integrity(SIL)

There is the Surveillance Level Integrity, which is dependent on the Containment Radius and Vertical Protection Limit (VPL). The two parameters are used to calculate the likelihood of reaching the three recorded Radius of Containment and Vertical Protection Limits without warning. SIL is also subject to vertical safety restrictions in the DO-260A. The Integrity Control Level ranges from 0 to 3, with a value of 0 to 3 per hour or per sample. The name is changed to Source Integrity

Level in the DO-260B. It only depends on the recorded horizontal location in this edition (Rc). A SIL supplement was also introduced, with only 0 and 1 values. If the unit was in per hour or sample was calculated by the zero or one value. Aside from that, the function is unchanged

SIL	Rcu	VPL
0	0	0
1	$< 1 \times 10^{-3}$	$< 1 \times 10^{-3}$
2	$< 1 \times 10^{-5}$	$< 1 \times 10^{-3}$
3	$< 1 \times 10^{-7}$	$< 1 \times 10^{-7}$

TABLE 2.11: Values for Surveillance Integrity Level

SIL	Probability of Exceeding RCu
0	$\leq 1 \times 10^{-3}$ or unknown
1	$\leq 1 \times 10^{-3}$
2	$\leq 1 \times 10^{-5}$
3	$\leq 1 \times 10^{-7}$

TABLE 2.12: Values for Source Integrity Level

SILsupp	Definition
0	Probability of exceeding NIC Rc based on "flight per hour"
1	Probability of exceeding NIC Rc based on "flight per sample"

TABLE 2.13: SIL supplement bit to define unit

2.3.7 Navigation Integrity Level

The Radius of Containment, Vertical Protection Limit, Navigation Integrity Category Supplement Bits, and Navigation Integrity Category Barometric are the four parameters that make up the Navigation Integrity Category (Musmann, n.d.). The Navigation Integrity Category Barometric (NICbaro) only appears on the DO-260B and shows if the barometric pressure switch has been cross-checked with other pressure level sources. The NICbaro values 1 and 0 indicate that 1 has been

cross-checked and 0 has not. The ADS-B version 1 NIC is better at dealing with confusion. The Type Code in the NIC has two levels: 7 for surface messages and 11,12,13 and 16 for air position messages. NICsupp is here to help at all of the levels it mentions. It is divided into three levels in ADS-B Version 2, namely NIC Supplement A (Type Code 31 = operational status message), NIC Supplement B (Type Code 9 to 18 = airborne position message), NIC Supplement C (Type Code 31 = operational status message but different with NICa). NICa to find in Type Code 31 about operational status messages. The NICb searches in Type Code 31 for operational status messages and the NICc searches in Type Code 9 through 18 for airborne location messages, but the message is slightly separated from the NICa. NIC Numbers 0 to 11 (The degree of radius containing smaller increases as the value increases). Vertical Radius of Containment (95%). for example from Soekarno-Hatta International Airport (IATA code: CGK) to Surakarta Airport (IATA code: SOC).The route takes about 1 hour 35 minutes. 95% mean, aircraft flying the 1 hour and 10-minute flight, there is a 95% chance that the aircraft is within the radius of detention. Meanwhile, there is always a 4.99% chance that the aircraft will leave the detention area for the rest.

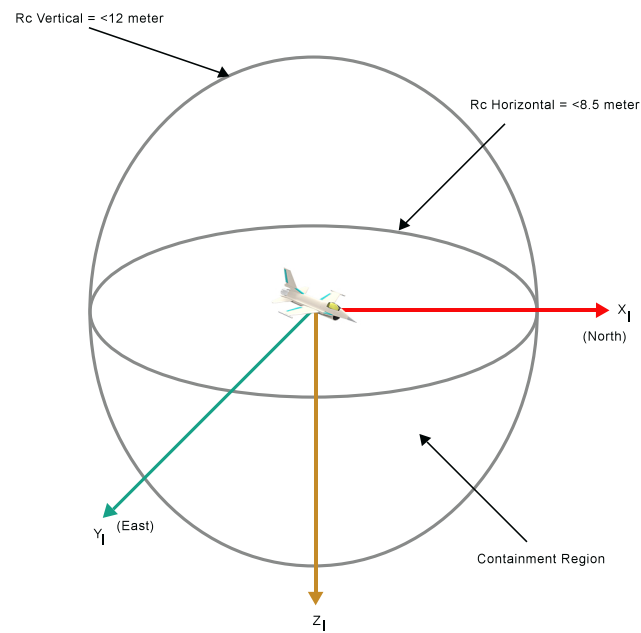


FIGURE 2.6: Vertical and Horizontal of radius of containment for
NIC

NIC	Rc Horizontal (m)	Rc Vertical (m)
0	>37 060 or unknown	-
1	<3760	-
2	<14 615	-
3	<7600	-
4	<4402	-
5	<1765	-
6	<1011	-
7	<360	-
8	<168	-
9	<72	<144
10	<22	<38.5
11	<8.5	<12

TABLE 2.14: Values of NIC for Version 1

NICbaro	Meaning
0	Barometric altitude has not been crosschecked
1	Barometric altitude has been crosschecked

TABLE 2.15: Values of NICbaro for Version 2

2.3.8 System Design Assurance(SDA)

System Design Assurance is a warning that a fault in the ADS-B system may result in a false location report. Included are the location source, ADS-B equipment, and any data-processing intermediary instruments. SDA values range from 0 to 3: unknown or no safety impact, minor support malfunction state, paramount, and dangerous. The Next Generation Air Transportation System is a technology developed by the Federal Aviation Administration (NextGEN).By altering the National Airspace System's operation, NextGEN was meant to increase protection and promote environmental movements. The FAA decided it was time to move from ground-based monitoring and navigation to airborne surveillance. Furthermore, NextGEN plans to replace ATC radar-based technologies with satellite-derived location technology.Furthermore, ADS-B technologies and facilities are an important core factor in the program's performance. One of NextGEN's minimum technical consistency criteria is that the System Design Assurance standard be equal to or greater than 2.

SDA	Failure	Probability of Undetected Fault	Design Assurance Level
0	Unknown	$>1 \times 10^{-3}$ per flight hour/unknown	Not Available
1	Minor	$\leq 1 \times 10^{-3}$ per flight hour	D
2	Major	$\leq 1 \times 10^{-5}$ per flight hour	C
3	Hazardous	$\leq 1 \times 10^{-7}$ per flight hour	B

TABLE 2.16: Values of SDA in version 2

2.3.9 Geometric Vertical Accuracy(GVA)

Only ADS-B Version 2 supports Geometric Vertical Accuracy. The horizontal and vertical components of ADS-B Version 2 are separated. The GVA stands for the

geometrical vertical location precision. GVA will help determine whether the barometric altitude system or the GPS receiver affects the mismatch between geometric and pressure altitude. Vertical Separation Minimum Is Required For This Application The Vertical Figure of Merit (VFOM) 95% from the GNSS position source used to encode the geometric altitude field airborne position message shall be used to set the GVA field in the airborne position message. It also considers the possibility of transmitting erroneous or inaccurate latitude, longitude, velocity, or accuracy, and honesty metrics.

GVA	Meaning
0	Unknown or >155 m
1	≤ 155 m
2	≤ 45 m
3	Reserved

TABLE 2.17: Values of GVA in version 2

2.4 Capability differences between the ADS-B Quality Indicator

ADS-B is a system that will continuously be updated, and each generation or each version of the ADS-B Quality indicator has differences and updates. The Capability Quality Indicator has six parameter quality indicators from all versions of ADS-B. ADS-B Version 0 (DO-260), which only has the Navigation Uncertainty Category (NUC) as a Quality Indicator for velocity and position. ADS-B Version 1 (DO-260 A) is the first update that has four parameters, namely Navigation Uncertainty Category (NUC), Navigation Accuracy Category (NAC), Source Integrity Level (SIL), Navigation Integrity Category (NAC). The latest version, ADS-B Version 2 (DO-260 B), has 5 Quality Indicator parameters, namely Accuracy Category (NAC), Source Integrity Level (SIL), Navigation Integrity Category (NAC), System Design Assurance (SDA), Geometric Vertical Accuracy (GVA)).

Capability of Quality Indicator	ADS-B Version 0 (DO-260)	ADS-B Version 1 (DO-260 A)	ADS-B Version 2 (DO-260 B)
NUC	✓	✓	
NAC		✓	✓
SIL		✓	✓
NIC		✓	✓
GVA			✓
SDA			✓

TABLE 2.18: Summarized differences

2.5 ADS-B data received by ATC

Land-based air traffic controllers guide aircraft on the ground and across regulated airspace and provide advisory services to aircraft flying in uncontrolled airspace. ATC receives ADS-B data from ADS-B ground station via aircraft transmitting of ADS-B OUT and receives ADS-B data from MLAT. ATC requires ADS-B data for Air Traffic Management needs so that the aircraft will continue to record. ADS-B data received by ATC has 12 parameters: Hex Code, Callsign, Latitude, Longitude, Altitude, Velocity, Position, Vertical Speed, Ground Speed, Track, Direction, Squawk (FAA, March 2020). On the Quality Indicator of ADS-B Version 0, ADS-B Version 1 and ADS-B Version 2, check the quality of latitude, longitude, altitude, velocity, position, vertical speed, ground speed.

ADS-B Data received from ATC	ADS-B Version 0 (DO-260)	ADS-B Version 1 (DO-260 A)	ADS-B Version 2 (DO-260 B)
Hex Code			
Callsign			
Latitude	✓	✓	✓
Longitude	✓	✓	✓
Altitude	✓	✓	✓
Velocity	✓	✓	✓
Position	✓	✓	✓
Vertical Speed	✓	✓	✓
Ground Speed	✓	✓	✓
Track			
Squawk			

TABLE 2.19: Parameters of ADS-B data

2.5.1 Time

Air Traffic Services units must utilize Coordinated Universal Time (UTC) and indicate time in hours, minutes, and, if necessary, seconds of a 24-hour day starting at midnight. Every station in the aviation telecommunication service must utilize Coordinated Universal Time (UTC). The time of reference UTC, or Coordinated Universal Time, is often known as "Zulu" time. Air Traffic Services units must have clocks that display the time in hours, minutes, and seconds and are visible from every operational position in operation (ICAO, 19 to 30 November 2012). A date-time group must have six digits, with the first two indicating the month's date and the final four indicating the hours and minutes in UTC. (See METARs and TAFs for examples.) Greenwich Mean Time (GMT) is used as the time base, with the Greenwich meridian at 0°. A country can choose its own "standard time" hour based on its location in the world. Instead of utilizing solar time or a locally determined meridian (longitude) to produce a local mean time standard, standard time synchronizes clocks within a geographical area or region to a single time standard. Each of these zones covers 15 degrees of longitude and divides the world

into twenty-four time zones. Finally, local, national standard time will vary around the world. UTC is also used to eliminate misunderstandings regarding time zones and daylight saving time for flight schedules in aviation. Clearances from air traffic control, weather predictions, and maps.

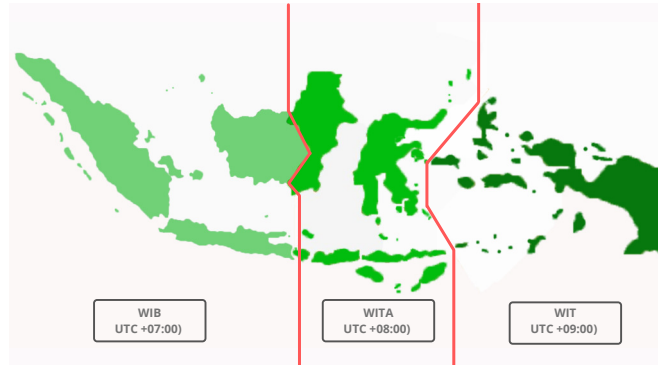


FIGURE 2.7: Coordinated Universal Time (UTC) in Indonesia

2.5.2 Hex Code and Call Sign

Mode S transponders are given a unique 24-bit address, commonly referred to as a hex code due to the way it is presented. The HEX code of an aircraft appears on its certificate of registration once it has been registered, and it is seldom altered. For example, the ADS-B data shows hex code 0X8A0711 that hex code mean the registration from ICAO for Lion Air JT (PK-LQP).

2.5.3 Position from Latitude and Longitude(Geographical Coordinates

A geographic coordinate that defines in degrees because Earth is a sphere. The north-south direction of a point on the Earth's surface is known as latitude (ϕ). The latitude angle varies from 0° at the Equator to 90° at the poles. Parallels, or lines of constant latitude, running east-west as circles parallel to the Equator. The east-west orientation of a point on the Earth's surface, or the surface of a celestial body, is defined by longitude. It is an angular measurement denoted by the Greek letter (λ) and typically expressed in degrees. 0° line is known as the Prime Meridian, from the North Pole to the South Pole through Greenwich, England (SailingIssues,

2021).For example,coordinate of aircraft crash landing site from Lion Air Flight 610 is latitude: $5^{\circ}46'15''\text{S}$ and longitude: $107^{\circ}07'16''\text{E}$. 5° expressed longitude north-south location, $45'$ is divided into minute and $15''$ is divided into second. (See figure:2.8)



FIGURE 2.8: Meaning of coordinates

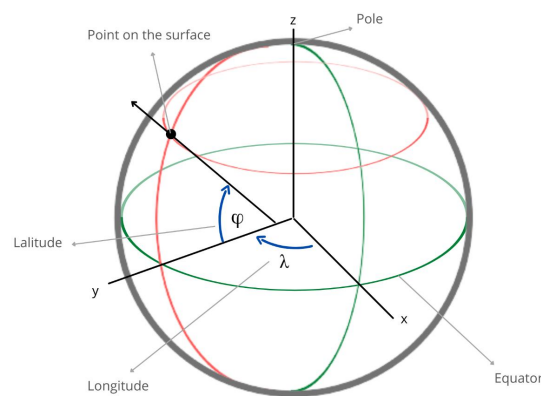


FIGURE 2.9: Parameter of latitude and longitude

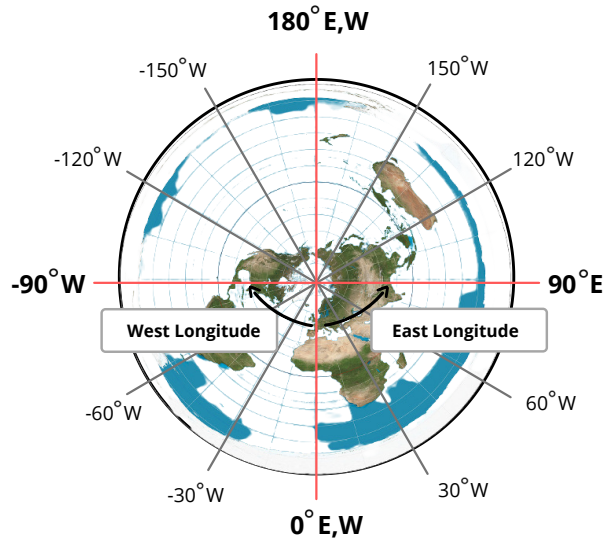


FIGURE 2.10: Longitudes in degree

2.5.4 Altitude

First and foremost, it must locate the Indicated Altitude, which can be found on the altitude indicator. It is also crucial to understand where and how to set QNH. An altitude above the MSL is referred to as altitude (Mean Sea Level). It is only valid if the local QNH is right. Altitude or height is a distance measurement between a reference datum and a point or object, usually in the vertical or "up" direction (also known as depth). The specific meaning and reference datum might vary depending on the situation (e.g., aviation, geometry, geographical survey, sport, or atmospheric pressure). Although the term "altitude" is often used to define a location's sea level, the term "elevation" is more widely used. Mean Sea Level (MSL) is the datum for measurement of elevation and altitude. Aircraft calculate altitude by 2 type called barometric altitude and geometric altitude (ICAO, 5 - 7 December 2012).

1. Barometric Altitude

- When a Secondary surveillance radar (SSR) interrogates an ATC transponder, the barometric altitude obtained from the onboard pressure altimeter is the same as the Mode C code transmitted by an ATC transponder. Aircraft altitude has been calculated from the mean sea level using onboard altimeters based on barometric pressure (MSL). The onboard altimeter is calibrated to display pressure as several feet or meters above sea level. The barometric altitude transmitted by aircraft to ground stations is often based on the International Standard Atmosphere (ISA) (i.e., standard sea level pressure at 1013.25 hPa at 15°C) (Ruijgrok, 2009). The ATM automation system will automatically correct the barometric altitude based on local QNH before showing it to ATC. The primary constants are used to calculate temperature, pressure, density and geometrical height as functions of geopotential altitude. Show how pressure and density in the International Standard Atmosphere (I.S.A). The higher the altitude, the lower the pressure effect. The higher the altitude, the lower the density effect.

Variable	Values
Sea-level pressure	$P_0 = 101325 N/m^2$
Sea-level temperature	$T_0 = 288.15 K (15^\circ C)$
Sea-level density	$\rho_0 = 1.225 kg/m^3$
Acceleration of gravity at sea level	$g_0 = 9.80665 m/s^2$
Universal gas constant	$R_a = 8314.32 J/K kmol$
Ratio of specific heats of air	$\gamma = C_p/C_v = 1.4$

TABLE 2.20: Values of parameter constant

- The altimeter indicates the vertical distance of the airplane above ground level using the atmosphere's static pressure and to provide an indicator of height instead of pressure, the scale is calibrated according to the pressure height relation in the international standard atmosphere (I.S.A) For use in the troposphere the calibration equation in terms of geopotential pressure height. The use of QNH (local pressure) will give the pressure setting information to know how high the aircraft above

sea level regarding the airport. Because of the difference in pressure in the atmosphere, the pilot must often be out of the setting. Standard pressure is used to provide the difference in altitude between aircraft at the flight level position (Ruijgrok, 2009).

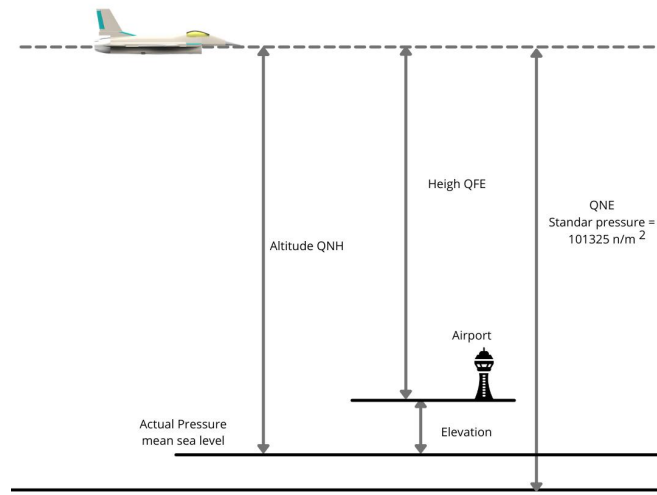


FIGURE 2.11: Definition of altimeter setting

2. Geometric Altitude

- aircraft and the MSL using a constellation of at least four GPS satellites, and this information is transmitted to ground stations via ADS-B. GPS uses WGS84 ellipsoid as an approximation to the MSL, which could have errors between 100m and 70m concerning the geoid, depending on the globe's location (González-Arribas, Soler, & Sanjurjo-Rivo, 2018). The best description of the MSL used as a reference for pressure altitude is the geoid. The accuracy of GPS's altitude measurement is less than that of its horizontal location measurement. Geometric altitude error is normally three times greater than horizontal location error, and it is generally found within 30-50 meters unless the satellite constellation is low. Geometric altitude is currently used to measure an aircraft's

altimeter device error (ASE) in height-keeping output control, but not for ATC purposes.

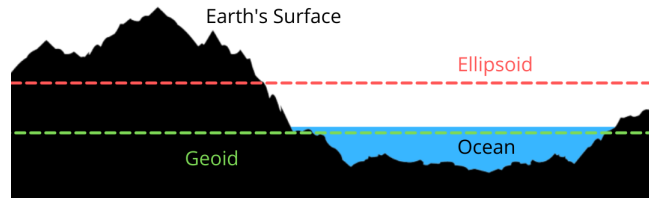


FIGURE 2.12: The parameter of geoid

2.5.5 Velocity

An object moving through the air generates aerodynamic forces. The square of the velocity between the target and the air, for example, determines aerodynamic lift. A positive velocity is known as a movement toward the aircraft's tail. A pitot tube can be used to calculate Airspeed directly on the aircraft. Higher ground speeds increased aerodynamic drag force, and decreased engine thrust and performance at higher altitudes usually are balanced at this level. A long-distance commercial passenger aircraft's average cruise speed is about 880–926 km/h (475–500 knot; 547–575 mph). The aircraft's velocity has several types called Ground speed, Indicated airspeed, calibrated Airspeed, equivalent Airspeed, true Airspeed (Ruijgrok, 2009).

- Ground speed is speed of the aircraft moving over the ground or the aircraft's speed about the ground, no relation with temperature, pressure, density.
- indicated Airspeed is a pitot-tube flow meter used to measure the velocity of fluid flow. It determines airspeed pressure between static pressure and dynamic pressure. Measure the airplane's speed as it moves through the air, the airplane's speed with the air mass flying according to the pitot tube. Suppose altitude increases the pressure of air decreases.
- Calibrated Airspeed is Indicated Airspeed corrected for position installation error. Calibrated airspeed measure by pitot-tube for any time airflow around

the body is going to change the pressure. Pitot tube would be measuring the airflow of the air uninterrupted by the airflow, skin friction, angle of attack and corrects for any error caused by the changing of the airflow from part of the airplane.

- Equivalent Airspeed is Calibrated Airspeed is about correct for compressibility of air at non-trivial Mach number. Determine the speed at sea level under International Standard Atmosphere (I.S.A.). At sea level under I.S.A., Equivalent Speed and Calibrated Airspeed are the same. 200-knot C.A.S. and altitude below 10,000 feet, the difference C.A.S. and E.A.S., is negligible.
- True Airspeed is Equivalent Airspeed corrected for temperature and pressure altitude, the aircraft's airspeed relative to the air it is flying. The general thumb rule that True Airspeed is an additional roughly 2% higher than indicated Airspeed for every 1000 feet above sea level. In still air, True Airspeed same as ground speed.

2.5.6 Track

Directional measurement path from one point to another can be determined in degrees using the meridians in a clockwise direction from true north. Draw a line on the map from the point of departure to the destination and calculate the angle this line makes with a meridian to signify a flight route. Although meridians converge toward the poles, a meridian at the midpoint of the course, rather than the point of departure, can be used to determine the path. The flight from point A to point B would have a TN of 150 degrees, while the return trip would have a TN of 330 degrees. The true heading (TH) is the true heading of the aircraft's longitudinal axis when measured in degrees clockwise from TN, or TH is the direction in which the aircraft's nose points during a flight as determined in degrees clockwise from TN. The planned horizontal path of travel is referred to as course. The track is the plane's accurate horizontal trajectory as it travels around the earth.

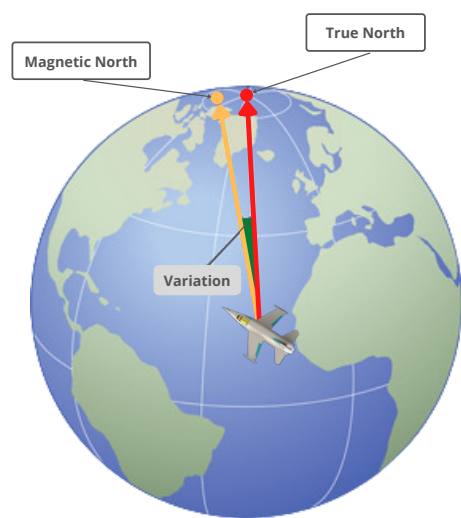


FIGURE 2.13: Reference of true north and magnitude north

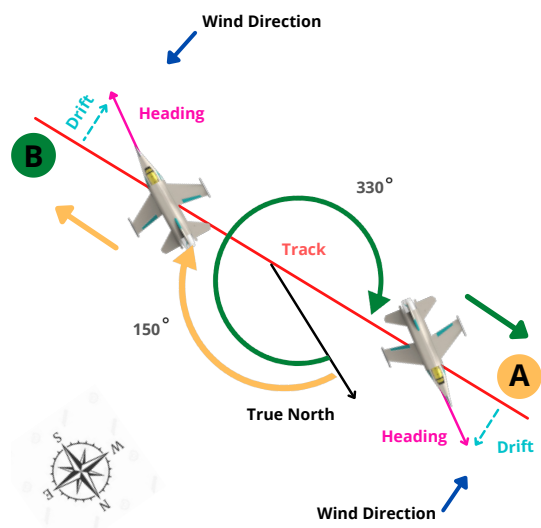


FIGURE 2.14: Track are determined by reference to true north on flight plan

2.5.7 Squawk

Each aircraft in a flight information area is assigned a discrete transponder code (also known as a squawk code) by air traffic controllers (FIR). This makes it easy to spot planes on radar. A transponder's dials range from zero to seven, and codes are made up of four octal digits. If the emergency code 7700 (squawking 7700) is used, all air traffic control facilities in the field are instantly notified that the aircraft is in an emergency condition. It may be a plane problem, a medical problem.

2.6 Multilateration

The process of multilateration is split into five sections called Mode A/C/S Interrogation; Mode A/C/S Reply, ADS-B, IFF; TDOA Processing; Hyperbolic Positioning; Aircraft position display in ATC. The ground station received replies from all aircraft fitted with a transponder, including legacy ADS-B radar and avionics. It used the difference in arrival time (TDOA) from the replies to assess the plane's location. Multilateration is accomplished by placing various earth stations in strategic locations around the airport, such as the nearby terminal area or a regional area that occupies a larger area of air space. This unit monitors the nearby SSR or multilateration station for "replies," typically interrogation signals. Since individual planes will be varying distances from each other and earth stations, their responses will be obtained fractionally at various times by each station. Multilateration uses responses from Mode A, C, and S transponders, the military IFF and ADS-B transponders, and does not include any extra avionics equipment. Although the radar and active multilateration "targets" tend to be the same control panel, the multilateration derived automatically identify the target due to its high renewal rate and smooth travel through the screen. A screen display multilateration information that can tune to update as fast as every second, compared to a 4 - 12 second position "jump" from a radar-lowered target (Pourvoyeur, Mathias, & Heidger, 2011).

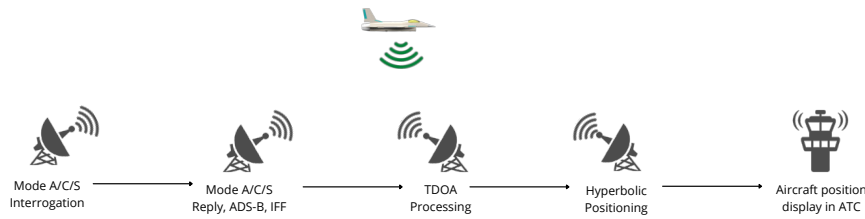


FIGURE 2.15: MLAT process to determine aircraft location

2.7 Regulation ADS-B from ICAO

ADS-B installation and operations guideline paper based on ICAO regulations (ICAO, September 2014). The ADS-B system will enable high-performance surveillance, improve flight safety, reduce separation minima, and meet user needs such as user-preferred trajectories. States should consider four factors when publishing ADS-B mandates or regulations:

- Identify the ADS-B standard that applies to the state. Standards for ADS-B aircraft location sources and ADS-B ground stations must be established by such legislation;
- Determine the airspace impacted by the restrictions and the types of aircraft that are subject to them;
- Determine the availability of time for operators, with many overseas operators in the Asia Pacific;
- Specify ground station ADS-B systems and air traffic management processes for ADS-B separation services, including related voice communications services, as well as systems and operational standards.

Factors to consider while utilizing ADS-B include the following:

- Use of ADS-B: Pressure altitude derived level information supplied by ADS-B is equal to Mode C level data supplied by an SSR sensor in terms of accuracy and integrity and is subject to the same operational procedures as in an SSR system;

- Position Reporting Performance: The aircraft's ADS-B data will contain a NUC/NIC/SIL classification of the horizontal position data's accuracy and integrity. This number is based on DO260A/B compliance avionics' NIC/NAC/ SIL values and DO260/ED102 compliant avionics' NUC values;
- GNSS Integrity Prediction Service: GNSS is likely to be used for location determination in early ADS-B installations. As a result, the availability of GNSS data has a direct impact on the surveillance service provided. ATC should not apply ADS-B separation to a specific aircraft reporting until its integrity has been established. The controller should verify with other aircraft in the area of the RAIM alert aircraft to see whether they have been affected and arrange alternate ways of separation;
- Sharing of ADS-B Data: Data-sharing through ADS-B for ATC operations. In order to optimize service advantages and improve operational safety, Member States should evaluate the benefits of exchanging ADS-B data received from aircraft flying near their international airspace boundaries with neighboring states with comparable technology;
- The synergy of ADS-B and GNSS: Surveillance is provided by ADS-B systems using a GNSS location source. For both air-air and ATC surveillance, ADS-B delivers excellent performance and high update rates. The expense of ground-based radar infrastructure can be avoided by switching to ADS-B. Acceptable GNSS equipment must be installed in the aircraft to provide the position source and integrity required by the ADS-B system.

2.8 Aircraft Performance

Aircraft performance refers to an airplane's ability to perform particular tasks that make it valuable for specific purposes. Standard atmospheric conditions, pressure altitude, or density altitude may be used to describe the performance. Pressure and temperature must be reviewed since the properties of the atmosphere have a significant impact on performance.

2.8.1 coordinates system

Earth-Centered-Earth-Fixed (ECEF) coordinates are three-dimensional Cartesian coordinates (x,y,z) derived from this framework. It is an Earth-fixed system because it is a right-handed orthogonal system that rotates with and is connected to the Earth. If the following model can be used to define a three-dimensional Cartesian coordinate system, it is right-handed: The right hand's extended forefinger represents the x-axis' positive orientation. The positive orientation of the y-axis is symbolized by the middle finger of the same hand extended at right angles to the forefinger. The positive orientation of the z-axis is symbolized by the extended thumb of the right hand, which is perpendicular to them both. The y-axis is projected from the geocenter to 90° East longitude in a line perpendicular to the x-axis in the same mean equatorial plane. That is, the y-axis intersects the genuine Earth in the Indian Ocean at the positive end. In any case, they all revolve along the Earth's z-axis, which runs from the geocenter to the International Reference Pole (IRP).

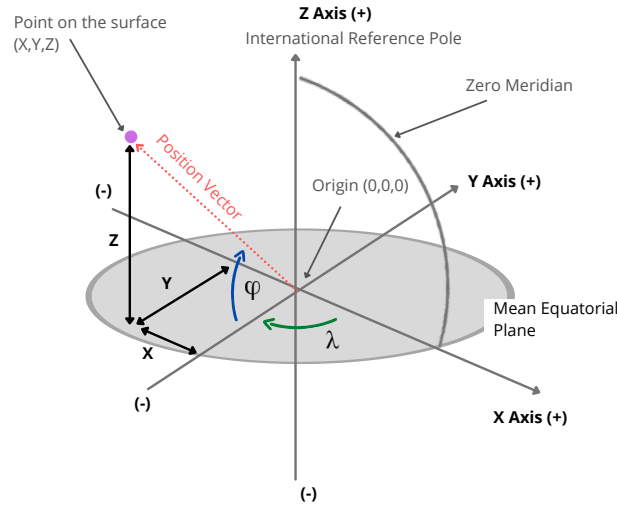


FIGURE 2.16: Three-Dimensional Cartesian Coordinate (ECEF)

The body coordinates systems

The system's origin lies at the center of gravity of the aircraft, which is represented by the subscript "b (body)." The x_b -axis is located in the plane of symmetry of the aircraft and extends from the nose. The z_b -axis is parallel to the x_b -axis. The y_b -axis is pointed out of the aircraft's right wing. The x_b -axis of the aircraft is parallel to the aircraft's longitudinal axis. The y_b -axis is commonly referred to as the lateral axis, whereas the z_b -axis is referred to as the normal axis. The roll, pitch, and yaw are the rotational components of x_b, y_b, z_b (Ruijgrok, 2009).

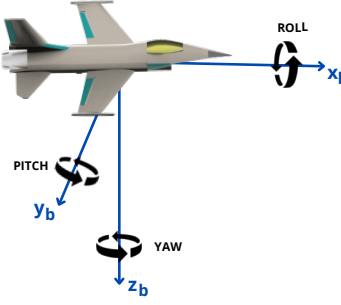


FIGURE 2.17: Body coordintes systems of aircraft

2.8.2 Flight-path angle

The angle between the flight path vector and the x-axes is known as the flight path angle (γ). The longitudinal of the x_b body coordinate system aircraft and flight path vector is known as the angle of attack (AOA). The angle of attack (AOA) is the difference between the pitch angle and the flight path angle. when the angle of the flight path is measured in relation to the atmosphere.because of the relationship of pitch angle, AOA and flight path angle. Pitch angle is angle between x_b body coordinate system and x-axes.

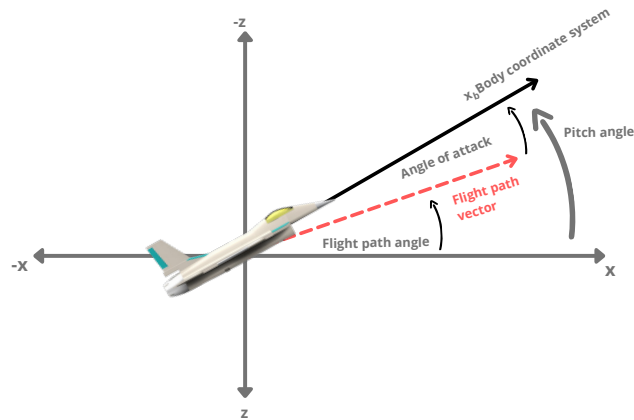


FIGURE 2.18: Definition of flight-path angle

2.8.3 Heading angle

The heading of an aircraft in navigation is the compass direction in which the ship's bow or nose is pointed. Due to gravity, heading, also known as yaw or azimuth, is one of the three rotational degrees of freedom naturally determined for land, sea, and air navigation. The orientation about the vertical direction vector is referred to as heading (where vertical is defined as usual to the reference ellipsoid). The crosswind is responsible for the drift angle—the angle between the aircraft heading and the trajectory in degrees. The pilot adjusts for the crosswind impact during the approach to landing by slipping or altering heading by an equivalent to the drift angle. For instance (figure: 2.19), the track angle is pointing north due to a wind direction that causes the body position coordinate system or heading angle to alter to stay on track. As a result, the track angle and heading angle are integrated to create a drift angle.

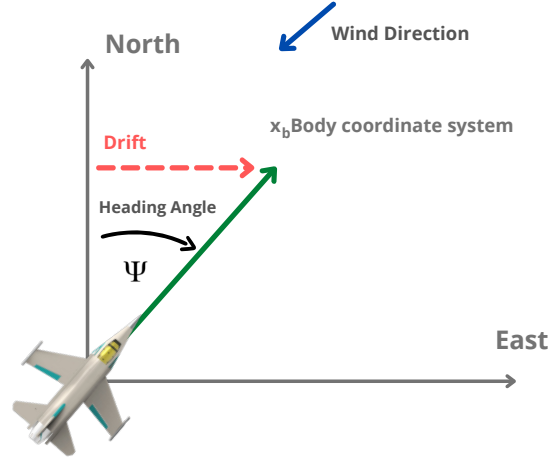


FIGURE 2.19: Definition of heading angle

2.8.4 Coefficient Lift

Airfoil is a phrase used to describe the cross-sectional form of an item that causes an aerodynamic force when propelled through a stream of air. Airfoils are used on aircraft as wings or propeller blades to provide lift and thrust. Both of these forces are generated in the opposite direction of the airflow. Drag occurs due to the generating of lift or thrust and acts in the same direction as the airflow (Anderson & Hughes, 2009). Tailplanes, fins, winglets, and rotary rotor blades are examples of other airfoil surfaces. Ailerons, elevators, and rudders are examples of control surfaces designed to contribute to a wing's entire airfoil section.

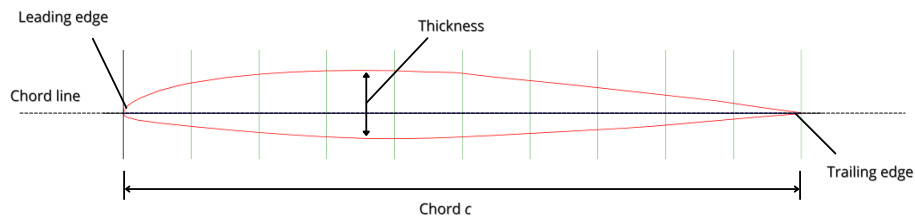


FIGURE 2.20: Airfoil of Boeing 737 MIDSPAN AIRFOIL (b737c-il). Source: (Tools, 27 May 2021).

Figure 2.20 shows an airfoil of Boeing 737. The leading edge and trailing edge are the most forward and backward locations. The chord line of the airfoil is the straight line connecting the leading edge and trailing edge, and chord c is the exact distance between the leading edge and trailing edge measured along the chord line. The thickness is measured perpendicular to the chord line and is the ratio between the upper and lower surfaces.

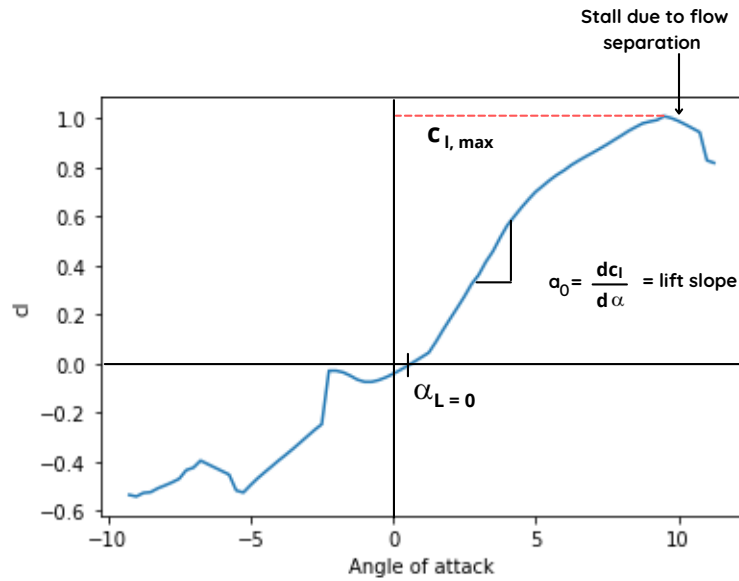


FIGURE 2.21: Schematic of lift coefficient variation with angle of attack for an airfoil Boeing 737 MIDSPAN AIRFOIL (b737c-il).
Source: (Tools, 27 May 2021).

The figure 2.21 shows a representation of coefficient lift (C_l) with the angle of attack (α) for an airfoil. Unless the airfoil is pitched to a negative angle of attack (α), the coefficient lift reduces to zero. The zero-lift angle of attack ($\alpha_{L=0}$) is defined as the (α) value when coefficient lift equals zero (C_l). Characteristic of this airfoil as a function of angle of attack to coefficient lift and from the graph indicate ($\alpha_{l=0}$) zero-lift angle of attack is 0.75° . (C_l) increases also with effects of

(α) till flow separation becomes noticeable. When (C_l) reaches its maximum value, (Cl, max) the airfoil stalls.

Lift for the finite wing:

$$C_L = a(\alpha - \alpha_{L=0}) \quad (2.1)$$

Where:

- a is lift slope;
- α is angle of attack;
- $\alpha_{L=0}$ is zero-lift angle of attack.

The formula (a) as follow:

$$a = \frac{a_0}{1 + (1 + \tau)} \left(\frac{a_0}{\pi AR} \right) \quad (2.2)$$

Where:

- a_0 is lift slope;
- τ is function of Fourier coefficient;
- AR is aspect ratio.

2.8.5 Coefficient Drag

Friction, pressure, and generated drag all contribute to the drag coefficient. The friction component is linked to the establishment of boundary layers, and its magnitude is determined by the fluid properties (i.e., viscosity). The pressure component is caused by the pressure differential between the profile's leading and trailing edges (Anderson & Hughes, 2009). The drag of an airplane cannot be calculated as the simple sum of the drag on each component. For example, drag is usually more significant for a wing-body combination than the sum of the independent drag forces on the wing and the body, resulting in an additional drag component known as

interference drag. Therefore, the simple modification for the complete aircraft will be discussed in this section.

For determine total drag of finite wing:

$$C_D = c_{d,0} + \frac{C_L^2}{\pi e AR} \quad (2.3)$$

Where:

- C_D is the total drag coefficient for the aircraft;
- $c_{d,0}$ is the parasite drag coefficient at at zero lift;
- e is Oswald efficiency factor;
- C_L is a coefficient finite wing.

the formula (e) as follow:

$$e = 1.78(1 - 0.045AR^{0.68}) - 0.64 \quad (2.4)$$

2.8.6 The Atmosphere

The atmosphere is the natural layer that surrounds the Earth. Earth's gravitational attraction keeps it close to the planet's surface. This gaseous combination is known as air. Because the Earth spins on its axis and the surface temperature is higher at the equator than at the poles, the atmosphere reaches the equator's space further than at the poles. As the airplanes climb higher in height, the density of the air decreases. The troposphere, stratosphere, mesopause, and thermosphere are the four layers of Earth. The troposphere is the atmosphere's lowest layer, and it is in this layer, weather and the local condition of temperature, pressure, density, and wind occur. The troposphere stretches from roughly 8 km at the poles to about 17 km at the equator. At the height of about 11 km, the temperature drops from 15°C at sea level to -56°C at the tropopause. The stratosphere has a constant temperature of -56°C up to a height of about 20 kilometers in this layer known as the lower stratosphere. The temperature rises to a high of 0°C at an altitude of 50 kilometers above 20 kilometers in the high stratosphere. As the temperature

drops from the stratopause to an altitude of 90 km in the mesosphere, it reaches a minimum of roughly -90°C at the mesopause. The atmosphere's temperature proliferates with increasing altitude until it reaches 500 km, at which point it is referred to as exospheric temperature (Ruijgrok, 2009).



FIGURE 2.22: Layers of Earth's atmosphere.

The ISA mathematical model separates the atmosphere into layers based on a linear relationship between absolute temperature (T) and geopotential height (h). The modification to geometric height (altitude above mean sea level) that compensates for gravity fluctuation with latitude and altitude is known as geopotential height or geopotential altitude. As a result, it is a "gravitational height." Thermodynamic temperature is a measure of absolute temperature and one of the thermodynamics' main parameters. The essential physical feature that imparts stuff with a temperature transferred kinetic energy owing to atomic movement, starting with a thermodynamic thermometer of zero. The Kelvin scale is used in science to quantify thermodynamic temperature, and the kelvin is the unit of measurement

(unit symbol: K). A temperature of 295 K, which is equal to 21.85°C and 71.33°F, is considered pleasant. The International Standard Atmosphere (ISA) is a model for airplane instrument standardization. It was created to give a standard reference for temperature and pressure, including tables of values for various elevations.

The standard sea level pressure/temperature in the ISA model is 101325 and (15°C). The temperature will decline at a conventional lapse rate when air pressure drops with altitude. The equation of temperature in the troposphere as follow:

$$T = T_0 + \lambda(H - H_0) \quad (2.5)$$

Where:

- T is temperature at a certain altitude;
- T_0 is the reference temperature at sea level 15°C
- H is altitude at a certain altitude;
- H_0 is the reference altitude zero.

$\lambda = \frac{dT}{dH}$ is the temperature gradient and T_0 is the temperature at altitude H_0 . The temperature gradient for each layer is different, which is shown in the following table:

Geopotential Height (Km)	\ λ	Value (K/m)	Layer
0 - 12	dT/dH	-0.0065	Troposphere
12 - 20	dT/dH	0	Tropopause
above 20	dT/dH	0.001	Stratosphere

TABLE 2.21: Temperature gradient λ at certain altitude

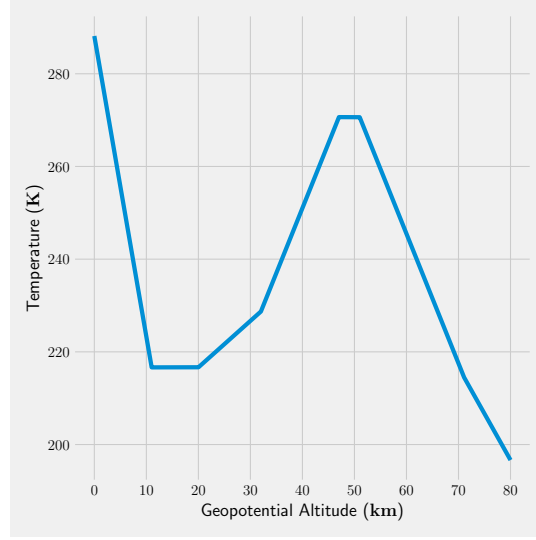


FIGURE 2.23: International Standard Atmosphere for temperature effect of geopotential altitude

The equation to determine pressure (P) at certain a geopotential altitude (H) in the layer troposphere, as follow:

$$P = P_0 \left(1 + \frac{\lambda(H)}{T_0} \right)^{-\frac{g_0}{R\lambda}} \quad (2.6)$$

Where:

- P is Pressure at a certain altitude;
- P_0 is the reference pressure at sea level 101325;
- g_0 is acceleration of gravity at sea level with 9.80665 m/s²;
- R is the spesific gas constant of air from relationship $R = \frac{R_a}{M} = 287.05 \text{ m}^2/\text{s}^2 \text{ K}$;
- T_0 is the temperature at 288.15 K.

The equation to determine pressure (P) at geopotential altitude 11 000 (m) - 20 000 (m) (H_s) in the layer lower stratosphere, as follow:

$$P = (P_s) e^{\left(-\frac{g_0}{R(T_s)} \right) (H - H_s)} \quad (2.7)$$

Where:

- P is Pressure at a certain altitude;
- H_s is geopotential altitude at 11 000 (m);
- P_s is the reference pressure geopotential altitude at 11 000 (m);
- T_s is the temperature geopotential altitude at 11 000 (m).

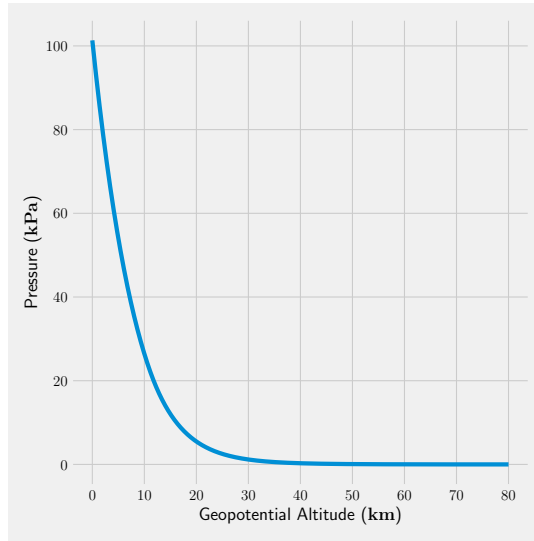


FIGURE 2.24: International Standard Atmosphere for pressure effect of geopotential altitude

The equation to determine density (ρ) at certain a geopotential altitude (H) in the upper troposphere, as follows:

$$\rho = \rho_0 \left(1 + \frac{\lambda(H)}{T_0} \right)^{-\frac{g_0}{R\lambda} + 1} \quad (2.8)$$

Where:

- ρ is density at a certain geopotential altitude;
- ρ_0 is the reference density at sea level 1.225 kg/m³.

The equation to determine density (ρ) at geopotential altitude 11 000 (m) - 20 000 (m) (H_s) in the layer lower stratosphere, as follow:

$$\rho = (\rho_s) e^{\left(-\frac{g_0}{R(T_s)}\right)(H-H_s)} \quad (2.9)$$

Where:

- ρ is Pressure at a certain altitude;
- H_s is geopotential altitude at 11 000 (m);
- ρ_s is the reference density geopotential altitude at 11 000 (m);
- T_s is the temperature geopotential altitude at 11 000 (m).

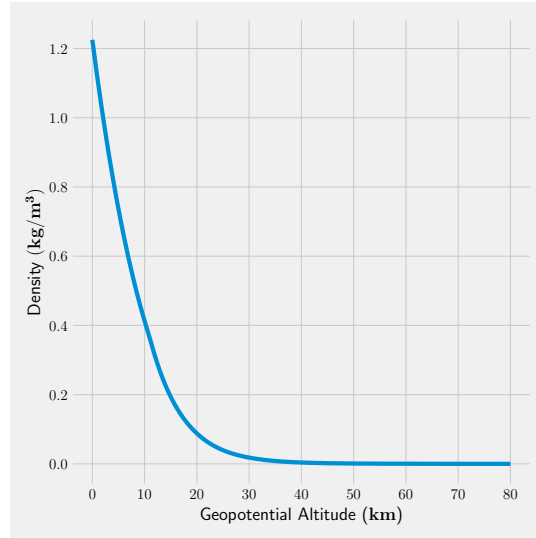


FIGURE 2.25: International Standard Atmosphere for density effect of geopotential altitude

2.8.7 Gravitation

Every aircraft's gravitational force changes as it rises in altitude. Because pressure can be easily detected with a pitot tube, planes implement the hydrostatic equation to estimate height or altitude. So airplanes use a pitot tube to determine pressure, which they can then input into the equation and solve for height. Gravity, on

the other hand, is not the same at different heights and varies with altitude. An airplane's ability to sense gravity in the air is challenging. As a result, geopotential altitude is commonly measured by airplanes.

The several concepts of height are acquainted, as are the changes in gravity-induced acceleration with height. For a given absolute height, the gravitational acceleration at sea level is (g_0), and the local gravitational constant is (g). For the acceleration of gravity at the Earth's surface, using calculation as follow (Ruijgrok, 2009):

$$g = \frac{uM_e}{(R_e)^2} - (\omega_e)^2 R_e = 9.827 - 0.034 = 9.793 \text{m/s}^2 \quad (2.10)$$

- u is a proportionality factor (universal gravitational constant) with $6.67 \times 10^{-11} \text{ m}^3 \text{kg}^{-1} \text{s}^{-2}$;
- M_e is the mass of the Earth with $5.8 \times 10^{24} \text{ kg}$;
- R_e is radius of Earth with $6.371 \times 10^6 \text{ m}$;
- ω_e is the Earth's angular velocity with $7.29 \times 10^{-5} \text{ s}^{-1}$.

The following variable of g develops significantly to 9.827 m/s^2 at the Poles 90° as the centrifugal force varies with latitude. Geographic latitude the sea-level acceleration of gravity at 45° , as follow:

$$g_0 = \frac{uM_e}{(R_e)^2} - (\omega_e)^2 R_e \cos^2 \theta = 9.827 - 0.034 \times 0.5 = 9.810 \text{m/s}^2 \quad (2.11)$$

, (g_0) and geometric altitude (h_g) is as follows:

$$g = g_0 \left(\frac{R_e}{R_e + h_g} \right)^2 \quad (2.12)$$

Where:

- g_0 is acceleration of gravity at sea level with 9.80665 m/s^2 ;
- R_e is radius of Earth with 6371 km ;

PREDICTION OF AIRCRAFT CRASH LANDING SITE FROM ADS-B DATA USING MONTE CARLO METHOD

- h_g is geometric altitude, the altitude as measured from the mean sea level.

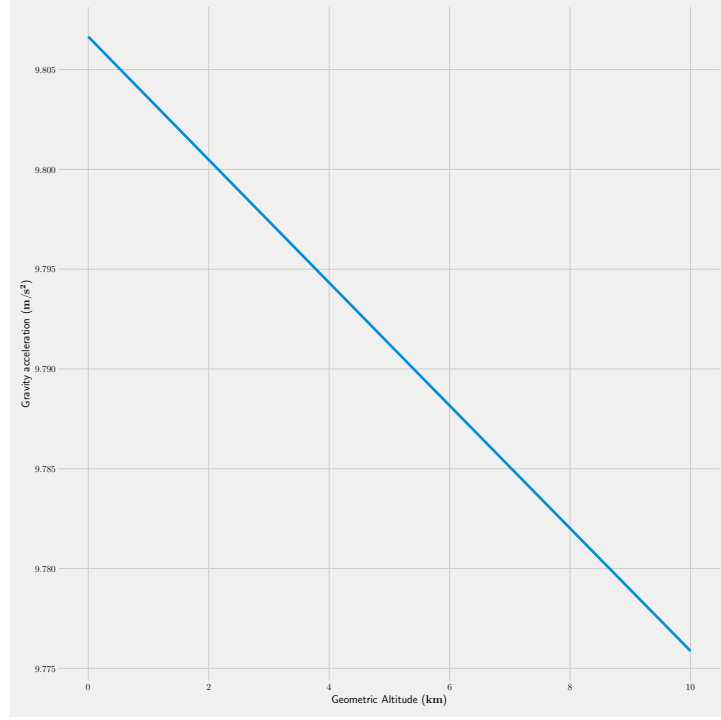


FIGURE 2.26: Gravity acceleration effect of geometric altitude

The impact of geometric altitudes on gravity acceleration is shown in the figure 2.26, where increasing altitude decreases gravitational acceleration at a distance of 0 to 10 km.

The altitude as measured from mean sea level is known as geometric altitude (h_g). An intermittent fluid's hydrostatic equation is:

$$P = \rho g h_g \quad (2.13)$$

where:

- P is hydrostatic pressure (Pa);
- ρ is fluid density (kg/m³);
- g is acceleration (m/s²) due to gravity corresponding to the geometric altitude (h_g).

The geometric altitude adjusted for gravity is called geopotential altitude (H). The reference for the adjustment is the Earth's mean sea level. to determine the equation, as follows:

$$P = \rho g_0 H \quad (2.14)$$

The correlation between the two hydrostatic equations, then derived using the two hydrostatic equations for geometric altitude (h_g) and geopotential altitude (H) are related in the following way:

$$h_g = \frac{R_e H}{R_e - H} \quad (2.15)$$

$$H = \frac{R_e H}{R_e + h_g} \quad (2.16)$$

2.9 Monte Carlo Simulation

Monte Carlo simulation is a computerized statistical methodology that helps people to account for probability in predictive forecasting, decision making, and multiple uncertainty simulation. Scientists working on the atomic bomb were the first to use the procedure, named Monte Carlo, the Monaco resort town known for its casinos. Monte Carlo simulation has been used to model many physical and mental structures since its implementation during World War II. For any given course of action, the Monte Carlo simulation provides the decision-maker with a set of potential possibilities and the probabilities that they will happen. It describes the significant results of going for a break and the most cautious statement to all potential outcomes for intermediate decisions.

The uncertainty distribution for each variable and an equation for calculating the desired quantity are inputs to Monte Carlo simulations for uncertainty propagation. The required amount is then computed by selecting at random from the input variables' defined uncertainty distributions. This computation is then performed several times, each time with different random drawings. The computed value's uncertainty distribution is derived directly from the many random trials. Monte Carlo uncertainty propagation benefits from being simple to understand while also accommodating a wide range of uncertainty distributions.

2.9.1 Normal Distribution

The theoretical equivalent of the mean (μ) and variance (σ^2) of the frequency distribution are the mean (\bar{x}) and variance (s^2) of the random variable X and its distribution. The distribution's dispersion variance (variability) and the position of the center are both defined by the mean. The mean or average (μ) is determined by:

$$(\text{Discrete distribution}) \implies \mu = \sum x_j f(x_j) \quad (2.17a)$$

$$(\text{Continuous distribution}) \implies \mu = \int_{-\infty}^{\infty} x f(x) dx \quad (2.17b)$$

The variance (σ^2) are as follows:

$$(\text{Discrete distribution}) \implies \sigma^2 = \sum (x_j - \mu)^2 f(x_j) \quad (2.18a)$$

$$(\text{Continuous distribution}) \implies \sigma^2 = \int_{-\infty}^{\infty} (x - \mu)^2 f(x) dx \quad (2.18b)$$

The standard deviation of X and its function is (σ) (the positive square root of (σ^2)). In both equations, (f) represents the probability function or density, respectively.

The mean (μ), which is frequently denoted by E (X), gives the expected value of X. It denotes the predicted average value of X across several trials. Parameters, such as (μ) and (σ^2), are numbers that quantify some properties of a distribution. The two most essential ones are (μ) and (σ^2).

$$\text{From equation 2.20, as we can see: } \implies \sigma^2 > 0 \quad (2.19)$$

(Expect a discrete "distribution" with only one possible value, resulting in ($\sigma^2 = 0$)). We assume that (μ) and (σ^2) exist (are finite), and so is the case for almost all effective distributions in applications.

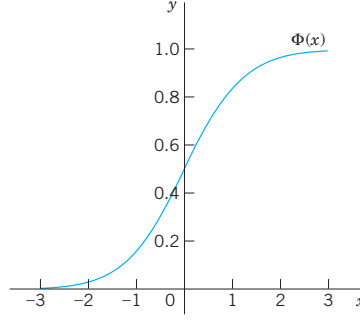


FIGURE 2.27: Example of distribution function (Kreyszig, 2009)

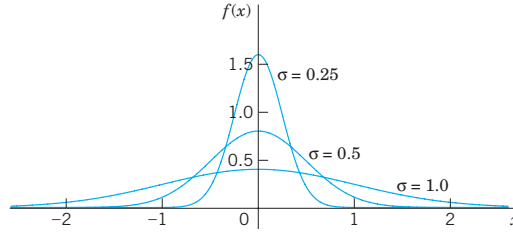


FIGURE 2.28: Example of normal distribution (Kreyszig, 2009)

2.9.2 Error Propagation Using Monte Carlo Simulation

The concept of Monte Carlo error propagation is to select from known initial conditions randomly. In this thesis, the initial conditions used from ADS-B data, such as variable velocity and initial position of aircraft, perform basic calculations from Newton's second law theory. Then the calculated results are entered into the table to be one point from a random initial condition but are parameterized using the standard deviation. Repeat the method as many times as needed to get a more precise probability. The average and standard deviation can measure the calculation of the number of points. The mean of the sample answers is the central value, and the standard deviation is the uncertainty (Toggerson, 2021).



FIGURE 2.29: Step of Monte Carlo Simulation

The initial conditions for the normal distribution are formed by an infinite set of values derived from potential observations of continuous variables such as speed, altitude, heading angle, flight-path angle.

- The mean (average) μ ;
- The standard deviation σ .

The mean (symbol) calculates the average of each variable in ADS-B, which is required as an initial condition. The equation of the mean is as follows:

$$\mu = \frac{1}{n} \sum_{i=1}^n a_i = \frac{a_1 + a_2 + a_3 \cdots + a_n}{n} \quad (2.20)$$

The probability distribution's standard deviation is the same as the random variable that has the distribution. The standard deviation does not apply to all random variables. If the distribution has infinitely, the standard deviation may not exist because the integral may not converge. Although the normal distribution has an infinite tail, the mean and standard deviation exists because the tail drops fast. The equation of the standard deviation:

$$\sigma = \sqrt{\frac{1}{n-1} \sum_{i=1}^n (a_i - \bar{a})^2} \quad (2.21)$$

2.10 Joint Density Function

Joint Density Function (JDF) is a technique for estimating an unknown probability density function from a set of data. To comprehend Joint Density Function

JDF, part of the data is first displayed as a histogram, since histogram plots give a straightforward method to view probability distributions and will be extremely beneficial in comprehending fine estimates of the fundamental Joint Density Function (JDF) (blog on science, 2020).

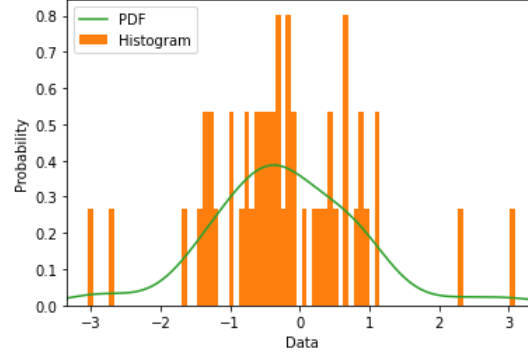


FIGURE 2.30: Example of plot difference between histogram and Probability Density Function (PDF)

In one variable condition, Joint Density Function (JDF) is quite simple. Assuming a set of (N) samples $(x_i = x_1, x_2, \dots, x_N)$, the Joint Density Function (JDF), (\hat{f}) , is described as follows:

$$\hat{f}(x, h) = \frac{1}{N} \sum_{i=1}^N K_h(x - x_i) \quad (2.22)$$

The Joint Density Function (JDF) method entails centering a smooth distributed kernel function at every data point and averaging the results. The Gaussian kernels as follow:

$$K(u) = \frac{1}{\sqrt{2\pi}} \exp\left(-\frac{u^2}{2}\right) \quad (2.23)$$

where:

- $(K_h) = \frac{1}{h} K\left(\frac{u}{h}\right)$ (the scale version of the kernel);
- $(h) = 0.9 \min\left(\hat{\sigma}, \frac{IQR}{1.34}\right) n^{-\frac{1}{5}}$ (the bandwidth of the kernel);
- $(\hat{\sigma})$ = standard deviation of data;

- IQR = Inter Quartile Range of data;
- n = length of data.

The bivariate Joint Density Function (JDF) is defined similarly in the case of two variables, x are tuples (x,y) :

$$\hat{f}(x, H) = \frac{1}{N} \sum_{i=1}^N K_H(X - X_i) \quad (2.24)$$

Where:

- H = a matrix in two variable case;
- $K_H(u) = \det(H)^{-0.5} K(H^{0.5}u)$ (The scale version of the kernel);
- $\det(H)$ = the determinant of the bandwidth Matrix H ;
- $K(u) = \frac{1}{2\pi} \exp(-0.5u^T u)$.

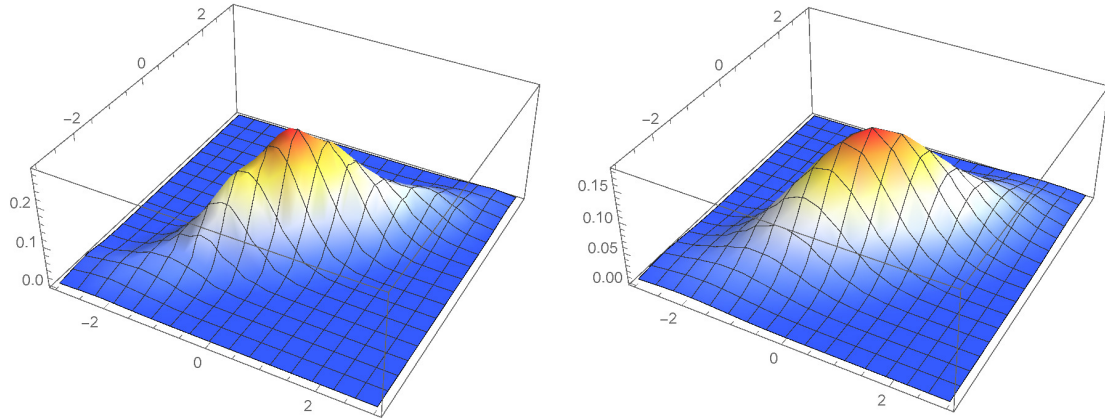


FIGURE 2.31: Example of Joint Density Function (JDF) source:
(blog on science, 2020)

CHAPTER 3

RESEARCH METHODOLOGY

The author will describe the steps to accomplishing the objective in this third chapter. The theoretical framework explains the steps involved in formulating needs and priorities because the data can be collected and processed. The technique for this research is created of many elements.

3.1 Overview

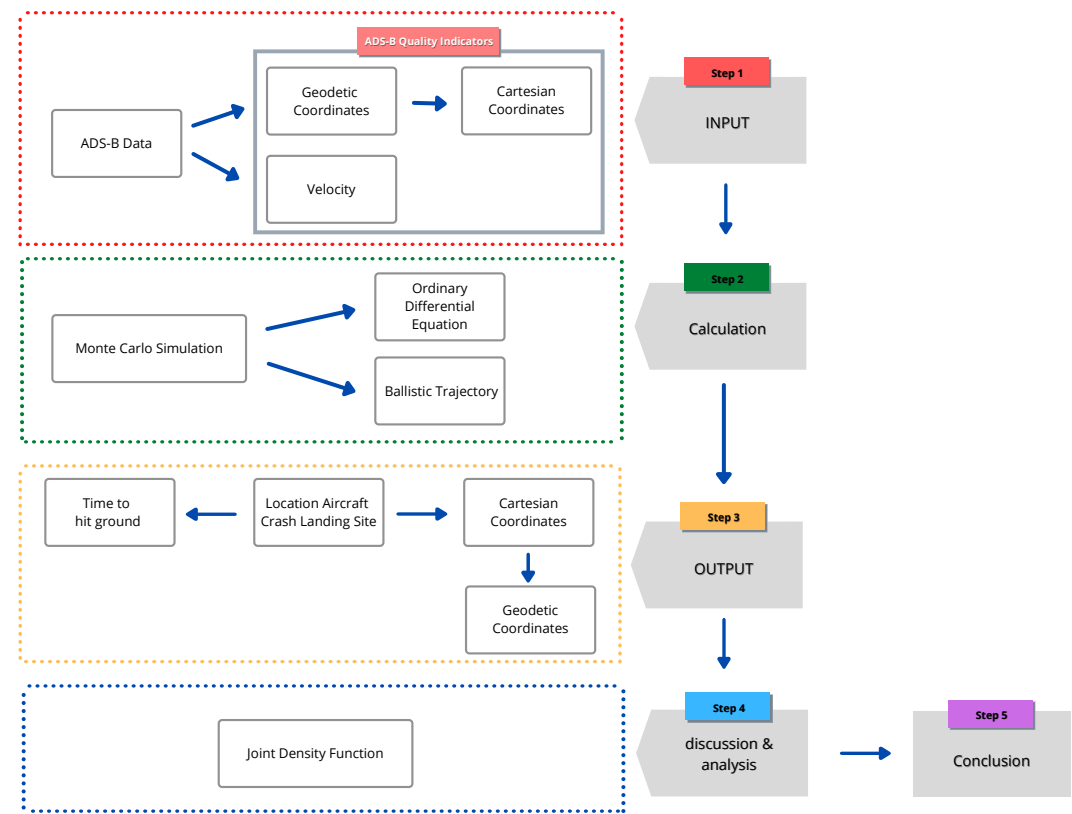


FIGURE 3.1: Reserach Framework

The research framework is divided into five parts: "Input, Calculation Process, and Output, discussion, and analysis, then the final stage, namely the conclusion." The first input step, the data required in the input step, is the last ADS-B data from the aircraft before losing contact with ATC (Air Traffic Control). The types of data variables needed in the ADS-B system are the speed and position that the ADS-B Quality Indicators have checked. Speed and position variables are mandatory inputs in this research process. The second step is the Monte Carlo Simulation. This second part of the phase will calculate the standard deviation, which provides a multiple probability simulation used to estimate the possible outcomes of an uncertain event. The third step is "OUTPUT," at this stage. It will provide the results of the calculations in the second step, namely the probability density function, the location of the aircraft landing location in the form of a time variable to touch the ground, and the discussion and analysis of Cartesian coordinates in the fourth step. It will consider the probability density function of the plane crash landing site.

3.2 Initial state

Initial state input is a variable where the plane is in the initial state (before it is used) and will be the initial state reference for calculation. The data needed as an initial state is from ADS-B data, where the data provided is about the coordinates, speed, weight of aircraft, angle of aircraft performance, which impacts the prediction of the fall of the aircraft and the earth's atmosphere. Variables or initial conditions that have been defined will be input and using Ordinary Differential Equation calculations. The data provided by ADS-B related to locations or coordinates, namely in the form of geodetic coordinates, at this stage, it needs to be converted into cartesian coordinates because the calculations used are in three-axes space or unit vector form.

3.2.1 ADS-B Data

Variable	Last Recorded	Sources
Time	23:31	KNKT Report
Latitude	-5.81346	KNKT Report
Longitude	107.12698	KNKT Report
Altitude (ft)	425 (130 m)	KNKT Report
Ground Speed (kts)	360	KNKT Report
Track Angle	30°	KNKT Report
Pitch Angle	-2°	KNKT Report
Coefficient Drag	0.11	Calculated
Frontal Area (m ²)	11.35	Calculated
Ballistic Coefficient	51.59	Calculated.
Density (kg/m ³)	1.225	ISA Model
Weight (kg)	63 974	KNKT Report

TABLE 3.1: The last recorded ADS-B of Lion Air JT610 (*Aircraft Accident Investigation Report PT. Lion Mentari Airlines Boeing 737-8 (MAX); PK-LQP, 2019*)

ADS-B data sample will be the initial state input using the Lion Air Boeing 737-8 (MAX) plane crash; PK-LQP Tanjung Karawang, Republic of Indonesia West Java, October 29, 2018. the data of ADS-B recorded at 23:31:54 UTC, and the CVR stopped recording, and the target aircraft LNI610 disappeared in ASD.



FIGURE 3.2: The last location of Lion Air (PK-LQP) (*Aircraft Accident Investigation Report PT. Lion Mentari Airlines Boeing 737-8 (MAX); PK-LQP, 2019*)

3.2.2 Convert geodetic coordinates to cartesian coordinates

In concepts x , y , and z , the coordinates of the longitude, latitude, and altitude of a position data. Relationship between two Calculations of the Cartesian coordinates of a point, including longitude, latitude, and altitude (Stelios, 2007). The following is the equation for translating geodetic coordinates into Cartesian coordinates:

$$x = (N + h)(\cos \phi)(\cos \lambda) \quad (3.1)$$

$$y = (N + h)(\cos \phi)(\sin \lambda) \quad (3.2)$$

$$z = (N(1 - e^2) + h)(\sin \phi) \quad (3.3)$$

where:

- N = radius of curvature: $N = \frac{a}{\sqrt{1 - e^2 \sin^2 \phi}}$
- f = flattening: $f = \frac{a - b}{a} = (f = 1/298.257223 = 0.003353 \text{ by WGS84})$
- e = first eccentricity: $e^2 = \frac{a^2 - b^2}{a^2}$
- a = semi-major axis of the ellipse (semi-diameter of the longest axis of a reference ellipsoid called equatorial axis) = (6378137 by WGS84)

- b = semi-minor axis of the ellipse (semi-diameter of the shortest axis of a reference ellipsoid called polar axis) = $a(1-f)$ = (6356752 by WGS84)

3.3 Calculation Development

The first identification to calculate is the implementation of a one-dimensional free body diagram that identifies the body using the Newton Second Law as follows:

$$\Sigma \vec{F} = m\vec{a} \quad (3.4)$$

The weight (W) is defined as the mass of the body (m) divided by the gravitational acceleration (a), (g) which is 9.8 meters per square second on the earth's surface. Free falling refers to an object that moves only force acting of gravity.

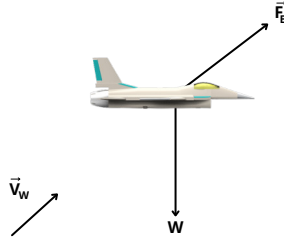


FIGURE 3.3: Free Body Diagram

3.3.1 Analytical approach - one dimensional

This is Newton's Second Law with the force acting on the body on the right side and left side of the equation resulting acceleration. Density, gravity, and a drag force proportional to velocity square are all taken into consideration in analytical formulas for the one-dimensional behavior of a ballistic trajectory. Vertical motion is one-dimensional, with drag proportional to velocity square (v^2), with the wind impact ignored by assuming constant gravity (g) and mass (s). The one-dimensional equation is as follows:

$$\Sigma F = m \frac{d^2 z}{dt^2} \quad (3.5)$$

$$\frac{1}{2} \rho v^2 S C_d - mg = m \frac{d^2 z}{dt^2} \quad (3.6)$$

$$m \frac{d^2 z}{dt^2} = \frac{1}{2} \rho v^2 \frac{S}{m} C_d - g \quad (3.7)$$

Define,

$$v_z \triangleq \frac{dz}{dt} \quad (3.8)$$

$$\frac{dz}{dt} = \frac{1}{2} \rho v^2 \frac{S}{m} C_d - g \quad (3.9)$$

$$v_z = \frac{dz}{dt} \quad (3.10)$$

Where:

- ρ is a density level with the reference from International Standard Atmosphere (ISA);
- S is a area of the body during vertical movement;
- C_d is a coefficient drag;
- m is mass of the aircraft;
- g is gravity on Earth.

The area on the body in vertical motion is assumed to be fuselage of the frontal area (S) of the plane (see figure 3.4) and constant gravity (g) of 9.81 m/s². Based on

the ICAO standard atmosphere and typical initial values of temperature (see figure 2.23), pressure (see figure 2.24), and air density (see figure 2.25) at Mean Sea Level, international standard atmospheric parameters have been measured as a function of geometric and geopotential heights at altitudes ranging from 2000 to 50000 meters (MSL). International Standard Atmosphere (ISA) with (ρ) of 1.225 kg/m^3 .

The drag coefficient is represented in the equation 3.9 in the method $\frac{1}{2}\rho v^2 \frac{S}{m} C_d - g$. The theory of ballistic trajectory will be substituted for the theory of drag coefficient in the equation 3.9, and the ballistic coefficient will be utilized for ballistic trajectory analysis. The following is the equation for the ballistic coefficient:

$$C_B = \frac{m}{C_d S} \quad (3.11)$$

Where:

- C_B is ballistic coefficient;
- m is mass of aircraft;
- C_d is coefficient drag;
- S is frontal area of aircraft.

In ballistic trajectory, it is assumed for the area on the plane using the front of the aircraft. Example of aircraft from Boeing 737-800 (see figure: 3.4).

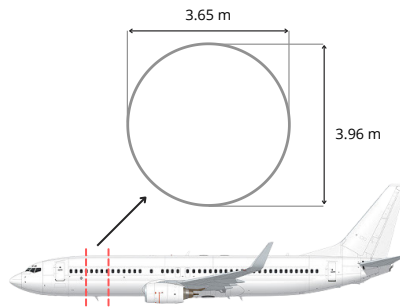


FIGURE 3.4: Frontal area of Boeing 737-800

3.3.2 Numerical approach - three dimensional

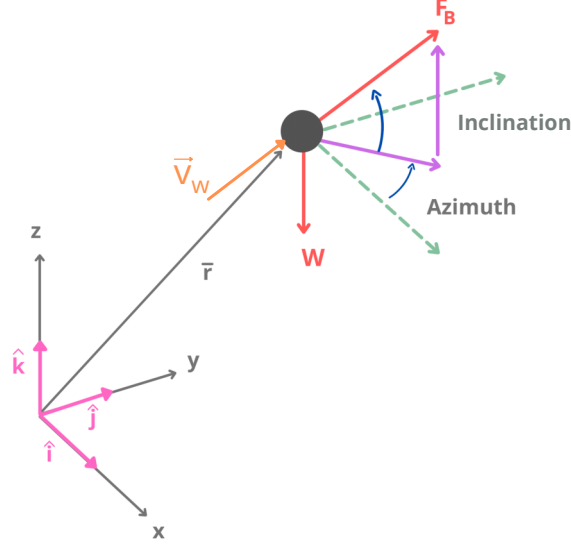


FIGURE 3.5: Free body diagram of three dimensionanl

The schema shows three-dimensional identification in the figure 3.5. The three-dimensional scheme considers the unit vector represented by the symbol $(\hat{i}, \hat{j}, \hat{k})$. The base vector space is usually defined as a unit vector. Linear combinations of unit vectors can be used to describe any vector in space. objects in vector space are affected by wind speed (wind speed symbol) which causes things to form angles called azimuths and meridians. The position of the aircraft is given by:

$$\vec{r} = x\hat{i} + y\hat{j} + z\hat{k} \quad (3.12)$$

The development of calculations from Newton's second law equations is also needed in three-dimensional objects, as follows:

$$m \frac{d^2 \vec{r}}{dt^2} = -\vec{W} + \vec{F}_B \quad (3.13)$$

For weight of the aircraft $(-\vec{W})$ opposite direction of unit vector $(z\hat{k})$ and volve with a diversity of variables $(mg\hat{h})$. (m) is a mass of aircraft that falls against the

earth's gravity (g) and is affected by the unit vector of altitude (\hat{h}). The equation becomes as follows:

$$-\vec{W} = mg\hat{h} \quad (3.14)$$

airspeed ($(V_{TAS})^2$). The density (ρ) at particular a geopotential altitude (H) refers to the International Standard Atmosphere (ISA). The area (S) for the equation in three-dimensional uses the frontal area of the aircraft shown in the figure 3.4. The ballistic trajectory (C_B) is considered as a substitute for the drag coefficient described in equation 3.11. For gravity, the numerical calculation will consider geometric altitude (hg) and radius of Earth. Geometric altitude on a unit vector called (z -axis) in cartesian coordinates and the equation as follows:

$$g = g_0 \left(\frac{R_e}{R_e + z} \right)^2 \quad (3.15)$$

Where:

- g_0 is acceleration of gravity at sea level with 9.80665 m/s^2 ;
- R_e is radius of Earth with 6371 km ;
- z is geometric altitude, the altitude as measured from the mean sea level.

True airspeed ($(V_{TAS})^2$) is affected by the unit vector of wind speed (\vec{V}_W), unit vector of ground speed (\vec{V}_{GND}), and calculation in the unit vector affected by the speed in the unit vector (\vec{V}_{TAS}). The equation becomes:

$$\vec{V}_{TAS} = \vec{V}_{GND} - \vec{V}_W \quad (3.16)$$

- For unit vector of wind speed: $\vec{V}_W = \vec{V}_{Wx}\hat{i} + \vec{V}_{Wy}\hat{j} + \vec{V}_{Wz}\hat{k}$
- For unit vector of ground speed: $\vec{V}_{GND} = \frac{dx}{dt}\hat{i} + \frac{dy}{dt}\hat{j} + \frac{dz}{dt}\hat{k}$

The equation of true airspeed (\vec{V}_{TAS}) in the unit vector becomes:

$$\vec{V}_{TAS} = \left(\frac{dx}{dt} - V_{wx} \right) \hat{i} + \left(\frac{dy}{dt} - V_{wy} \right) \hat{j} + \left(\frac{dz}{dt} - V_{wz} \right) \hat{k} \quad (3.17)$$

The equation of aircraft's force \vec{F}_B in three-dimensional:

$$\vec{F}_B = \frac{1}{2}\rho SC_B(V_{TAS})\vec{V}_{TAS} \quad (3.18)$$

The final equation of Newton's second law in three-dimensional is as follows:

$$\frac{d^2x}{dt^2} = g - \frac{1}{2}\frac{\rho SC_B}{m} \left(\frac{dx}{dt} - V_{wx} \right) \vec{V}_{TAS} \quad (3.19a)$$

$$\frac{d^2y}{dt^2} = g - \frac{1}{2}\frac{\rho SC_B}{m} \left(\frac{dy}{dt} - V_{wy} \right) \vec{V}_{TAS} \quad (3.19b)$$

$$\frac{d^2z}{dt^2} = g - \frac{1}{2}\frac{\rho SC_B}{m} \left(\frac{dz}{dt} - V_{wz} \right) \vec{V}_{TAS} \quad (3.19c)$$

Equation 3.13 is the second order of ordinary differential equations (ODEs), which in this thesis is solved numerically with `scipy solve_ivp` and uses an "event," which considers when an object falls to the ground or when its altitude reaches 0 ($z = 0$).

3.4 Final state

This thesis research aims to find the probability of the location of the plane crash, which is at the output stage. The calculations at step two use Ordinary Differential Equations (ODEs) and the Monte Carlo Method theory. The output stage produces two variables, and the first is time to hit the ground. Time to hit the ground is the estimated travel time of the aircraft when at the initial state point it reaches the altitude zero point ($z=0$). The second output variable is the plane's coordinates at the time of the ground hit.

3.4.1 Cartesian Coordinates systems

One of the calculations in the second step is to use unit vectors or Cartesian coordinates systems, which produce locations in the form (x, y, z) on the earth. Because regulations in the aviation industry use variable geodetic coordinates, the

value must convert from Cartesian coordinates to geodetic coordinates (Gerdan & Deakin, 1999). Convert cartesian coordinates to geodetic coordinates as follow:

$$\tan \lambda = \frac{y}{x} \quad (3.20)$$

$$\tan \phi = \frac{z + Ne^2 \sin \phi}{p} \quad (3.21)$$

$$h = \frac{p}{\cos \phi} - v \quad (3.22)$$

where p is the perpendicular distance from the rotational axis:

$$p = \sqrt{x^2 + y^2} \quad (3.23)$$

3.4.2 Time to hit ground

The category prediction in this study is time to hit the ground, which is where the aircraft travel time is in the initial state position to the ground or final state considering the earth's atmosphere, the drag of aircraft, angle of the aircraft, wind speed, etc. This travel time will be provided by calculations using Ordinary Differential Equations (ODEs).

the aircraft that affects the earth's ground. where the variables shown in the 3D illustration of simulation are as follows:

- x_i, y with green color are the inertia coordinate system of the aircraft;
- x_i, y_i, z_i with red color are inertia reference axes;
- x_i, y_i, z_i with black color, which is the origin of coordinates system point on the inertia earth's surface;
- V_W is a wind direction in simulation;
- Altitude is the height from between the center of gravity of the aircraft to the ground surface;
- F_B is the force body of aircraft in the simulation;
- Azimuth (φ) is the angle of aircraft generated by the primary control surface (rudder) called yaw. the angle of azimuth (φ) which is between x_i and x_b or can be called the heading angle (yaw angle);
- Inclination is the angle generated by the primary control surface (elevator) called pitch. The angle of inclination (δ) between F_B and x_b can be called the flight-path angle (pitch angle).

4.2 Simulation without uncertainty

In this study, the simulation stage will be different from the initial conditions, divided into five simulations with different initial conditions (see table: 4.1). The initial state of the aircraft includes the last ADS-B data of Lion Air (PK-LQP) (see table: 3.1) and considers wind speed in the second to fifth simulations, but in the first simulation, the wind speed is ignored. The angle of azimuth (φ) was also considered in this study in the second to fifth simulations at the impact of azimuth (φ) angle on-ground location. However, the angle of azimuth (φ) in the first simulation is ignored. The inclination angle will also play a role in the final result of the location on the ground, input in the third and fifth simulations. However, the first, second, and fourth simulations are neglected.

Variable	Simulation				
	1	2	3	4	5
Altitude (m)	130	130	130	1000	1000
Wind Speed (m/s)	0	10	10	10	10
Angle of Azimuth	0°	30°	30°	30°	30°
Angle of Inclination	0°	0°	30°	0°	30°
x-axes (m)	0	0	0	0	0
y-axes (m)	0	0	0	0	0
Time to hit ground (s)	0	0	0	0	0

TABLE 4.1: Simulation without uncertainty.

4.2.1 Simulation without uncertainty case 1

The first simulation uses an altitude of 130 meters with a wind speed of 0 m/s. This simulation does not consider the angle of azimuth ($\varphi = 0^\circ$) and the angle of inclination ($\delta = 0^\circ$).

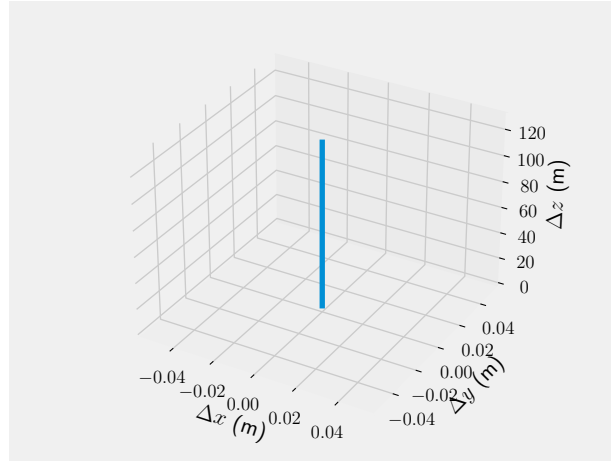


FIGURE 4.2: Result of simulation 1.

In the first simulation using calculations using Ordinary Differential Equation (ODEs) with the plane falling from a height of 130 m to the hit ground or ($z = 0$). Wind speed, angle of azimuth (φ), and angle of inclination are ignored. The result

is that there is no effect on the distance of displacement of x-axes and displacement of y-axes.

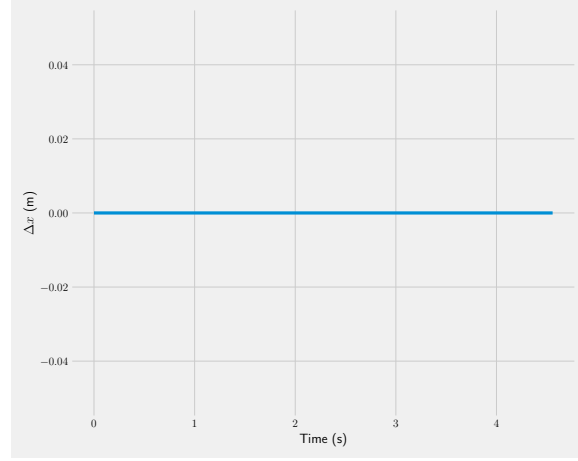


FIGURE 4.3: Result of simulation 1 at displacement x-axis on time.

The result (see figure: 4.3) is that there is no effect of the x-axis displacement distance because the wind speed, (φ) azimuth angle, and inclination angle are ignored, and the aircraft travel time to reach the ground almost 5 seconds.

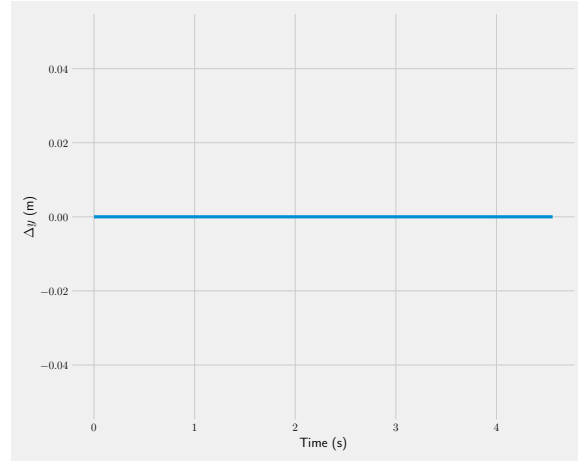


FIGURE 4.4: Result of simulation 1 at displacement y-axis on time.

The result (see figure: 4.4) is that there is no effect of the y-axis displacement distance because the wind speed, (φ) azimuth angle, and inclination angle are ignored, and the aircraft travel time to reach the ground almost 5 seconds.

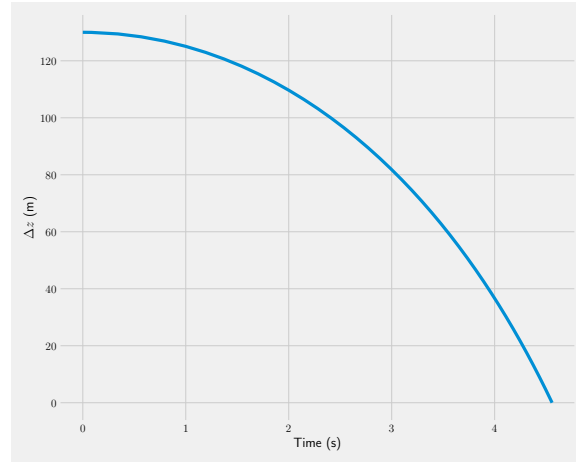


FIGURE 4.5: Result of simulation 1 at displacement z-axis on time.

The initial state of the aircraft at an altitude of 130 m ($z=130$) free fall to the ground until ($z=0$) without any disturbance from wind speed, angle of azimuth (φ), and angle of inclination with a recovery time almost 5 seconds (see figure: 4.5).

Variable	Initial state	Final Condition
Altitude (m)	130	0
Wind Speed (m/s)	10	10
Angle of Azimuth (degree)	0°	
Angle of Inclination (degree)	0°	
x-axes (m)	0	0
y-axes (m)	0	0
Time to hit ground (s)	0	5

TABLE 4.2: Result of simulation 1.

4.2.2 Simulation without uncertainty case 2

The second simulation uses an altitude of 130 meters with a wind speed of 10 m/s. This simulation does consider the angle of azimuth ($\varphi = 30^\circ$) and the angle of inclination ($\delta = 0^\circ$).

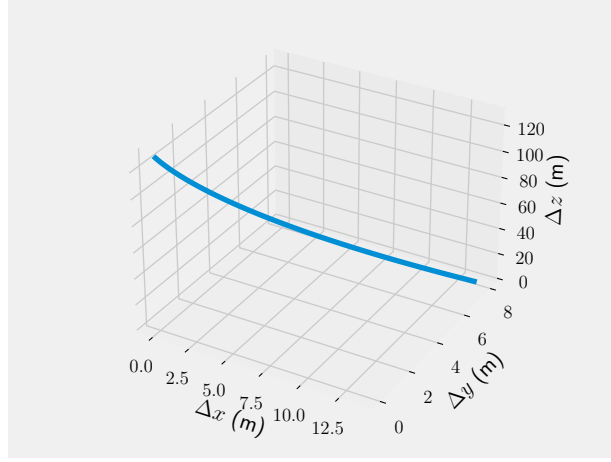


FIGURE 4.6: Result of simulation 2.

In the second simulation using calculations using Ordinary Differential Equation (ODEs) with the plane falling from a height of 130 m ($z = 130$) to the ground or ($z = 0$). The wind speed is at 10 m/s, and the azimuth angle (φ) is (30°). The angle of inclination is neglected. Consequently, the x-axis displacement impact is 14 meters, and the y-axis displacement is 8 meters compared to the initial position.

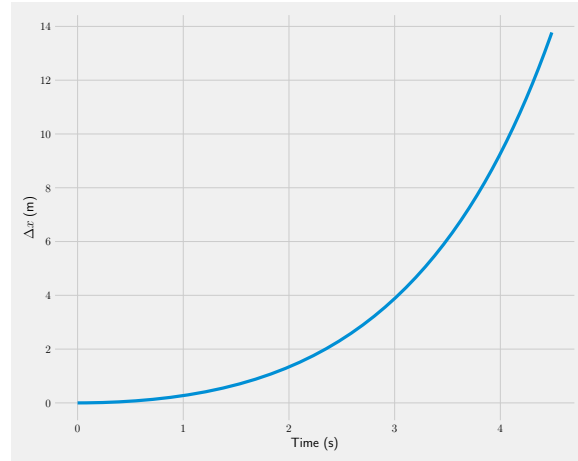


FIGURE 4.7: Result of simulation 2 at displacement x-axis on time.

The result (see figure: 4.7) is 14 meters of the x-axis displacement distance because the wind speed 10 m/s, azimuth angle ($\varphi = 30^\circ$), and inclination angle (0°), and the aircraft travel time to reach the ground in almost 5 seconds.

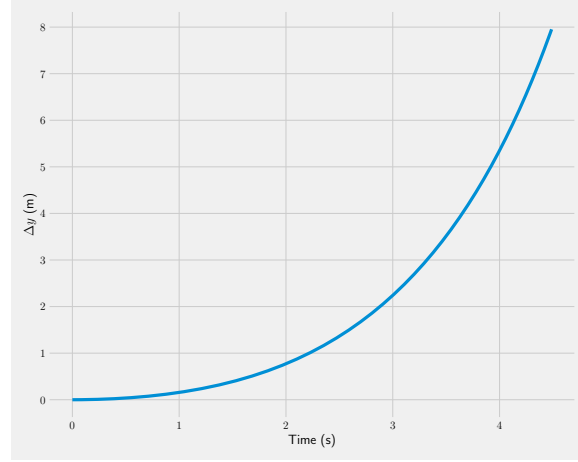


FIGURE 4.8: Result of simulation 2 at displacement y-axis on time.

The result (see figure: 4.8) is 8 meters of the y-axis displacement distance because the wind speed 10 m/s, azimuth angle ($\varphi = 30^\circ$), and inclination angle (0°), and the aircraft travel time to reach the ground in almost 5 seconds.

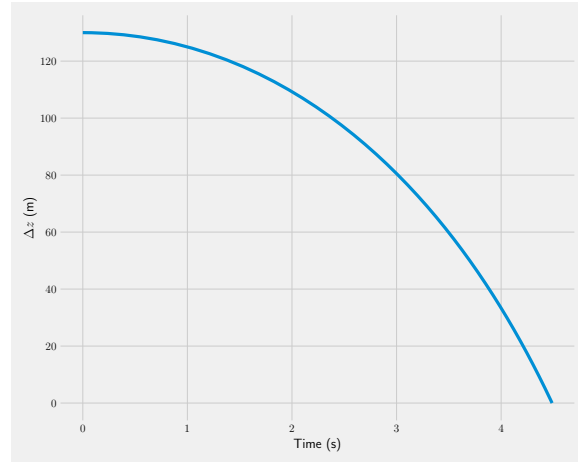


FIGURE 4.9: Result of simulation 2 at displacement z-axis on time.

The aircraft's initial position was a free fall to the earth from an altitude of 130 m ($z=130$) with a wind speed of 10 m/s till altitude ($z=0$). The angles of azimuth ($\varphi = 30^\circ$), inclination ($\delta = 0^\circ$) are calculated in this simulation, and travel time almost 5 seconds to hit the ground (see figure: 4.9).

Variable	Initial state	Final Condition
Altitude (m)	130	0
Wind Speed (m/s)	10	10
Angle of Azimuth (degree)	30°	
Angle of Inclination (degree)	0°	
x-axes (m)	0	14
y-axes (m)	0	8
Time to hit ground (s)	0	5

TABLE 4.3: Result of simulation 2.

4.2.3 Simulation without uncertainty case 3

The third simulation starts at an altitude of 130 meters with a wind speed of 10 meters per second. The angles of azimuth (30°) and inclination (30°) are considered in this simulation.

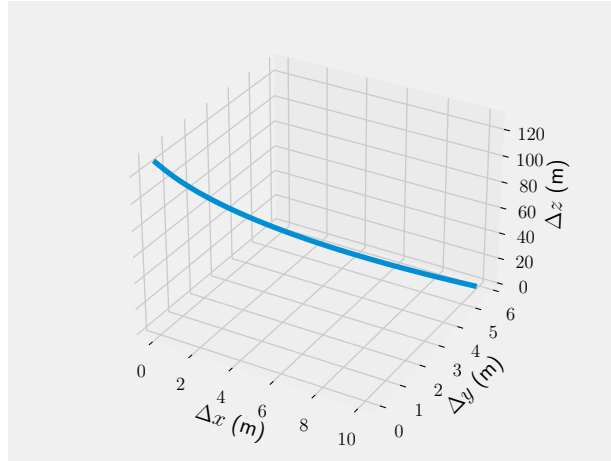


FIGURE 4.10: Result of simulation 3.

In the third simulation using calculations using Ordinary Differential Equation (ODEs) with the plane falling from a height of 130 m ($z = 130$) to the ground or ($z = 0$). The wind speed is at 10 m/s, and the azimuth angle is (30°). The angle of inclination ($\delta = 30^\circ$). Consequently, the x-axis displacement impact is 10 meters,

and the y-axis displacement is 6 meters compared to the initial position (see figure: 4.10).

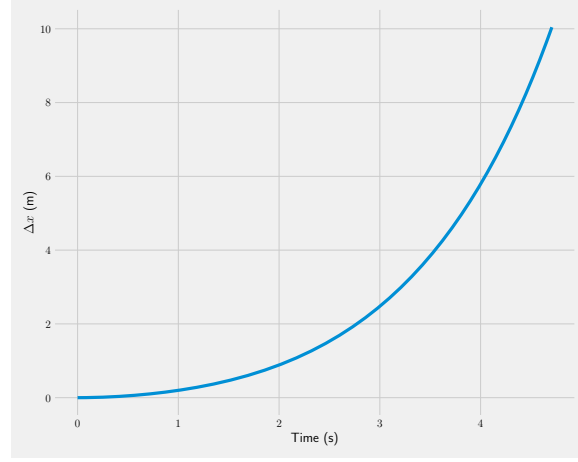


FIGURE 4.11: Result of simulation 3 at displacement x-axis on time.

The result (see figure: 4.11) is 10 meters of the x-axis displacement distance because the wind speed 10 m/s, azimuth angle ($\varphi = 30^\circ$), and inclination angle ($\delta = 30^\circ$), and the aircraft travel time to reach the ground in almost 5 seconds.

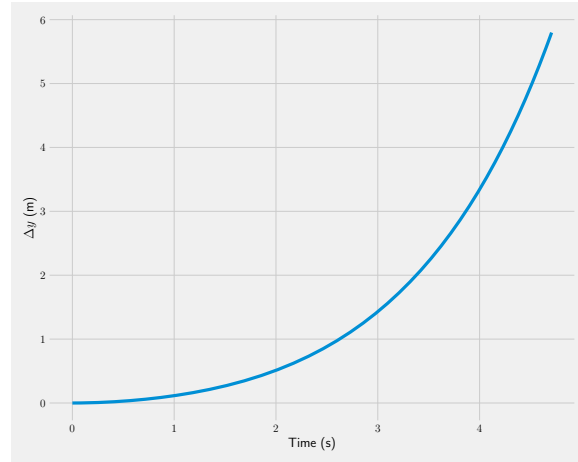


FIGURE 4.12: Result of simulation 3 at displacement y-axis on time.

The result (see figure: 4.12) is 6 meters of the y-axis displacement distance because the wind speed 10 m/s, azimuth angle ($\varphi = 30^\circ$), and inclination angle ($\delta = 30^\circ$), and the aircraft travel time to reach the ground in almost 5 seconds.

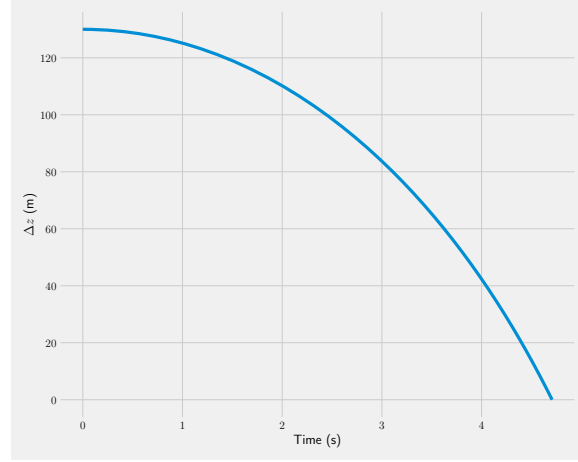


FIGURE 4.13: Result of simulation 3 at displacement z-axis on time.

The aircraft was in free fall to the ground from an altitude of 130 meters ($z=130$) with a wind speed of 10 meters per second until it reached height ($z=0$). This simulation calculates azimuth ($(\varphi) = 30^\circ$), inclination ($(\delta) = 30^\circ$), and travel time of about 5 seconds to hit the ground (see figure: 4.13).

Variable	Initial state	Final Condition
Altitude (m)	130	0
Wind Speed (m/s)	10	10
Angle of Azimuth (degree)	30°	
Angle of Inclination (degree)	30°	
x-axes (m)	0	10
y-axes (m)	0	6
Time to hit ground (s)	0	5

TABLE 4.4: Result of simulation 3.

4.2.4 Simulation without uncertainty case 4

The fourth simulation starts at an altitude of 1000 meters with a wind speed of 10 meters per second. The angles of azimuth ($(\varphi) = 30^\circ$) and inclination ($(\delta) = 0^\circ$) are considered in this simulation.

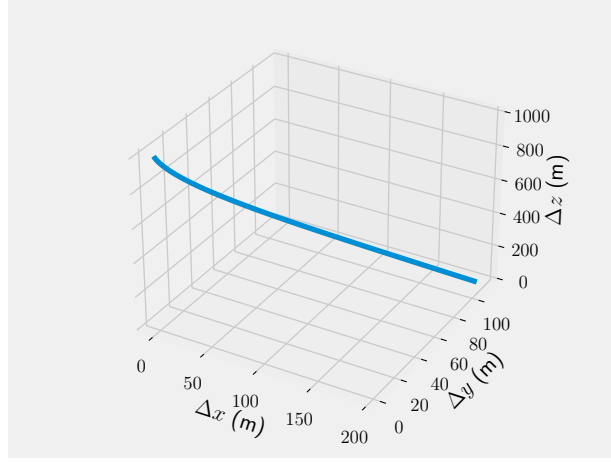


FIGURE 4.14: Result of simulation 4.

In the fourth simulation using calculations using Ordinary Differential Equation (ODEs) with the plane falling from a height of 1000 m ($z = 1000$) to the ground or ($z = 0$). The wind speed is at 10 m/s, and the azimuth angle is ($\varphi = 30^\circ$). The angle of inclination ($\delta = 0^\circ$). Consequently, the x-axis displacement impact is almost 200 meters, and the y-axis displacement is almost 120 meters compared to the initial position (see figure: 4.14).

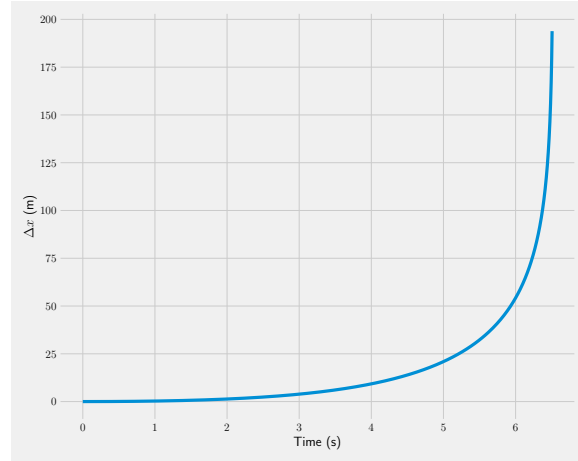


FIGURE 4.15: Result of simulation 4 at displacement x-axis on time.

The result (see figure: 4.15) is almost 200 meters of the x-axis displacement distance because the wind speed 10 m/s, azimuth angle ($\varphi = 30^\circ$), and inclination angle ($\delta = 0^\circ$), and the aircraft travel time to reach the ground in almost 6 seconds.

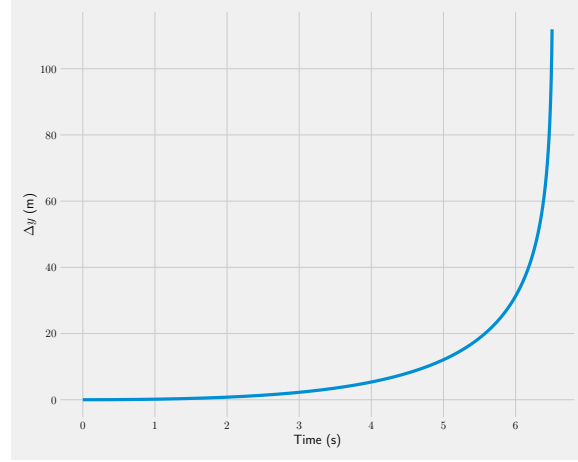


FIGURE 4.16: Result of simulation 4 at displacement y-axis on time.

The result (see figure: 4.16) is almost almost 120 meters of the y-axis displacement distance because the wind speed 10 m/s, azimuth angle ($(\varphi) = 30^\circ$), and inclination angle ($\delta = 0^\circ$), and the aircraft travel time to reach the ground in almost 6 seconds.

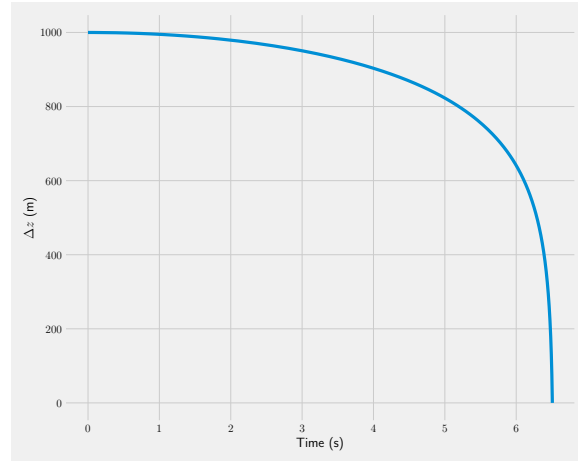


FIGURE 4.17: Result of simulation 4 at displacement z-axis on time.

The aircraft was in free fall to the ground from an altitude of 1000 meters ($z=1000$) with a wind speed of 10 meters per second until it reached height ($z=0$). This simulation calculates azimuth ($(\varphi) = 30^\circ$), inclination ($\delta = 0^\circ$), and travel time of about 6 seconds to hit the ground (see figure: 4.17).

Variable	Initial state	Final Condition
Altitude (m)	1000	0
Wind Speed (m/s)	10	10
Angle of Azimuth (degree)	30°	
Angle of Inclination (degree)	0°	
x-axes (m)	0	almost 200
y-axes (m)	0	almost 120
Time to hit ground (s)	0	6

TABLE 4.5: Result of simulation 4.

4.2.5 Simulation without uncertainty case 5

Altitude 1000 m, Wind speed 10 m/s, Azimuth (φ) 30 degree, inclination (δ) 30 degree. The fifth simulation starts at an altitude of 1000 meters with a wind speed of 10 meters per second. The angles of azimuth ($\varphi = 30^\circ$) and inclination ($\delta = 30^\circ$) are considered in this simulation.

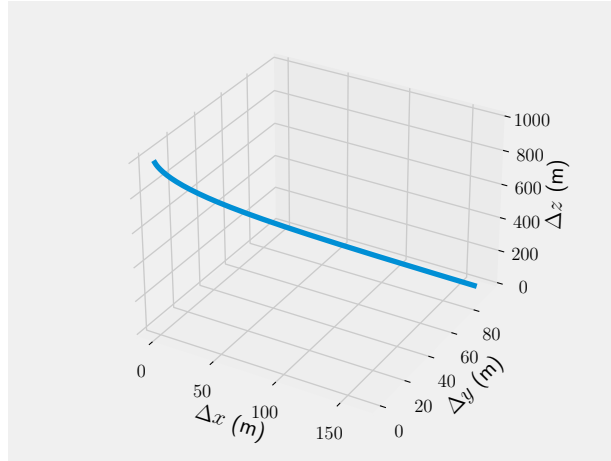


FIGURE 4.18: Result of simulation 5.

In the fifth simulation using calculations using Ordinary Differential Equation (ODEs) with the plane falling from a height of 1000 m ($z = 1000$) to the ground or ($z = 0$). The wind speed is at 10 m/s, and the azimuth angle (φ) is (30°). The angle of inclination ($\delta = 30^\circ$). Consequently, the x-axis displacement impact is

almost 170 meters, and the y-axis displacement is almost 90 meters compared to the initial position (see figure: 4.18).

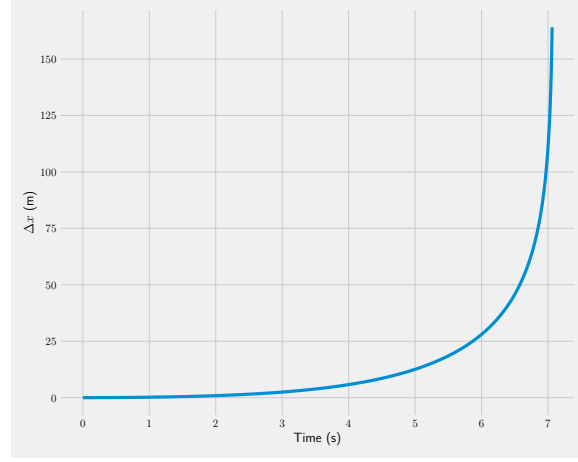


FIGURE 4.19: Result of simulation 5 at displacement x-axis on time.

The result (see figure: 4.19) is almost almost 170 meters of the x-axis displacement distance because the wind speed 10 m/s, azimuth angle ($(\varphi) = 30^\circ$), and inclination angle ($\delta = 30^\circ$), and the aircraft travel time to reach the ground in almost 7 seconds.

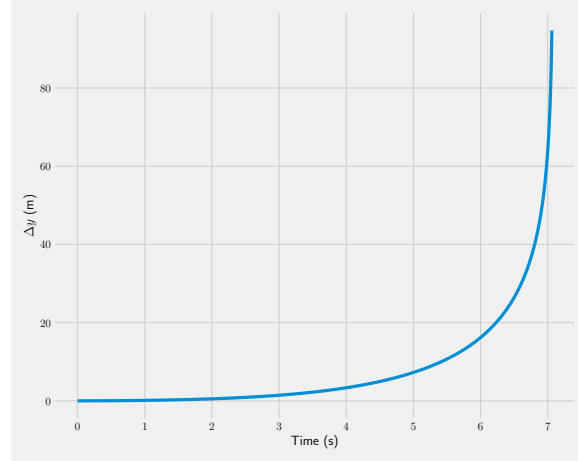


FIGURE 4.20: Result of simulation 5 at displacement y-axis on time.

The result (see figure: 4.20) is almost almost 90 meters of the y-axis displacement distance because the wind speed 10 m/s, azimuth angle ($(\varphi) = 30^\circ$), and

inclination angle ($\delta = 30^\circ$), and the aircraft travel time to reach the ground in almost 7 seconds.

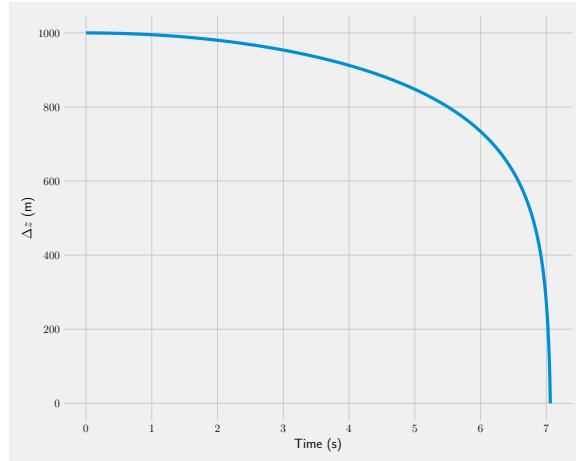


FIGURE 4.21: Result of simulation 5 at displacement z-axis on time.

The aircraft was in free fall to the ground from an altitude of 1000 meters ($z=1000$) with a wind speed of 10 meters per second until it reached height ($z=0$). This simulation calculates azimuth ($\varphi = 30^\circ$), inclination ($\delta = 30^\circ$), and travel time of about 7 seconds to hit the ground (see figure: 4.21).

Variable	Initial state	Final Condition
Altitude (m)	1000	0
Wind Speed (m/s)	10	10
Angle of Azimuth (degree)	30°	
Angle of Inclination (degree)	30°	
x-axes (m)	0	almost 170
y-axes (m)	0	almost 90
Time to hit ground (s)	0	7

TABLE 4.6: Result of simulation 5.

4.3 Simulation with uncertainty

This simulation will consider the value of uncertainty provided by the ADS-B Quality indicator in NUCp and NUCv with an estimate of tens of thousands of aircraft crash points. This simulation is with variable wind speed and negligible. The simulation results will be displayed in a 3-dimensional form in unit vector or inertial reference (x , y , z) and two dimensions (x -axis and y -axis), showing only ten thousand points of potential accident locations. After that, the ten thousand points generated from the theory in chapter 3 and chapter 4. will be shown in the form of a Kernel Density estimation plot to predict the most significant potential location of the plane crash.

4.3.1 Simulation with uncertainty

In simulation this simulation (see figure: ??), it is assumed that the plane fell from an altitude of 1000 meters without considering the wind speed or wind direction. Hence, the plane immediately fell vertically to the ground.

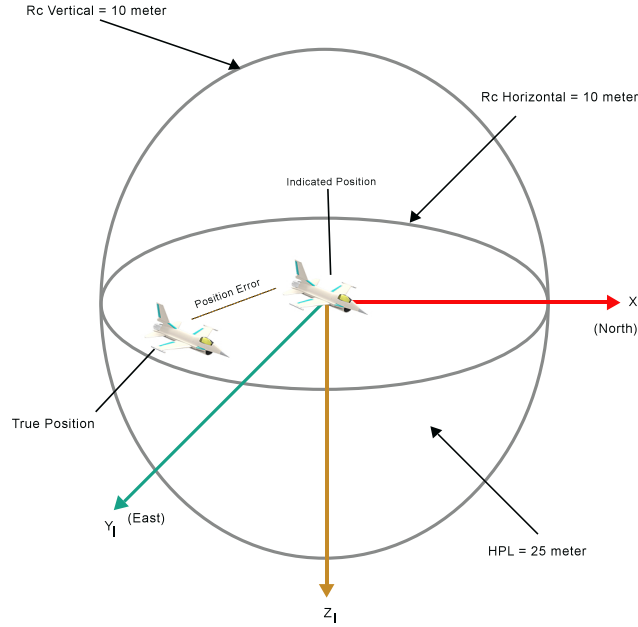


FIGURE 4.22: Illustration with uncertainty of ADS-B Quality Indicators of score 8 in NUCp and $V_w = 0$

The initial position of the aircraft identified through ADS-B Quality Indicators is assumed to have a value score of 8 of (NUCp) Navigation Uncertainty Category for Position (see table: 2.6). Value score 8 states that Horizontal Protection Level (HPL) is less than 25, Rc Horizontal at less than 10 meters, and Rc Vertical at less than 15 meters, which means the data accurately.

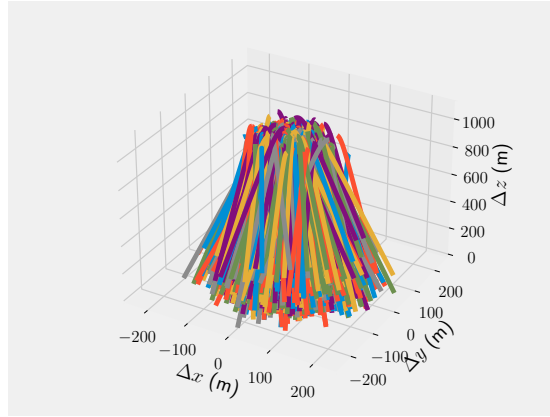


FIGURE 4.23: Result of 10 000 point crash site

Even though ADS-B Quality Indicators stated that it scored 8, there will still be uncertainty in the Horizontal Protection Level (HPL) because it has a 5% certainty armpit. The probability position of the aircraft and the HPL inside is 95% accurate. So to minimize the search area for the location of the plane crash, the theory from Monte Carlo is used, which will use the standard deviation of the value score of 8 NUCp. The results of simulation with the uncertainty of the aircraft crash location are shown in (see figure: 4.23) and (see figure: 4.24) with a number of sampling 10 thousand point prediction of aircraft crash site.

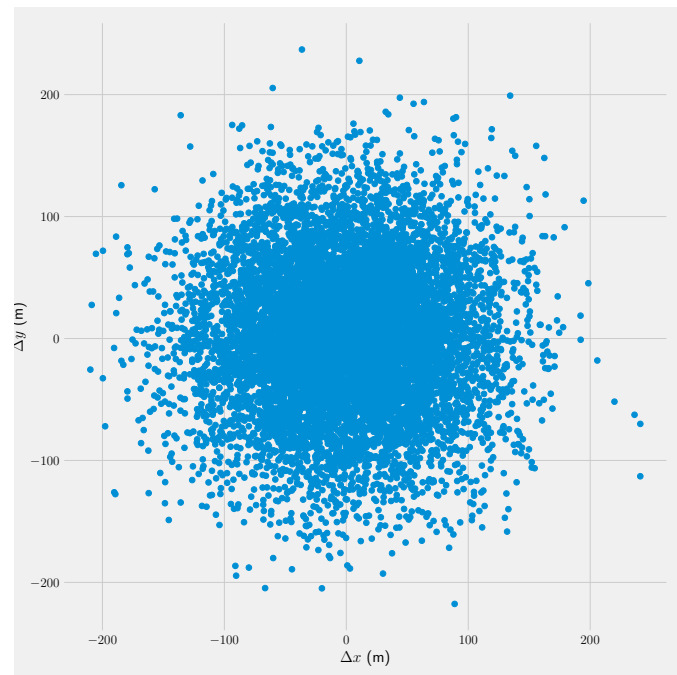


FIGURE 4.24: Result of 10 000 point crash site

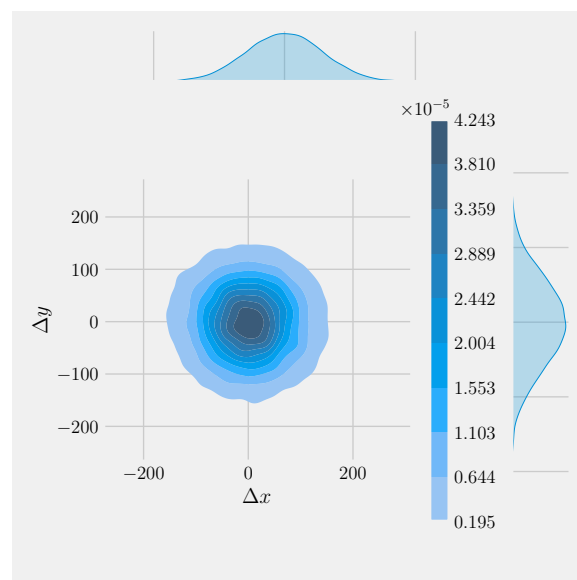


FIGURE 4.25: Joint Density Function (JDF) for prediction of aircraft crash site.

The results will be shown in the form of Join Density Function in 2D as the final result of the study with parameters from an initial state in chapter (3), and input

initial state velocity wind at (0 m/s) and initial altitude at 1000 m. Joint Density Function in 2D is a prediction of aircraft crash site shown in two dimensional with parameters in Cartesian coordinates (Δx and Δy) with several sampling 10 000 uncertainty points. Δx and Δy are assumed in Figure 4.25 will be ground on earth, which will be the aim of this study and valuable for investigators.

4.4 Simulation 11 cases with uncertainty

In the simulation, case C will identify 11 different cases, referred to in (table: 4.7), which will be the initial conditions. Initial conditions for altitude there are three categories, namely 1000 meters, 3000 meters, 5000 meters. NUCp is a Navigation Uncertainty Category for the position by showing a score. The higher the score, the higher the accuracy level NUCp and the Navigation Uncertainty Category for velocity (NUCv), which has the same characteristics in terms of scores as NUCp. The description for the two ADS-B Quality Indicators is shown in (figure: 4.26 and 4.27). the category C simulation will consider ground speed, angle of azimuth, and inclination angle. The Joint Density Function will show the final result of this simulation.

PREDICTION OF AIRCRAFT CRASH LANDING SITE FROM ADS-B DATA USING
MONTE CARLO METHOD

Simulation	Variable						
	Alt(m)	NUCp	NUCv	Gnd speed	Wnd speed	Azimuth	Inclination
Case 1	1000	9	0	0	0	0	0
Case 2	1000	4	0	0	0	0	0
Case 3	3000	9	4	0	0	0	0
Case 4	3000	6	4	0	0	0	0
Case 5	3000	6	2	0	0	0	0
Case 6	5000	6	2	0	0	0	0
Case 7	5000	1	1	0	0	0	0
Case 8	5000	6	2	0	20 (m/s)	30°	0
Case 9	5000	6	2	0	20 (m/s)	0	30
Case 10	5000	6	2	0	20 (m/s)	30°	30°
Case 11	5000	6	2	50 (m/s)	20 (m/s)	30°	30°

TABLE 4.7: Initial state of Simulation with uncertainty .

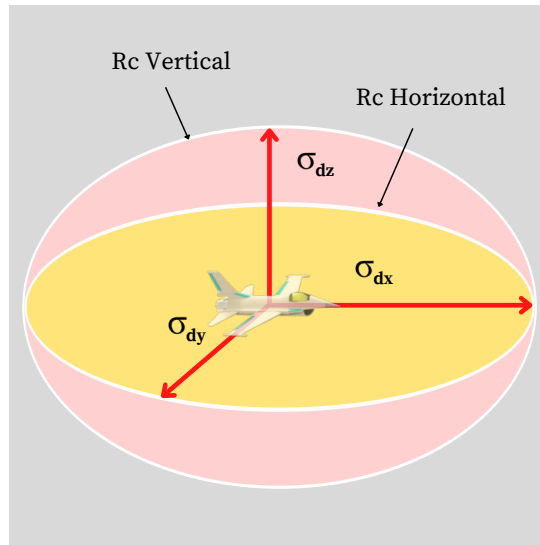


FIGURE 4.26: Parameters of uncertainties for position

Figure 4.26 shows the parameter of Navigation Uncertainty Category for the position (NUCp), which has the parameter of $(\sigma_{dx}, \sigma_{dy}, \sigma_{dz})$.

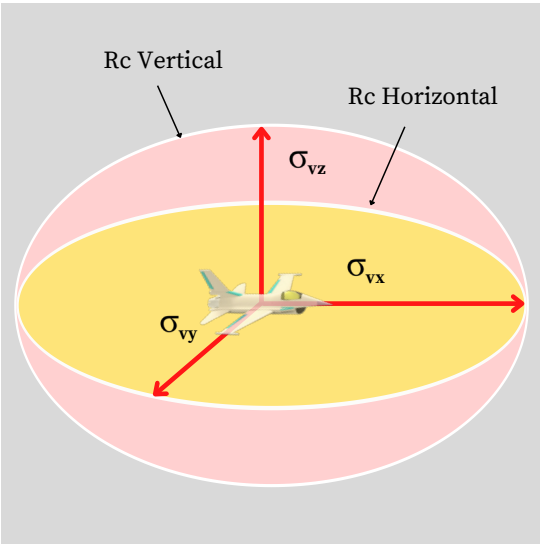


FIGURE 4.27: Parameters of uncertainties for velocity

Figure 4.27 shows the parameter of Navigation Uncertainty Category for the velocity (NUCv), which has the parameter of ($\sigma_{vx}, \sigma_{vy}, \sigma_{vz}$).

4.4.1 Simulation with uncertainty case 1

Simulation with uncertainty 1 using the initial state for altitude at 1000 meters. Ground speed, wind speed, and NUCv are neglected. Navigation Uncertainty Category for the position (NUCp) has a score of 9, which is shown in table 4.8 .

Uncertainties for position		
σ_{dx}	σ_{dy}	σ_{dz}
7.5 (m)	7.5 (m)	3 (m)

TABLE 4.8: Score 9 of NUCp

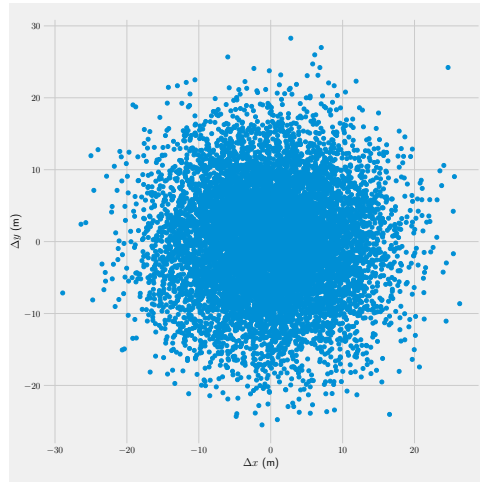


FIGURE 4.28: Result: crash site of simulation with uncertainty 1 in 2D.

The result of simulation with uncertainty 1 with the uncertainty of the aircraft crash location are shown in (figure: 4.28) with several sampling ten thousand point prediction of aircraft site. The maximum point of fall of the aircraft location is not more than between -30 m and 30 m at (Δy) and maximum at the point between -30 m and 30 m at (Δx). in simulation with uncertainty 1, the plane immediately fell vertical because there was no effect from the wind.

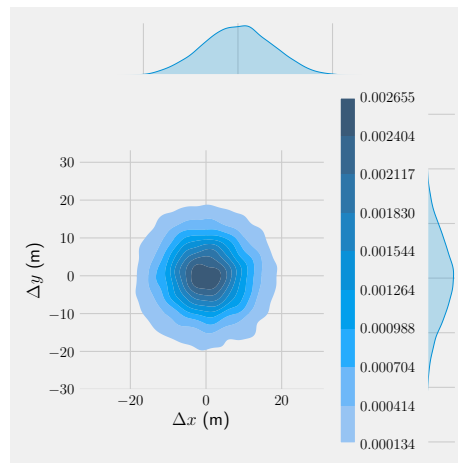


FIGURE 4.29: Joint Density Function (JDF) for simulation with uncertainty 1.

The results will be presented in the form of graphs a Join Density Function in 2D as the final result of the study with parameters from the initial conditions in the chapter (3), and input the initial conditions of wind speed at (0 m/s) and initial altitude of 1000 m with a score of 9 NUCp. The Joint Density Function in 2D is a prediction of the location of the crash that is displayed in two dimensions with parameters in Cartesian coordinates (Δx and Δy) with some sampling of 10,000 points of uncertainty. Δx resulting between displacement -19 meters and 19 meters and Δy resulting between -19 meters and 19 meters displacement. The most significant probability of the plane crashing location is between Δx resulting between displacement -5 meters and 5 meters and Δy resulting in a displacement of -5 meters and 5 meters. Δx and Δy is assumed in Figure 4.29 to be ground on earth, which will be the aim of this study and valuable for investigators.

4.4.2 Simulation with uncertainty case 2

Simulation with uncertainty 2 using the initial state for altitude at 1000 meters. Ground speed and wind speed are neglected. Navigation Uncertainty Category for the position (NUCp) has a score of 9 and Navigation Uncertainty Category for the velocity (NUCv) has a score 4, which is shown in table 4.9 and 4.10.

Uncertainties for position		
σ_{dx}	σ_{dy}	σ_{dz}
7.5 (m)	7.5 (m)	3 (m)

TABLE 4.9: Score 9 of NUCp

Uncertainties for velocity		
σ_{vx}	σ_{vy}	σ_{vz}
0.3 (m/s)	0.3 (m/s)	0.46 (m/s)

TABLE 4.10: Score 4 of NUCv

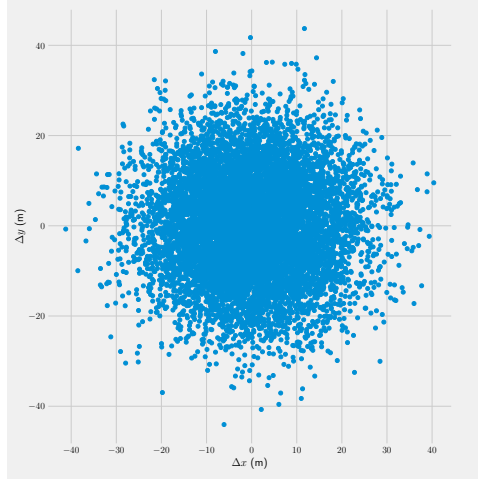


FIGURE 4.30: Result: crash site of simulation with uncertainty 2 in 2D.

The result of simulation with uncertainty 2 with the uncertainty of the aircraft crash location are shown in (figure: 4.30) with several sampling ten thousand point prediction of aircraft site. The maximum point of fall of the aircraft location is not more than between -50 m and 50 m at (Δy) and maximum at the point between -50 m and 50 m at (Δx). in simulation with uncertainty 2, the plane immediately fell vertical because there was no effect from the wind.

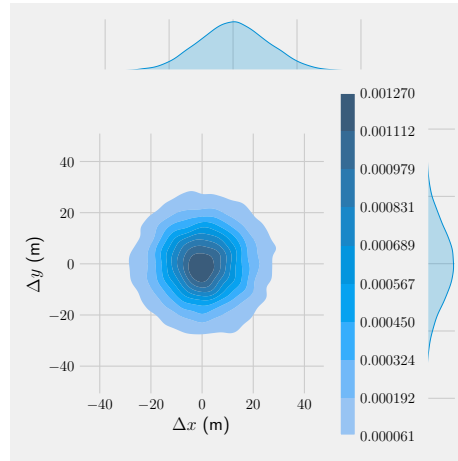


FIGURE 4.31: Joint Density Function (JDF) for simulation with uncertainty 2.

The results will be presented in the form of graphs a Join Density Function in 2D as the final result of the study with parameters from the initial conditions in the chapter (3), and input the initial conditions of wind speed at (0 m/s) and initial altitude of 1000 m with a score of 9 NUCp and Navigation Uncertainty Category for the velocity (NUCv) has a score 4. The Joint Density Function in 2D is a prediction of the location of the crash that is displayed in two dimensions with parameters in Cartesian coordinates (Δx and Δy) with some sampling of 10,000 points of uncertainty. Δx resulting between displacement -28 meters and 25 meters and Δy resulting between -28 meters and 25 meters displacement. The most significant probability of the plane crashing location is between Δx resulting between displacement -5 meters and 5 meters and Δy resulting in a displacement of 5 meters and -8 meters. Δx and Δy is assumed in Figure 4.31 to be ground on earth, which will be the aim of this study and valuable for investigators.

4.4.3 Simulation with uncertainty case 3

Simulation with uncertainty 3 using the initial state for altitude at 3000 meters. Ground speed and wind speed are neglected. Navigation Uncertainty Category for the position (NUCp) has a score of 9 and Navigation Uncertainty Category for the velocity (NUCv) has a score 4, which is shown in table 4.9 and 4.10.

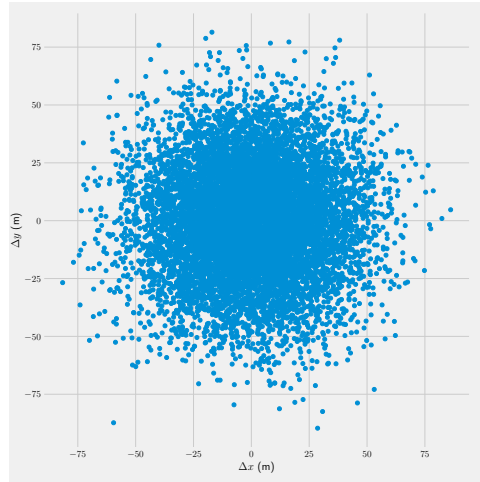


FIGURE 4.32: Result: crash site of simulation with uncertainty 3 in 2D.

The result of simulation with uncertainty 3 with the uncertainty of the aircraft crash location are shown in (figure: 4.32) with several sampling ten thousand point prediction of aircraft site. The maximum point of fall of the aircraft location is not more than between -100 m and 100 m at (Δy) and maximum at the point between -100 m and 100 m at (Δx). in simulation with uncertainty 3.

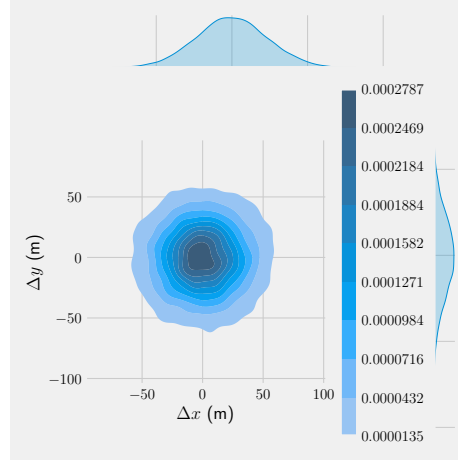


FIGURE 4.33: Joint Density Function (JDF) for simulation with uncertainty 3.

The results will be presented in the form of graphs a Join Density Function in 2D as the final result of the study with parameters from the initial conditions in the chapter (3), and input the initial conditions of wind speed at (0 m/s) and initial altitude of 3000 m with a score of 9 NUCp and Navigation Uncertainty Category for the velocity (NUCv) has a score 4. The Joint Density Function in 2D is a prediction of the location of the crash that is displayed in two dimensions with parameters in Cartesian coordinates (Δx and Δy) with some sampling of 10 000 points of uncertainty. Δx resulting between displacement -60 meters and 60 meters and Δy resulting between -60 meters and 60 meters displacement. The most significant probability of the plane crashing location is between Δx resulting between displacement -10 meters and 10 meters and Δy resulting in a displacement of -10 meters and 10 meters. Δx and Δy is assumed in Figure 4.33 to be ground on earth, which will be the aim of this study and valuable for investigators.

4.4.4 Simulation with uncertainty case 4

Simulation with uncertainty 4 using the initial state for altitude at 3000 meters. Ground speed and wind speed are neglected. Navigation Uncertainty Category for the position (NUCp) has a score of 6 and Navigation Uncertainty Category for the velocity (NUCv) has a score 4, which is shown in table 4.11 and 4.12.

Uncertainties for position		
σ_{dx}	σ_{dy}	σ_{dz}
370 (m)	370 (m)	185 (m)

TABLE 4.11: Score 6 of NUCp

Uncertainties for velocity		
σ_{vx}	σ_{vy}	σ_{vz}
0.3 (m/s)	0.3 (m/s)	0.46 (m/s)

TABLE 4.12: Score 4 of NUCv

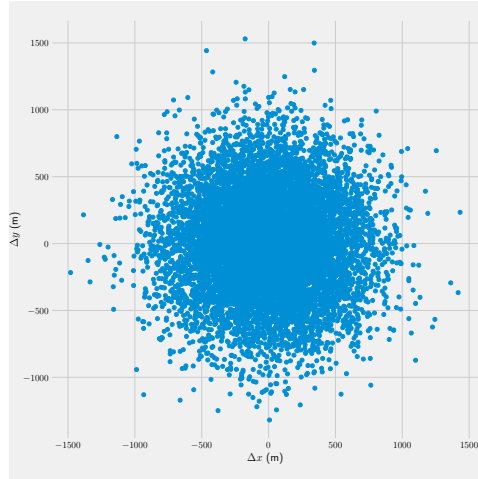


FIGURE 4.34: Result: crash site of simulation with uncertainty 4 in 2D.

The result of simulation with uncertainty 4 with the uncertainty of the aircraft crash location are shown in (figure: 4.34) with several sampling ten thousand point

prediction of aircraft site. The maximum point of fall of the aircraft location is not more than between -1500 m and 1500 m at (Δy) and maximum at the point between -1500 m and 1500 m at (Δx). in simulation with uncertainty 4.

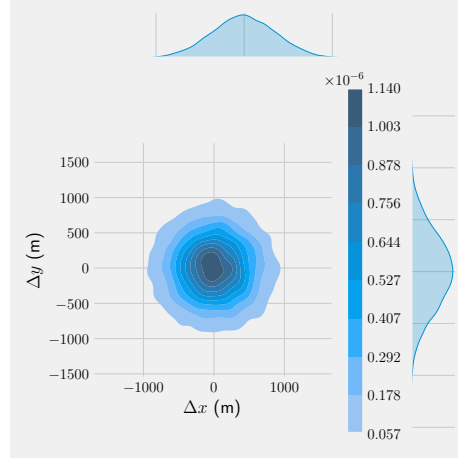


FIGURE 4.35: Joint Density Function (JDF) for simulation with uncertainty 4.

The results will be presented in the form of graphs as the final result of the study with parameters from the initial conditions in the chapter (3), and input the initial conditions of wind speed at (0 m/s) and initial altitude of 3000 m with a score of 6 NUCp and Navigation Uncertainty Category for the velocity (NUCv) with a score of 4. The Joint Density Function in 2D is a two-dimensional forecast of the crash's position, with parameters in Cartesian coordinates (Δx and Δy) and a sample of 10 000 points of uncertainty. Δx resulting between displacement -1000 meters and 1000 meters and Δy resulting between -900 meters and 1000 meters displacement. The most significant probability of the plane crashing location is between Δx resulting between displacement -100 meters and 100 meters and Δy resulting in a displacement of -150 meters and 100 meters. Δx and Δy is assumed in Figure 4.35 to be ground on earth, which will be the aim of this study and valuable for investigators.

4.4.5 Simulation with uncertainty case 5

Simulation with uncertainty 5 using the initial state for altitude at 3000 meters. Ground speed and wind speed are neglected. Navigation Uncertainty Category for

the position (NUCp) has a score of 6 and Navigation Uncertainty Category for the velocity (NUCv) has a score 2, which is shown in table 4.13 and 4.14.

Uncertainties for position		
σ_{dx}	σ_{dy}	σ_{dz}
370 (m)	370 (m)	185 (m)

TABLE 4.13: Score 6 of NUCp

Uncertainties for velocity		
σ_{vx}	σ_{vy}	σ_{vz}
3 (m/s)	3 (m/s)	4.5 (m/s)

TABLE 4.14: Score 2 of NUCv

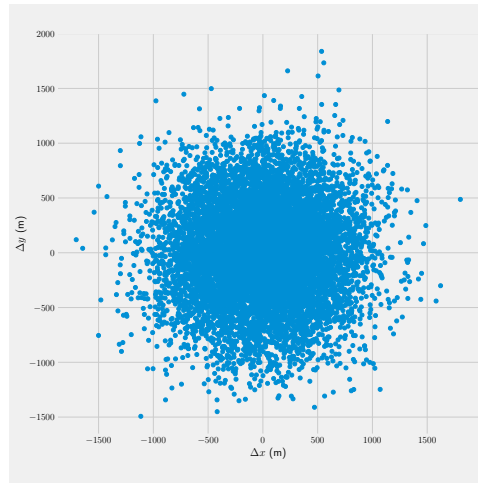


FIGURE 4.36: Result: crash site of simulation with uncertainty 5 in 2D.

The result of simulation with uncertainty 5 with the uncertainty of the aircraft crash location are shown in (figure: 4.36) with several sampling ten thousand point prediction of aircraft site. The maximum point of fall of the aircraft location is not more than between -2000 m and 2000 m at (Δy) and maximum at the point between -1500 m and 2000 m at (Δx). in simulation with uncertainty 5.

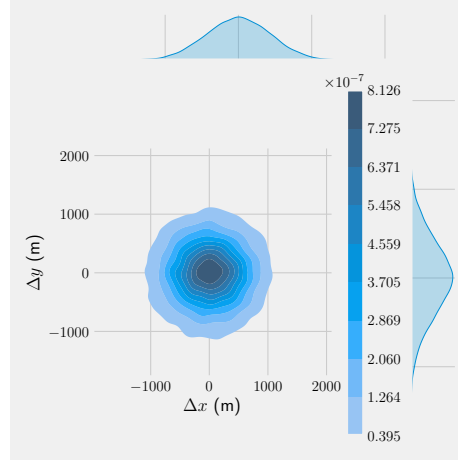


FIGURE 4.37: Joint Density Function (JDF) for simulation with uncertainty 5.

The results will be presented in the form of graphs as the final result of the study with parameters from the initial conditions in the chapter (3), and input the initial conditions of wind speed at (0 m/s) and initial altitude of 3000 m with a score of 6 NUCp and Navigation Uncertainty Category for the velocity (NUCv) with a score of 2. The Joint Density Function in 2D is a two-dimensional forecast of the crash's position, with parameters in Cartesian coordinates (Δx and Δy) and a sample of 10 000 points of uncertainty. Δx resulting between displacement -1100 meters and 1100 meters and Δy resulting between -1100 meters and 1100 meters displacement. The most significant probability of the plane crashing location is between Δx resulting between displacement -300 meters and 300 meters and Δy resulting in a displacement of -300 meters and 300 meters. Δx and Δy is assumed in Figure 4.37 to be ground on earth, which will be the aim of this study and valuable for investigators.

4.4.6 Simulation with uncertainty case 6

Simulation with uncertainty 6 using the initial state for altitude at 5000 meters. Ground speed and wind speed are neglected. Navigation Uncertainty Category for the position (NUCp) has a score of 6 and Navigation Uncertainty Category for the velocity (NUCv) has a score 2, which is shown in table 4.13 and 4.14.

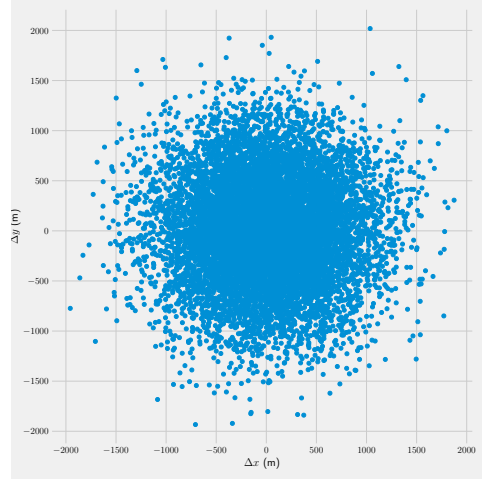


FIGURE 4.38: Result: crash site of simulation with uncertainty 6 in 2D.

The result of simulation with uncertainty 6 with the uncertainty of the aircraft crash location are shown in (figure: 4.38) with several sampling ten thousand point prediction of aircraft site. The maximum point of fall of the aircraft location is not more than between -2000 m and 2000 m at (Δy) and maximum at the point between -2000 m and 2000 m at (Δx). in simulation with uncertainty 6.

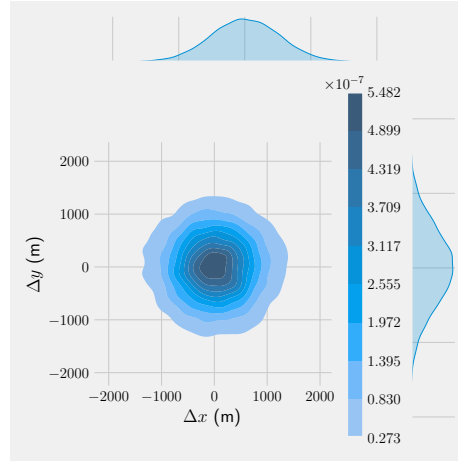


FIGURE 4.39: Joint Density Function (JDF) for simulation with uncertainty 6.

The results will be presented in the form of graphs as the final result of the study with parameters from the initial conditions in the chapter (3), and input the

initial conditions of wind speed at (0 m/s) and initial altitude of 5000 m with a score of 6 NUCp and Navigation Uncertainty Category for the velocity (NUCv) with a score of 2. The Joint Density Function in 2D is a two-dimensional forecast of the crash’s position, with parameters in Cartesian coordinates (Δx and Δy) and a sample of 10 000 points of uncertainty. Δx resulting between displacement -1300 meters and 1300 meters and Δy resulting between -1400 meters and 1400 meters displacement. The most significant probability of the plane crashing location is between Δx resulting between displacement -400 meters and 400 meters and Δy resulting in a displacement of -400 meters and 400 meters . Δx and Δy is assumed in Figure 4.37 to be ground on earth, which will be the aim of this study and valuable for investigators.

4.4.7 Simulation with uncertainty case 7

Simulation with uncertainty 7 using the initial state for altitude at 5000 meters. Ground speed and wind speed are neglected. Navigation Uncertainty Category for the position (NUCp) has a score of 1 and Navigation Uncertainty Category for the velocity (NUCv) has a score 1, which is shown in table 4.15 and 4.16.The score of NUC is deficient, so the data is assumed to be inaccurate.

Uncertainties for position		
σ_{dx}	σ_{dy}	σ_{dz}
37040 (m)	37040 (m)	18520 (m)

TABLE 4.15: Score 1 of NUCp

Uncertainties for velocity		
σ_{vx}	σ_{vy}	σ_{vz}
10 (m/s)	10 (m/s)	15.2 (m/s)

TABLE 4.16: Score 1 of NUCv

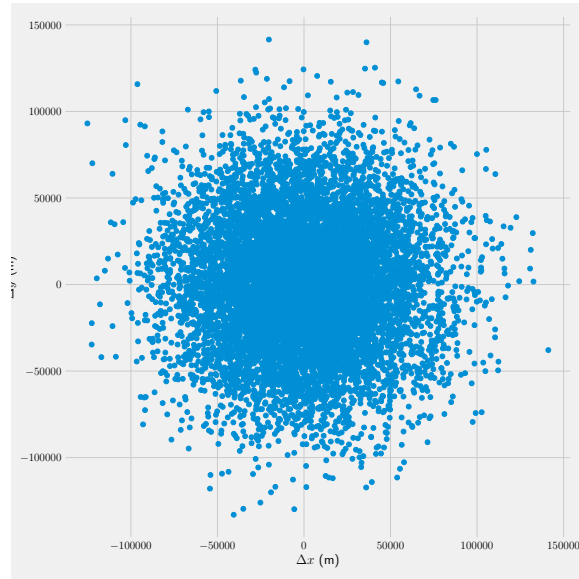


FIGURE 4.40: Result: crash site of simulation with uncertainty 7 in 2D.

The result of simulation with uncertainty 7 with the uncertainty of the aircraft crash location are shown in (figure: 4.40) with several sampling ten thousand point prediction of aircraft site. The maximum point of fall of the aircraft location is not more than between -100000 m and 150000 m at (Δy) and maximum at the point between -100000 m and 150000 m at (Δx). in this simulation. Because the NUC score is so low that the radius of the containment of NUC is extensive and impacts predicting the location of the plane crash, the search location area will be the more comprehensive and low prediction.

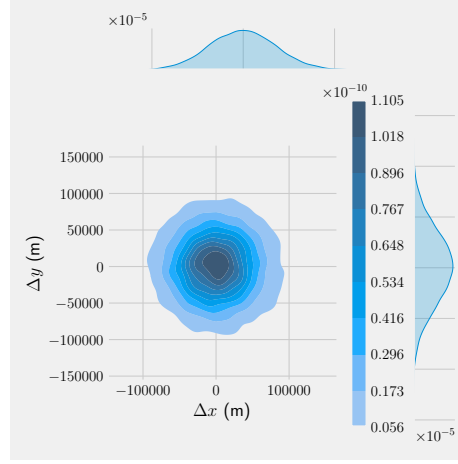


FIGURE 4.41: Joint Density Function (JDF) for simulation with uncertainty 7.

The results will be presented in the form of graphs as the final result of the study with parameters from the initial conditions in the chapter (3), and input the initial conditions of wind speed at (0 m/s) and initial altitude of 5000 m with a score of 1 NUCp and Navigation Uncertainty Category for the velocity (NUCv) with a score of 1. The Joint Density Function in 2D is a two-dimensional forecast of the crash's position, with parameters in Cartesian coordinates (Δx and Δy) and a sample of 10 000 points of uncertainty. Δx resulting between displacement -80 000 meters and 80 000 meters and Δy resulting between -80 000 meters and 80 000 meters displacement. The most significant probability of the plane crashing location is between Δx resulting between displacement -20 000 meters and 20 000 meters and Δy resulting in a displacement of -20 000 meters and 20 000 meters. Δx and Δy is assumed in Figure 4.37. The results show that a low NUC data score will impact the location on the ground, and the search area will be extensive.

4.4.8 Simulation with uncertainty case 8

Simulation with uncertainty 8 using the initial state for altitude at 5000 meters. Ground speed and inclination angle are neglected. Wind velocity at 20 m/s and the angle of azimuth ($\varphi = 30^\circ$). Navigation Uncertainty Category for the position (NUCp) has a score of 6 and Navigation Uncertainty Category for the velocity (NUCv) has a score 2, which is shown in table 4.17 and 4.18.

not more than between -1500 m and 3000 m at (Δy) and maximum at the point between 500 m and 5200 m at (Δx). in this case,the results showed that the presence of wind disturbance and angle of azimuth impacted the location on the ground by shifting towards positive x-axes displacement.

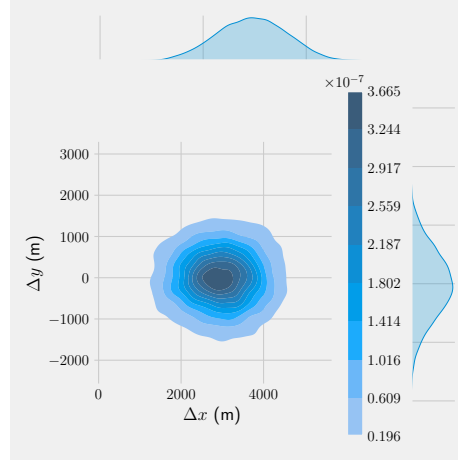


FIGURE 4.43: Joint Density Function (JDF) for simulation with uncertainty 8.

The results will be presented in the form of graphs as the final result of the study with parameters from the initial conditions in the chapter (3), and input the initial conditions of wind speed at (20 m/s), the angle of azimuth ($(\varphi) = 30^\circ$). and initial altitude of 5000 m with a score of 6 NUCp and NUCv with a score of 1. The Joint Density Function in 2D is a two-dimensional forecast of the crash's position, with parameters in Cartesian coordinates (Δx and Δy) and a sample of 10 000 points of uncertainty. Δx resulting between displacement 1500 meters and 4300 meters and Δy resulting between -1500 meters and 1400 meters displacement. The most significant probability of the plane crashing location is between Δx resulting between displacement 2500 meters and 3200 meters and Δy resulting in a displacement of -300 meters and 200 meters. The results showed that the presence of wind disturbance and azimuth angle affects the ground location by shifting the displacement of the positive x-axis. And the (Δy) does not change between the minus y-axis and the plus y-axis.

4.4.9 Simulation with uncertainty case 9

Simulation with uncertainty 9 using the initial state for altitude at 5000 meters. Ground speed and angle of azimuth are neglected. Wind velocity at 20 m/s and inclination angle (δ) = 30° . Navigation Uncertainty Category for the position (NUCp) has a score of 6 and Navigation Uncertainty Category for the velocity (NUCv) has a score 2, which is shown in table 4.17 and 4.18.

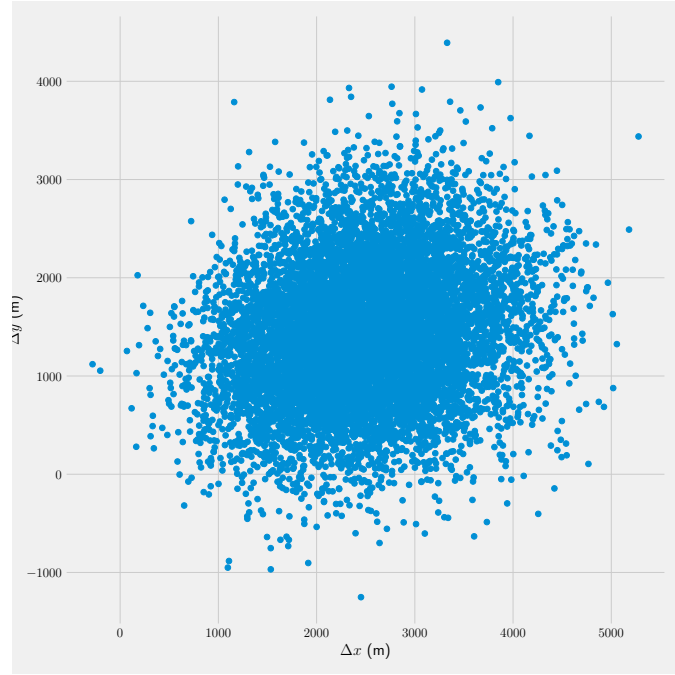


FIGURE 4.44: Result: crash site of simulation with uncertainty 9 in 2D.

The result of simulation with uncertainty 9 with the uncertainty of the aircraft crash location are shown in (figure: 4.44) with several sampling ten thousand point prediction of aircraft site. The maximum point of fall of the aircraft location is not more than between 4500 m and -1200 m at (Δy) and maximum at the point between -200 m and 5200 m at (Δx). in this case. The results showed that wind disturbances and inclination angles impact the location on the ground by shifting in the direction of displacement of the positive x-axis and positive y-axis.

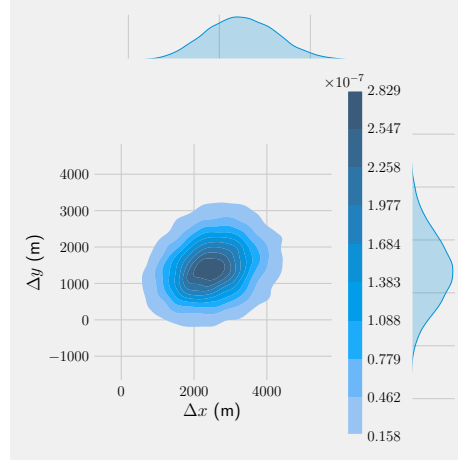


FIGURE 4.45: Joint Density Function (JDF) for simulation with uncertainty 9.

The results will be presented in the form of graphs as the final result of the study with parameters from the initial conditions in the chapter (3), and input the initial conditions of wind speed at (20 m/s), the inclination angle ($(\delta) = 30^\circ$). and initial altitude of 5000 m with a score of 6 NUCp and NUCv with a score of 1. The Joint Density Function in 2D is a two-dimensional forecast of the crash's position, with parameters in Cartesian coordinates (Δx and Δy) and a sample of 10 000 points of uncertainty. Δx resulting between displacement 800 meters and 4200 meters and Δy resulting between -100 meters and 3100 meters displacement. The most significant probability of the plane crashing location is between Δx resulting between displacement 2000 meters and 2800 meters and Δy resulting in a displacement of 1000 meters and 1600 meters. The results showed that wind disturbance and inclination angle affect the ground location by shifting the displacement of the positive x-axis and the positive y-axis.

4.4.10 Simulation with uncertainty case 10

Simulation with uncertainty 10 using the initial state for altitude at 5000 meters. Ground speed is neglected. Wind velocity at 20 m/s, inclination angle ($(\delta) = 30^\circ$) and the angle of azimuth ($(\varphi) = 30^\circ$). Navigation Uncertainty Category for the position (NUCp) has a score of 6 and Navigation Uncertainty Category for the velocity (NUCv) has a score 2, which is shown in table 4.17 and 4.18.

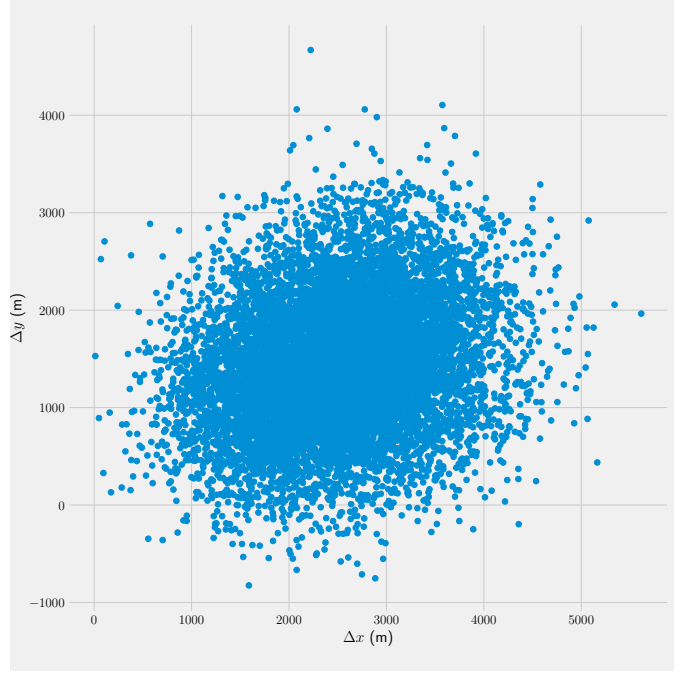


FIGURE 4.46: Result: crash site of simulation with uncertainty 10 in 2D.

The result of simulation with uncertainty 10 with the uncertainty of the aircraft crash location are shown in (figure: 4.46) with several sampling ten thousand point prediction of aircraft site. The maximum point of fall of the aircraft location is not more than between 5000 m and -900 m at (Δy) and maximum at the point between 0 m and 5800 m at (Δx). in simulation with uncertainty 10. The results show that wind disturbances, inclination angles and angle of azimuth impact the location on the ground by shifting the direction of displacement of the positive x-axis and positive y-axis, similar to case 9.

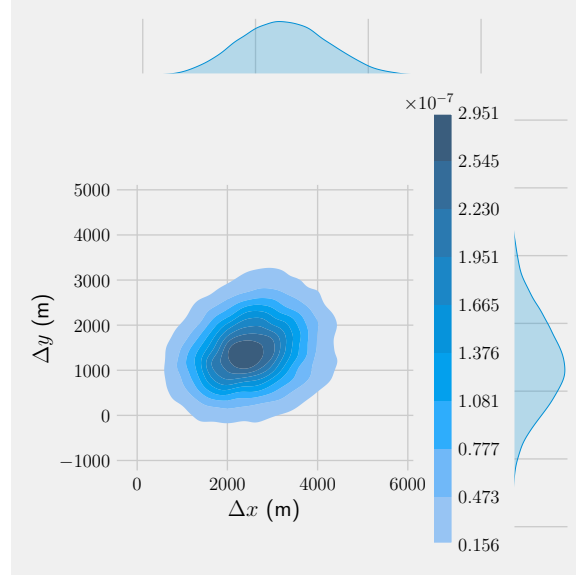


FIGURE 4.47: Joint Density Function (JDF) for simulation with uncertainty 10.

The results will be presented in the form of graphs as the final result of the study with parameters from the initial conditions in the chapter (3), and input the initial conditions of wind speed at (20 m/s), the inclination angle ($(\delta) = 30^\circ$), the angle of azimuth ($(\varphi) = 30^\circ$) and initial altitude of 5000 m with a score of 6 NUCp and NUCv with a score of 1. The Joint Density Function in 2D is a two-dimensional forecast of the crash's position, with parameters in Cartesian coordinates (Δx and Δy) and a sample of 10 000 points of uncertainty. Δx resulting between displacement 800 meters and 3200 meters and Δy resulting between -100 meters and 3100 meters displacement. The most significant probability of the plane crashing location is between Δx resulting between displacement 2000 meters and 2800 meters and Δy resulting in a displacement of 1000 meters and 1600 meters. The results showed that wind disturbance, inclination angle, and azimuth angle affect the location of the ground with a smaller search area.

4.4.11 Simulation with uncertainty case 11

Simulation with uncertainty 11 using the initial state for altitude at 5000 meters. Wind velocity at 20 m/s, ground speed at 50 mls, inclination angle ($(\delta) = 30^\circ$) and the angle of azimuth ($(\varphi) = 30^\circ$). Navigation Uncertainty Category for the

position (NUCp) has a score of 6 and Navigation Uncertainty Category for the velocity (NUCv) has a score 2, which is shown in table 4.17 and 4.18.

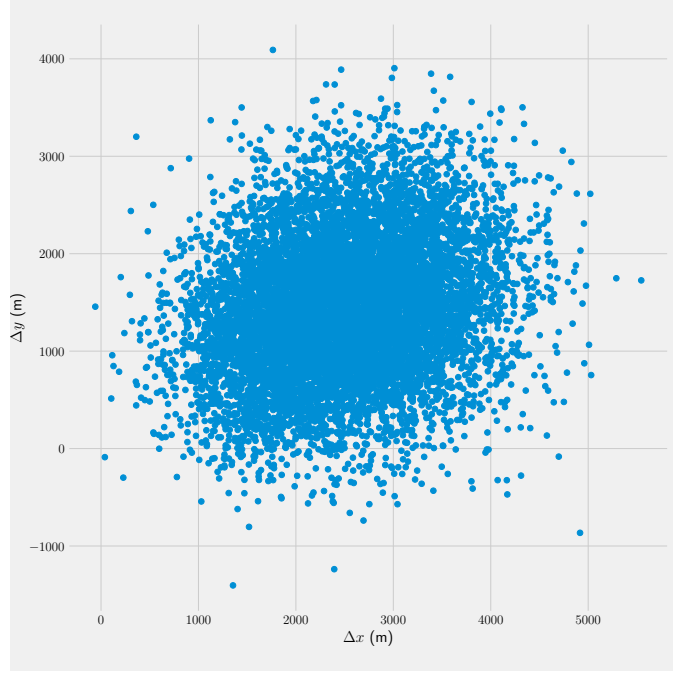


FIGURE 4.48: Result: crash site of simulation with uncertainty 11 in 2D.

The result of simulation with uncertainty 11 with the uncertainty of the aircraft crash location are shown in (figure: 4.48) with several sampling ten thousand point prediction of aircraft site. The maximum point of fall of the aircraft location is not more than between 4000 m and -1500 m at (Δy) and maximum at the point between 0 m and 5500 m at (Δx). in simulation with uncertainty 10. Wind disturbance, ground speed, inclination angle, and azimuth angle all impact position on the ground by altering the direction of displacement of the positive x-axis and positive y-axis, according to the results.

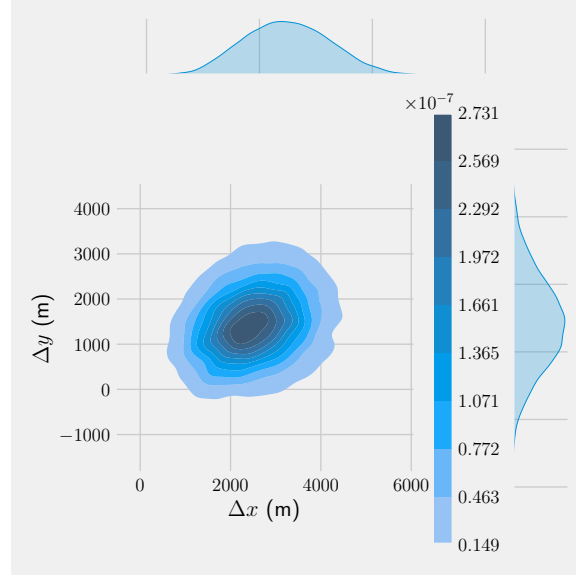


FIGURE 4.49: Joint Density Function (JDF) for simulation with uncertainty 11.

The results will be presented in the form of graphs as the final result of the study with parameters from the initial conditions in the chapter (3), and input the initial conditions of wind speed at (20 m/s), ground speed at 50 m/s, the inclination angle ($\delta = 30^\circ$), the angle of azimuth ($\varphi = 30^\circ$) and initial altitude of 5000 m with a score of 6 NUCp and NUCv with a score of 1. The Joint Density Function in 2D is a two-dimensional forecast of the crash's position, with parameters in Cartesian coordinates (Δx and Δy) and a sample of 10 000 points of uncertainty. Δx resulting between displacement 500 meters and 4200 meters and Δy resulting between -100 meters and 3100 meters displacement. The most significant probability of the plane crashing location is between Δx resulting between displacement 2000 meters and 2700 meters and Δy resulting in a displacement of 1000 meters and 1600 meters. The results show that wind disturbance, ground speed, elevation angle, and azimuth angle affect the location of the ground with a smaller search area, so it will be beneficial for investigators to reduce the search area.

CHAPTER 5

SUMMARY, CONCLUSION, RECOMMENDATION

5.1 Conclusion

This study results will be summarized in Chapter five, and the technique of developing a numerical solution for ballistic trajectory analysis issues will be described.

For some investigations, ballistic trajectory research has been the key to many vital investigations, particularly in the transportation industry. However, no program is designed mainly for thesis research that considers ADS-B information as an initial state. In addition, the changeable gravity, the earth's atmosphere (International Standard Atmosphere (ISA)), the assumption of the aircraft's dimensions, the impact of the aircraft's free motion or the angle acting on the aircraft, and the variable wind profile are all put into consideration. All of the variable parameters are input into differential equations (ODEs), which are then solved numerically.

This study presents a confirmed numerical solution for an unidentified plane accident based on the latest ADS-B data. The result will offer investigators information on the location of the crash site in the form of a Joint Density Function in 2D (show in figure: 4.25), which is regarded as a forecast of the aircraft site. The result is as follows:

1. Simulation without uncertainty

Variable	Simulation				
	A.1	A.2	A.3	A.4	A.5
x-axes (m)	0	14	10	200	170
y-axes (m)	0	8	6	120	90
Time to hit ground (s)	5	5	5	6	7

TABLE 5.1: Simulation without uncertainty.

The results in simulation without uncertainty have x-axes and y-axes at 0 points falling from an altitude of 130 meters because they are not affected by wind direction or wind speed and are not affected by the plane's angle that the plane falls vertically in the same position—the same from the initial position which is 0 points. However, at the same altitude, which is 130 meters, simulation 2 and simulation 3 have x-coordinate and y-coordinate points due to the wind speed of 10 m/s. The only difference is the angle of inclination. In simulation A.3 it has an angle of inclination ($\delta = 30^\circ$). In simulations A.4 and simulation A.5, the initial altitude position is 1000 meters and produces different coordinates on x-axes and y-axes because they have different angles of inclination (δ). This result of category simulation A shows that the altitude and angle of the aircraft affect displacement the aircraft will reach the ground in inertia coordinates x-axes and y-axes.

2. Simulation with uncertainty The result of simulation with uncertainty is shown in the figure: 4.25. The results show the Monte Carlo theory of error propagation, which states that each variable corresponds to the target in terms of position and is combined into a Joint Density Function in the form of a vector of 2 state variables (Δx and Δy), The distribution, in this case, defines the potential state values, implying that the distribution's mode describes the most likely state value of the aircraft crash site at the inertia x-coordinate between point -30 to point 30, and at the inertia y-coordinate between point -30 to point 30 with 4243 points.
3. Simulation 11 cases with uncertainty

In simulation with uncertainty, there are 11 cases, and each case has a different altitude and ADS-B Quality Indicator and considers aircraft performance, angle of aircraft, wind speed. Moreover, the results of the simulation are as follows:

Case	Alt(m)	Δx (m)	Δy (m)	Area (m ²)
1	1000	-5 \rightarrow 5	-5 \rightarrow 5	78.5
2	1000	-5 \rightarrow 5	-8 \rightarrow 5	102.05
3	3000	-10 \rightarrow 10	-10 \rightarrow 10	314
4	3000	-100 \rightarrow 100	-150 \rightarrow 100	39250
5	3000	-300 \rightarrow 300	-300 \rightarrow 300	282600
6	5000	-400 \rightarrow 400	-400 \rightarrow 400	502400
7	5000	-20 000 \rightarrow 20 000	-20 000 \rightarrow 20 000	1 256 000 000
8	5000	2500 \rightarrow 3200	-300 \rightarrow 200	274 750
9	5000	2000 \rightarrow 2800	1000 \rightarrow 1600	376 800
10	5000	2000 \rightarrow 2800	1000 \rightarrow 1600	376 800
11	5000	2000 \rightarrow 2700	1000 \rightarrow 1600	329 700

TABLE 5.2: Final state with uncertainty.

The results of the simulation with uncertainty prove that altitude and ADS-B Quality Indicators affect the search area results. Suppose the ADS-B Quality Indicators data gives a high score of NUCp and NUCv and the altitude is at 5000 m. It will have a more negligible impact on the search area, as in the example case 11 with the prediction of aircraft crash area 329 700 m². Compared to case 7 with a predicted area of 1 260 000 000 m², ADS-B Quality Indicators with a low score so that the impact on predictions on the ground will be extensive. In the event of an accident, ADS-B Quality Indicators should provide higher and more accurate score in NUCp and NUCv data so that investigators predict a smaller search area.

5.2 Recommendation

Although this study has shown the prediction of the results of the crash site, many variables can be considered to improve the crash site prediction results. The following are possible things to consider:

- Consider the explosion of the plane in the air causing debris. Because even though it is not cold, it will feel as if there is an explosion in the air. An analysis considering an aircraft explosion is provided;
- Because in this final project using ADS-B Quality Indicators from NUC. for further evaluation may consider the NIC;
- To get the best prediction results, it is necessary to get accurate data from the value of ADS-B Quality Indicator in Navigation Uncertainty Category in position and Navigation Uncertainty Category in Velocity;
- Suppose there is an accident of aircraft in the ocean and the potential to fall in the ocean. Sea currents that change according to the direction of the wind can consider.

References

- Aircraft accident investigation report pt. lion mentari airlines boeing 737-8 (max); pk-lqp* (Tech. Rep.). (2019). KOMITE NASIONAL KESELAMATAN TRANSPORTASI REPUBLIC OF INDONESIA.
- Anderson, J., & Hughes, W. (2009). *Fundamentals of aerodynamics + schaum's outline of fluid dynamics*. McGraw-Hill Education. Retrieved from <https://books.google.co.id/books?id=TOiUSQAACAAJ>
- blog on science, A. (2020). *A gentle introduction to kernel density estimation*. <https://ekamperi.github.io/math/2020/12/08/kernel-density-estimation.html>. (Accessed: 18 May 2021)
- Crider, D. A. (2015). Trajectory analysis for accident investigation. In *Aiaa modeling and simulation technologies conference* (p. 0147).
- Do, R. (2009). 260b. *Minimum operational performance standards for, 1090*.
- FAA, A. M. D. (March 2020). *Public ads-b performance report (papr) user's guide* (Tech. Rep.). FAA.
- Gerdan, G. P., & Deakin, R. E. (1999). Transforming cartesian coordinates x, y, z to geographical coordinates ϕ, λ, h . *Australian surveyor*, 44(1), 55–63.
- González-Arribas, D., Soler, M., & Sanjurjo-Rivo, M. (2018). Robust aircraft trajectory planning under wind uncertainty using optimal control. *Journal of Guidance, Control, and Dynamics*, 41(3), 673–688.
- Greaves, M. (2012). *Revisiting trajectory analysis-evolving the cranfield model* (Tech. Rep.). Tech. rep., safety and Accident Investigation Centre, Cranfield University.
- ICAO. (19 to 30 November 2012). *Twelfth air navigation conference* (Tech. Rep.). International Civil Aviation Organization.
- ICAO. (5 - 7 December 2012). *Use of barometric altitude and geometric altitude information in ads-b message for atc applications* (Tech. Rep.). International Civil Aviation Organization.

- ICAO. (September 2014). *Ads-b implementation and operations guidance document* (Tech. Rep.). Author.
- KNKT. (1 JANUARY 2007). *Aircraft accident investigation report: Boeing 737-4q8 pk-kkw* (Tech. Rep.). Author.
- Kreyszig, E. (2009). *Advanced engineering mathematics 10th edition*. Publisher John Wiley & Sons.
- Martin Strohmeier, V. L., Matthias Schäfer, & Martinovic, I. (May 2014). *Realities and challenges of nextgen air traffic management: The case of ads-b* (Tech. Rep.).
- Musmann, F. (n.d.). Ads-b and functions for flight inspection.
- Pourvoyeur, K., Mathias, A., & Heidger, R. (2011). Investigation of measurement characteristics of mlat/wam and ads-b. In *2011 tyrrhenian international workshop on digital communications-enhanced surveillance of aircraft and vehicles* (pp. 203–206).
- Ruijgrok, G. (2009). *Elements of airplane performance*. Vssd Pub. Retrieved from <https://books.google.co.id/books?id=RQE8cgAACAAJ>
- SailingIssues. (2021). *Navigation course*. https://www.sailingissues.com/navcourse_723A0zQ45-6li0.pdf. (Accessed: April 2021)
- SC-186, R. F. (2006). *Minimum operational performance standards for 1090 mhz extended squitter: Automatic dependent surveillance-broadcast (ads-b) and traffic information services-broadcast (tis-b)*. RTCA.
- Stelios, K. (2007). Conversion of gps data to cartesian coordinates via an application development adapted to a cad modelling system.
- Strohmeier, M. (2016). *Security in next generation air traffic communication networks* (Doctoral dissertation). doi: 10.13140/RG.2.2.21924.48006
- Sun, J. (2021). *The 1090 megahertz riddle: A guide to decoding mode s and ads-b signals* (2nd ed.). TU Delft OPEN Publishing. doi: 10.34641/mg.11
- Tesi, S., & Pleninger, S. (2017). Analysis of quality indicators in ads-b messages. *MAD-Magazine of Aviation Development*, 5(3), 6–12.
- Toggerson, D. (2021). *Monte carlo error propagation*. <http://openbooks.library.umass.edu/p132-lab-manual/chapter/monte-carlo-error-propagation/>. (Accessed: 10 June 2021)

Tools, A. (27 May 2021). *Boeing 737 midspan airfoil (b737c-il)*. <http://airfoiltools.com/airfoil/details?airfoil=b737c-il>. (Accessed: 27 May 2021)

Appendices

Appendix A: Python Codes

```
1  #!/usr/bin/env python3
2
3  import numpy as np
4  from numpy import random
5  from scipy.integrate import solve_ivp
6
7  import matplotlib
8  import matplotlib.pyplot as plt
9  from mpl_toolkits.mplot3d import Axes3D
10 from ballistic import ballistic_fall_3D
11 from gravity import g0_from_latitude
12
13 matplotlib.rcParams["text.usetex"] = True
14 plt.style.use("fivethirtyeight")
15
16 # Simulation Parameters
17 LAT = -5.81346
18 g0 = g0_from_latitude(LAT)
19 RE = 6356.766 # Earth's radius (km)
20 # g0 = g0_from_latitude(LAT)
21
22
23 TMAX = 24 * 3600 # In seconds
24 atol = 1e-08
25 rtol = 1e-13
26
27 # Case 1: NUCP = 9, Vw=0, VO = 0
28 # ALTO = 425 * 0.3048 # m
29 ALTO = 5000
30
31
32 # Uncertainties in positions
33 sigma_dx = 370 # meter
```

PREDICTION OF AIRCRAFT CRASH LANDING SITE FROM ADS-B DATA USING MONTE CARLO METHOD

```
34 sigma_dy = 370 # meter
35 sigma_dz = 185 # meter
36
37 # Uncertainties in velocities
38 sigma_vx = 3 # m/s
39 sigma_vy = 3 # m/s
40 sigma_vz = 4.5 # m/s
41
42
43 # Mean initial conditions
44 y_state0 = [0, 0, ALTO, 0, 0, 0] # [m, m, m, m/s, m/s, m/s]
45
46 x0 = 0
47 y0 = 0
48 z0 = ALTO
49 vx0 = 0
50 vy0 = 0
51 vz0 = 0
52
53
54 def hit_ground(t, y_state):
55     """
56     Define terminal condition for ballistic fall.
57     Keyword Arguments:
58         t -- time (second)
59         y_state -- State vector: [x, y, z, vx, vy, vz]
60     """
61     return y_state[2]
62
63
64 hit_ground.terminal = True
65 hit_ground.direction = -1
66
67
68 # FIG4 = plt.figure()
69 # ax = FIG4.add_subplot(111, projection="3d")
70
71
72 # for N in np.arange(Ns):
73 #     xr0 = random.normal(x0, sigma_dx, 1)[0]
```

PREDICTION OF AIRCRAFT CRASH LANDING SITE FROM ADS-B DATA USING MONTE CARLO METHOD

```
74 #     yr0 = random.normal(y0, sigma_dy, 1)[0]
75 #     zr0 = random.normal(z0, sigma_dy, 1)[0]
76 #     vxr0 = random.normal(vx0, sigma_vx, 1)[0]
77 #     vyr0 = random.normal(vy0, sigma_vy, 1)[0]
78 #     vzr0 = random.normal(vz0, sigma_vz, 1)[0]
79 #     y_state0 = [xr0, yr0, zr0, vxr0, vyr0, vzr0]
80
81 #     sol = solve_ivp(
82 #         ballistic_fall_3D,
83 #         [0, TMAX],
84 #         y_state0,
85 #         method="RK45",
86 #         atol=atol,
87 #         rtol=rtol,
88 #         events=hit_ground,
89 #     )
90
91 #     xs = sol.y[0, :]
92 #     ys = sol.y[1, :]
93 #     zs = sol.y[2, :]
94 #     ts = sol.t
95
96 #     ax.plot(xs, ys, zs)
97
98 # ax.set_xlabel(r"$\Delta x$ (m)")
99 # ax.set_ylabel(r"$\Delta y$ (m)")
100 # ax.set_zlabel(r"$\Delta z$ (m)")
101 # plt.tight_layout()
102 # plt.savefig("Displacement-3D.pdf", dpi=600)
103
104 # plt.show()
105
106
107 Ns = 10000
108
109
110 FIG1 = plt.figure(figsize=(10, 10))
111 ax1 = FIG1.add_subplot(111)
112
113 xyxs = np.array([])
```

PREDICTION OF AIRCRAFT CRASH LANDING SITE FROM ADS-B DATA USING MONTE CARLO METHOD

```
114
115 for N in np.arange(Ns):
116     print(str(N))
117     xr0 = random.normal(x0, sigma_dx, 1)[0]
118     yr0 = random.normal(y0, sigma_dy, 1)[0]
119     zr0 = random.normal(z0, sigma_dy, 1)[0]
120     vxr0 = random.normal(vx0, sigma_vx, 1)[0]
121     vyr0 = random.normal(vy0, sigma_vy, 1)[0]
122     vzr0 = random.normal(vz0, sigma_vz, 1)[0]
123     y_state0 = [xr0, yr0, zr0, vxr0, vyr0, vzr0]
124
125     sol = solve_ivp(
126         ballistic_fall_3D,
127         [0, TMAX],
128         y_state0,
129         method="RK45",
130         # atol=atol,
131         # rtol=rtol,
132         events=hit_ground,
133     )
134
135     xc = sol.y[0, :][-1]
136     yc = sol.y[1, :][-1]
137
138     xyc = np.array([xc, yc])
139     xyxs = np.append(xyxs, xyc)
140
141
142 xyxs = xyxs.reshape(-1, 2)
143 np.savetxt("Case10.txt", xyxs)
144 ax1.plot(xyxs[:, 0], xyxs[:, 1], "o")
145 ax1.set_xlabel(r"$\Delta x$ (m)")
146 ax1.set_ylabel(r"$\Delta y$ (m)")
147 ax1.set_aspect("equal")
148 plt.tight_layout()
149 plt.savefig("crash_site_2D_Case10.pdf", dpi=600)
150
151 plt.show()
152
153
```

PREDICTION OF AIRCRAFT CRASH LANDING SITE FROM ADS-B DATA USING MONTE CARLO METHOD

```
154 # FIG1 = plt.figure(figsize=(10, 8))
155 # ax1 = FIG1.add_subplot(111)
156 # ax1.plot(ts, xs)
157 # ax1.set_xlabel(r"Time (s)")
158 # ax1.set_ylabel(r"$\Delta x$ (m)")
159 # plt.tight_layout()
160 # plt.savefig("Displacement-x-axis.pdf", dpi=600)
161
162 # FIG2 = plt.figure(figsize=(10, 8))
163 # ax1 = FIG2.add_subplot(111)
164 # ax1.plot(ts, ys)
165 # ax1.set_xlabel(r"Time (s)")
166 # ax1.set_ylabel(r"$\Delta y$ (m)")
167 # plt.tight_layout()
168 # plt.savefig("Displacement-y-axis.pdf", dpi=600)
169
170 # FIG3 = plt.figure(figsize=(10, 8))
171 # ax1 = FIG3.add_subplot(111)
172 # ax1.plot(ts, zs)
173 # ax1.set_xlabel(r"Time (s)")
174 # ax1.set_ylabel(r"$\Delta z$ (m)")
175 # plt.tight_layout()
176 # plt.savefig("Displacement-z-axis.pdf", dpi=600)
177
178
179 # ax.legend()

1 #!/usr/bin/env python3
2
3 import numpy as np
4
5 from gravity import g_geometric_altitude, h2H, g0_from_latitude
6 from isamodel import isa
7 from wind import wind_aloft
8
9
10 CB = 51.59
11 s = 11.35 # m2
12 m = 63974 # kg
13
14
```

PREDICTION OF AIRCRAFT CRASH LANDING SITE FROM ADS-B DATA USING MONTE CARLO METHOD

```
15 def ballistic_fall_3D(t, y_state):
16     """
17     Returns gradient of 3 dimensional ballistic fall that complied
18     with scipy's solve_ivp
19     Keyword Arguments:
20     t          -- time (second)
21     y_state -- state vectors = [x, y, z, vx, vy, vz]
22     """
23     x = y_state[0]
24     y = y_state[1]
25     z = y_state[2]
26
27     vx = y_state[3]
28     vy = y_state[4]
29     vz = y_state[5]
30
31     g0 = 9.81
32     g = g_geometric_altitude(g0, z)
33     H = h2H(z) / 1e3
34     [_, _, rho, _, _] = isa(H)
35
36     grad0 = vx
37     grad1 = vy
38     grad2 = vz
39
40     [vw_x, vw_y, vw_z] = wind_aloft(20, z, 30, 30) # (m/s, m, deg, deg)
41
42     vx_tas = vx + vw_x
43     vy_tas = vy + vw_y
44     vz_tas = vz + vw_z
45
46     v_tas = np.sqrt(vx_tas ** 2 + vy_tas ** 2 + vz_tas ** 2)
47
48     grad3 = 0.5 * rho * CB * (s / m) * vx_tas * v_tas
49     grad4 = 0.5 * rho * CB * (s / m) * vy_tas * v_tas
50     grad5 = -g + 0.5 * rho * CB * (s / m) * vz_tas * v_tas
51
52     return [grad0, grad1, grad2, grad3, grad4, grad5]
53
54
```

PREDICTION OF AIRCRAFT CRASH LANDING SITE FROM ADS-B DATA USING MONTE CARLO METHOD

```
55 def ballistic_fall_1D_v2(t, y_state):
56     """
57     Returns gradient of one diemnsional ballistic fall that complied
58     with scipy's solve_ivp
59     Keyword Arguments:
60     t          -- time (second)
61     y_state -- state vectors = [x, vx]
62     """
63     z = y_state[0]
64     v_z = y_state[1]
65
66     g = g0
67     rho = 1.225
68
69     grad0 = v_z
70     grad1 = -g + 0.5 * rho * CB * (s / m) * grad0 ** 2
71
72     return [grad0, grad1]

```

```
1  #!/usr/bin/env python3
2
3  import numpy as np
4
5  RE = 6356.766 * 1e3  # Earth's radius (m)
6  g0 = 9.80665  # Earth gravity at RE
7
8
9  def g0_from_latitude(phi):
10     """
11     Computes gravity-acceleration (m/s2) as function of latitude.
12
13     Keyword Arguments:
14     phi -- Latitude angle (deg)
15     """
16     phi = np.radians(phi)
17
18     g0 = 9.80616 * (1 - 0.0026373 * np.cos(2 * phi) + 0.0000059 * np.cos(phi) ** 2)
19
20     return g0
21
22
```

PREDICTION OF AIRCRAFT CRASH LANDING SITE FROM ADS-B DATA USING MONTE CARLO METHOD

```
23 def g_geometric_altitude(g0, h):
24     """
25     Computes gravity acceleration (m/s2) as function of geometric altitude.
26     Keyword Arguments:
27     g0 -- gravity acceleration at h = 0
28     h  -- geometric altitude (m)
29     """
30     g = g0 * (RE / (RE + h)) ** 2
31
32     return g
33
34
35 def h2H(h):
36     """
37     Computes geopotential altitude (km) from geometric altitude.
38
39     Keyword Arguments:
40     h -- geometric altitude (m)
41     """
42     H = RE * h / (RE + h)
43
44     return H
45
46
47 def H2h(H):
48     """
49     Computes geometric altitude (km) from geopotential altitude.
50
51     Keyword Arguments:
52     H -- geopotential altitude (m)
53     """
54     h = RE * H / (RE - H)
55
56     return h
57
58
59 if __name__ == "__main__":
60     import matplotlib
61     import matplotlib.pyplot as plt
62
```


PREDICTION OF AIRCRAFT CRASH LANDING SITE FROM ADS-B DATA USING MONTE CARLO METHOD

```
63     matplotlib.rcParams["text.usetex"] = True
64     plt.style.use("fivethirtyeight")
65
66     # Atmospheric properties for 0 km <= h <= 10 km
67     hs = np.arange(0, 10 * 1e3)
68     Hs = np.array([])
69     gs = np.array([])
70
71     for h in hs:
72         H = h2H(h)
73         Hs = np.append(Hs, H)
74         g = g_geometric_altitude(g0, h)
75         gs = np.append(gs, g)
76
77     FIG = plt.figure(figsize=(15, 15))
78     ax1 = FIG.add_subplot(111)
79     ax1.plot(hs / 1e3, gs)
80     ax1.set_ylabel(r"Gravity acceleration ( $\mathbf{m/s^2}$ )")
81     ax1.set_xlabel(r"Geometric Altitude ( $\mathbf{km}$ )")
82     # ax1.grid(True)
83
84     # ax2 = ax1.twinx()
85     # ax2.plot(hs/1e3, gs, "b")
86     # ax2.set_xlabel(r"Geopotential Altitude ( $\mathbf{km}$ )")
87     # # ax2.grid(True)
88     plt.tight_layout()
89     plt.savefig("gravitymodel.pdf", dpi=600)
90     plt.show()
91
92 1  #!/usr/bin/env python3
93 2
94 3  import numpy as np
95 4  import matplotlib
96 5  import matplotlib.pyplot as plt
97 6  from scipy.optimize import curve_fit
98 7
99 8  matplotlib.rcParams["text.usetex"] = True
100 9  plt.style.use("fivethirtyeight")
101 10
102 11
103 12 def curve_fit_with_r2score(func, xdata, ydata):
```

PREDICTION OF AIRCRAFT CRASH LANDING SITE FROM ADS-B DATA USING MONTE CARLO METHOD

```
13     """
14     Perform curve fitting using scipy's curve fitting with also return the  $R^2$  score.
15     Keyword Arguments:
16     func -- The model function,  $f(x, \dots)$ 
17     xdata -- array_like or object
18     ydata -- array_like or object
19     """
20     popt, pcov = curve_fit(func, xdata, ydata)
21     residuals = ydata - func(xdata, *popt)
22     ss_res = np.sum(residuals ** 2)
23     ss_tot = np.sum((ydata - np.mean(ydata)) ** 2)
24     r_squared = 1 - (ss_res / ss_tot)
25
26     return popt, r_squared
27
28
29 def linear_model(x, a, b):
30     """
31     Linear model for curve fitting:
32      $y = ax + b$ .
33     Keyword Arguments:
34     x -- variable
35     a -- constant
36     b -- constant
37     """
38     y = a * x + b
39
40     return y
41
42
43 def quadratic_model(x, a, b, c):
44     """
45     Quadratic model for curve fitting:
46      $y = ax^2 + bx + c$ .
47     Keyword Arguments:
48     x -- variable
49     a -- constant
50     b -- constant
51     c -- constant
52     """
```

PREDICTION OF AIRCRAFT CRASH LANDING SITE FROM ADS-B DATA USING MONTE CARLO METHOD

```
53     y = a * x ** 2 + b * x + c
54
55     return y
56
57
58     # Loading data
59     FILE = "Wind_aloft_data.csv" # data are in feet and knot
60     wind_data = np.genfromtxt(FILE, skip_header=1, delimiter=",")
61     xdata = wind_data[:, 0] * 0.3048 # in m
62     ydata = wind_data[:, 1] * 0.514444 # in m/s
63
64     # Curve fitting
65     popt1, r_squared1 = curve_fit_with_r2score(linear_model, xdata, ydata)
66
67     popt2, r_squared2 = curve_fit_with_r2score(quadratic_model, xdata, ydata)
68
69     # Plotting
70     fig1, ax1 = plt.subplots(figsize=(10, 10))
71     plt.plot(xdata, ydata, "o", label="Wind Aloft")
72     plt.plot(
73         xdata,
74         linear_model(xdata, *popt1),
75         "--",
76         label=r"Linear fit: a=%5.3f, b=%5.3f,  $R^2$ =%5.3f"
77         % tuple(np.append(popt1, r_squared1)),
78     )
79     plt.plot(
80         xdata,
81         quadratic_model(xdata, *popt2),
82         "--",
83         label=r"Qudratic fit: a=%5.3f, b=%5.3f, c=%5.3f,  $R^2$ =%5.3f"
84         % tuple(np.append(popt2, r_squared2)),
85     )
86     ax1.set_xlabel(r"Geometric Altitude (m)")
87     ax1.set_ylabel(r"Wind Velocity (m/s)")
88     ax1.legend()
89     plt.tight_layout()
90     plt.show()
91
92     #!/usr/bin/env python3
```

PREDICTION OF AIRCRAFT CRASH LANDING SITE FROM ADS-B DATA USING MONTE CARLO METHOD

```
3 import numpy as np
4 import matplotlib
5 import matplotlib.pyplot as plt
6 from scipy.optimize import curve_fit
7
8 matplotlib.rcParams["text.usetex"] = True
9 plt.style.use("fivethirtyeight")
10
11
12 def curve_fit_with_r2score(func, xdata, ydata):
13     """
14     Perform curve fitting using scipy's curve fitting with also return the  $R^2$  score.
15     Keyword Arguments:
16     func -- The model function,  $f(x, \dots)$ 
17     xdata -- array_like or object
18     ydata -- array_like or object
19     """
20     popt, pcov = curve_fit(func, xdata, ydata)
21     residuals = ydata - func(xdata, *popt)
22     ss_res = np.sum(residuals ** 2)
23     ss_tot = np.sum((ydata - np.mean(ydata)) ** 2)
24     r_squared = 1 - (ss_res / ss_tot)
25
26     return popt, r_squared
27
28
29 def linear_model(x, a, b):
30     """
31     Linear model for curve fitting:
32      $y = ax + b$ .
33     Keyword Arguments:
34     x -- variable
35     a -- constant
36     b -- constant
37     """
38     y = a * x + b
39
40     return y
41
42
```

PREDICTION OF AIRCRAFT CRASH LANDING SITE FROM ADS-B DATA USING MONTE CARLO METHOD

```
43 def quadratic_model(x, a, b, c):
44     """
45     Quadratic model for curve fitting:
46      $y = ax^2 + bx + c$ .
47     Keyword Arguments:
48     x -- variable
49     a -- constant
50     b -- constant
51     c -- constant
52     """
53     y = a * x ** 2 + b * x + c
54
55     return y
56
57
58 def wind_aloft(vw, h, az, inc):
59     """
60     Returns wind vector velocities (m/s).
61
62     The direction and the magnitude of the wind
63     are assumed to be constant along the altitude.
64
65     Keyword Arguments:
66     vw -- Wind velocity (m/s)
67     h   -- Altitude (m)
68     az  -- Wind's azimuth (deg)
69     inc -- Wind's inclination (deg)
70     """
71     az = np.radians(az)
72     inc = np.radians(inc)
73
74     vwx = vw * np.cos(inc) * np.cos(az)
75     vwy = vw * np.cos(inc) * np.sin(az)
76     vwz = vw * np.sin(inc)
77
78     return [vwx, vwy, vwz]
79
80
81 # # Loading data
82 # FILE = "Wind_aloft_data.csv" # data are in feet and knot
```

PREDICTION OF AIRCRAFT CRASH LANDING SITE FROM ADS-B DATA USING MONTE CARLO METHOD

```
83 # wind_data = np.genfromtxt(FILE, skip_header=1, delimiter=",")
84 # xdata = wind_data[:, 0] * 0.3048 # in m
85 # ydata = wind_data[:, 1] * 0.514444 # in m/s
86
87 # # Curve fitting
88 # popt1, r_squared1 = curve_fit_with_r2score(linear_model, xdata, ydata)
89
90 # popt2, r_squared2 = curve_fit_with_r2score(quadratic_model, xdata, ydata)
91
92 # # Plotting
93 # fig1, ax1 = plt.subplots(figsize=(10, 10))
94 # plt.plot(xdata, ydata, "o", label="Wind Aloft")
95 # plt.plot(
96 #     xdata,
97 #     linear_model(xdata, *popt1),
98 #     "--",
99 #     label=r"Linear fit: a=%5.3f, b=%5.3f,  $R^2$ =%5.3f"
100 #     % tuple(np.append(popt1, r_squared1)),
101 # )
102 # plt.plot(
103 #     xdata,
104 #     quadratic_model(xdata, *popt2),
105 #     "--",
106 #     label=r"Quadratic fit: a=%5.3f, b=%5.3f, c=%5.3f,  $R^2$ =%5.3f"
107 #     % tuple(np.append(popt2, r_squared2)),
108 # )
109 # ax1.set_xlabel(r"Geometric Altitude (m)")
110 # ax1.set_ylabel(r"Wind Velocity (m/s)")
111 # ax1.legend()
112 # plt.tight_layout()
113 # plt.show()
```

Turnitin Report

PREDICTION OF AIRCRAFT CRASH LANDING SITE FROM ADS-B DATA USING MONTE CARLO METHOD

ORIGINALITY REPORT

12%

SIMILARITY INDEX

9%

INTERNET SOURCES

6%

PUBLICATIONS

5%

STUDENT PAPERS

PRIMARY SOURCES

1

soaneemrana.com

Internet Source

1%

2

mode-s.org

Internet Source

1%

3

Ye Yao, Mengwei Huang, Jing Chen. "State-space model for dynamic behavior of vapor compression liquid chiller", International Journal of Refrigeration, 2013

Publication

1%

4

www.icao.int

Internet Source

<1%

5

www.sgu.ac.id

Internet Source

<1%

6

Van Sickle, . "Building a coordinate system", Basic GIS Coordinates, 2004.

Publication

<1%

7

adsb.tc.faa.gov

Internet Source

<1%

8	Van Sickle, . "Building a Coordinate System", Basic GIS Coordinates Second Edition, 2010. Publication	<1 %
9	www.skybrary.aero Internet Source	<1 %
10	Stojče Dimov Ilčev. "Global Aeronautical Distress and Safety Systems (GADSS)", Springer Science and Business Media LLC, 2020 Publication	<1 %
11	Submitted to Emirates Aviation College, Aerospace & Academic Studies Student Paper	<1 %
12	mapref.org Internet Source	<1 %
13	Submitted to Institute Of Applied Technology Student Paper	<1 %
14	arc.aiaa.org Internet Source	<1 %
15	Submitted to RMIT University Student Paper	<1 %
16	Submitted to Cranfield University Student Paper	<1 %
17	livingsafelywithhumanerror.wordpress.com Internet Source	<1 %

18	www.anteninet.net Internet Source	<1 %
19	www.masterclock.com Internet Source	<1 %
20	www.multilateration.com Internet Source	<1 %
21	Submitted to University of Leicester Student Paper	<1 %
22	media.readthedocs.org Internet Source	<1 %
23	Submitted to Glyndwr University Student Paper	<1 %
24	hdl.handle.net Internet Source	<1 %
25	www.faa.gov Internet Source	<1 %
26	psasir.upm.edu.my Internet Source	<1 %
27	Chris Binns. "Aircraft Systems", Wiley, 2018 Publication	<1 %
28	Francesco Papi, Dario Tarchi, Michele Vespe, Franco Oliveri, Francesco Borghese, Giuseppe Aulicino, Antonio Vollero. "Radiolocation and tracking of automatic identification system"	<1 %

signals for maritime situational awareness",
IET Radar, Sonar & Navigation, 2015

Publication

-
- | | | |
|---|---|-----------------------|
| <div style="background-color: #008000; color: white; display: inline-block; width: 40px; height: 40px; text-align: center; line-height: 40px;">39</div> | <p>Submitted to University of Central Lancashire
Student Paper</p> | <p><1 %</p> |
|---|---|-----------------------|
-
- | | | |
|---|---|-----------------------|
| <div style="background-color: #8B4513; color: white; display: inline-block; width: 40px; height: 40px; text-align: center; line-height: 40px;">30</div> | <p>file.yizimg.com
Internet Source</p> | <p><1 %</p> |
|---|---|-----------------------|
-
- | | | |
|---|---|-----------------------|
| <div style="background-color: #8B4513; color: white; display: inline-block; width: 40px; height: 40px; text-align: center; line-height: 40px;">31</div> | <p>commons.und.edu
Internet Source</p> | <p><1 %</p> |
|---|---|-----------------------|
-
- | | | |
|---|---|-----------------------|
| <div style="background-color: #00008B; color: white; display: inline-block; width: 40px; height: 40px; text-align: center; line-height: 40px;">32</div> | <p>www.tandfonline.com
Internet Source</p> | <p><1 %</p> |
|---|---|-----------------------|
-
- | | | |
|---|---|-----------------------|
| <div style="background-color: #800080; color: white; display: inline-block; width: 40px; height: 40px; text-align: center; line-height: 40px;">33</div> | <p>Anjia Yang, Xiao Tan, Joonsang Baek, Duncan S. Wong. "A New ADS-B Authentication Framework Based on Efficient Hierarchical Identity-Based Signature with Batch Verification", IEEE Transactions on Services Computing, 2017
Publication</p> | <p><1 %</p> |
|---|---|-----------------------|
-
- | | | |
|---|---|-----------------------|
| <div style="background-color: #008000; color: white; display: inline-block; width: 40px; height: 40px; text-align: center; line-height: 40px;">34</div> | <p>repository.tudelft.nl
Internet Source</p> | <p><1 %</p> |
|---|---|-----------------------|
-
- | | | |
|---|--|-----------------------|
| <div style="background-color: #00008B; color: white; display: inline-block; width: 40px; height: 40px; text-align: center; line-height: 40px;">35</div> | <p>mafiadoc.com
Internet Source</p> | <p><1 %</p> |
|---|--|-----------------------|
-
- | | | |
|---|--|-----------------------|
| <div style="background-color: #00008B; color: white; display: inline-block; width: 40px; height: 40px; text-align: center; line-height: 40px;">36</div> | <p>S.J. Claessens. "Efficient transformation from Cartesian to geodetic coordinates", Computers & Geosciences, 2019
Publication</p> | <p><1 %</p> |
|---|--|-----------------------|
-

37	Submitted to University of Sussex Student Paper	<1 %
38	id.scribd.com Internet Source	<1 %
39	www.tailstrike.com Internet Source	<1 %
40	Submitted to University of Ruhuna Matara Student Paper	<1 %
41	James Gregory, Tianshu Liu. "Introduction to Flight Testing", Wiley, 2021 Publication	<1 %
42	Submitted to Queen Mary and Westfield College Student Paper	<1 %
43	Submitted to University of Queensland Student Paper	<1 %
44	www.eurocontrol.int Internet Source	<1 %
45	www.open.org Internet Source	<1 %
46	hss.ulb.uni-bonn.de Internet Source	<1 %
47	Submitted to Preston College Student Paper	<1 %

48	Submitted to University of Ghana Student Paper	<1 %
49	Submitted to University of Sydney Student Paper	<1 %
50	etheses.bham.ac.uk Internet Source	<1 %
51	Kenneth Gade. "The Seven Ways to Find Heading", Journal of Navigation, 2016 Publication	<1 %
52	Submitted to West Hills Community College Student Paper	<1 %
53	fossen.biz Internet Source	<1 %
54	publicapps.caa.co.uk Internet Source	<1 %
55	www.fedoa.unina.it Internet Source	<1 %
56	www.grc.nasa.gov Internet Source	<1 %
57	www.nexoncn.com Internet Source	<1 %
58	Submitted to The Hong Kong Polytechnic University Student Paper	<1 %

59	Submitted to University of Essex Student Paper	<1 %
60	Submitted to University of Sheffield Student Paper	<1 %
61	Submitted to University of Strathclyde Student Paper	<1 %
62	Submitted to University of Wales, Bangor Student Paper	<1 %
63	en.wikipedia.org Internet Source	<1 %
64	ethesis.nitrkl.ac.in Internet Source	<1 %
65	Matthias Schafer, Martin Strohmeier, Matthew Smith, Markus Fuchs, Rui Pinheiro, Vincent Lenders, Ivan Martinovic. "OpenSky report 2016: Facts and figures on SSR mode S and ADS-B usage", 2016 IEEE/AIAA 35th Digital Avionics Systems Conference (DASC), 2016 Publication	<1 %
66	Submitted to Oxford Brookes University Student Paper	<1 %
67	Submitted to University of Liverpool Student Paper	<1 %
68	Xiangyang Wang, Xiaming Yuan, Jihong Zhu, Yunjie Yang. "Stability Analysis of Tailsitters in	<1 %

Vertical Takeoff and Landing Flights", Journal of Aircraft, 2019

Publication

69	slidelegend.com Internet Source	<1 %
70	www.flightradar24.com Internet Source	<1 %
71	www.mygeodesy.id.au Internet Source	<1 %
72	Joonho Son, Ryoichi Hara, Hiroyuki Kita. "Determination of the optimal DR capacity for a commercial building with chiller system and energy storage system", IEEJ Transactions on Electrical and Electronic Engineering, 2017 Publication	<1 %
73	Submitted to Leiden University Student Paper	<1 %
74	Submitted to Military Technological College Student Paper	<1 %
75	Submitted to Ohio University Student Paper	<1 %
76	edoc.pub Internet Source	<1 %
77	utpedia.utp.edu.my Internet Source	<1 %

78	B. L. Granovskii, S. M. Ermakov. "The Monte Carlo method", Journal of Soviet Mathematics, 1977 Publication	<1 %
79	Kanako YASUE, Keisuke SAWADA. "CFD-Aided Evaluation of Reynolds Number Scaling Effect Accounting for Static Model Deformation", TRANSACTIONS OF THE JAPAN SOCIETY FOR AERONAUTICAL AND SPACE SCIENCES, 2012 Publication	<1 %
80	Submitted to Kuala Lumpur Infrastructure University College Student Paper	<1 %
81	Submitted to University of Zululand Student Paper	<1 %
82	lfcps.org Internet Source	<1 %
83	Ali, Busyairah Syd, Wolfgang Schuster, Washington Ochieng, Arnab Majumdar, and Thiam Kian Chiew. "Framework for ADS-B Performance Assessment: the London TMA Case Study : Automatic Dependent Surveillance Broadcast", Navigation, 2014. Publication	<1 %
84	Busyairah Syd Ali, Wolfgang Schuster, Washington Yotto Ochieng. "Evaluation of the Capability of Automatic Dependent	<1 %

Surveillance Broadcast to Meet the Requirements of Future Airborne Surveillance Applications", Journal of Navigation, 2016

Publication

-
- | | | |
|-----------|---|----------------|
| 85 | Submitted to Embry Riddle Aeronautical University
Student Paper | <1 % |
|-----------|---|----------------|
-
- | | | |
|-----------|--|----------------|
| 86 | Submitted to Massey University
Student Paper | <1 % |
|-----------|--|----------------|
-
- | | | |
|-----------|-------------------------------------|----------------|
| 87 | d-nb.info
Internet Source | <1 % |
|-----------|-------------------------------------|----------------|
-
- | | | |
|-----------|---|----------------|
| 88 | www.mpi-hd.mpg.de
Internet Source | <1 % |
|-----------|---|----------------|
-
- | | | |
|-----------|--|----------------|
| 89 | www.vehicular.isy.liu.se
Internet Source | <1 % |
|-----------|--|----------------|
-
- | | | |
|-----------|--|----------------|
| 90 | Ali, Busyairah Syd. "System specifications for developing an Automatic Dependent Surveillance-Broadcast (ADS-B) monitoring system", International Journal of Critical Infrastructure Protection, 2016.
Publication | <1 % |
|-----------|--|----------------|
-
- | | | |
|-----------|---|----------------|
| 91 | Submitted to Florida International University
Student Paper | <1 % |
|-----------|---|----------------|
-
- | | | |
|-----------|---|----------------|
| 92 | Inas Alhussein, Ali H. Ali. "Application of DBSCAN to Anomaly Detection in Airport Terminals", 2020 3rd International Conference | <1 % |
|-----------|---|----------------|

on Engineering Technology and its Applications (IICETA), 2020

Publication

93	Submitted to Republic Polytechnic Student Paper	<1 %
94	Submitted to Rushmore Business School Student Paper	<1 %
95	documents.mx Internet Source	<1 %
96	idus.us.es Internet Source	<1 %
97	Mark E. Dreier. "Introduction to Helicopter and Tiltrotor Flight Simulation", American Institute of Aeronautics and Astronautics (AIAA), 2007 Publication	<1 %
98	Submitted to Monash University Student Paper	<1 %
99	Yan Fang, Ma Zan. "Study on Airworthiness Requirement for the Position Quality of ADS-B System", Procedia Engineering, 2011 Publication	<1 %
100	azdoc.tips Internet Source	<1 %
101	code7700.com Internet Source	<1 %

102	discovery.ucl.ac.uk Internet Source	<1 %
103	www.nikhef.nl Internet Source	<1 %
104	www.scribd.com Internet Source	<1 %
105	Gowri Thumbur, N.B. Gayathri, P. Vasudeva Reddy, Md. Zia Ur Rahman, Aime' Lay-Ekuakille. "Efficient Pairing-Free Identity-Based ADS-B Authentication Scheme With Batch Verification", IEEE Transactions on Aerospace and Electronic Systems, 2019 Publication	<1 %
106	ijarcsse.com Internet Source	<1 %
107	jurnal.kominfo.go.id Internet Source	<1 %
108	peer.asee.org Internet Source	<1 %
109	www.coursehero.com Internet Source	<1 %
110	www.secureav.com Internet Source	<1 %
111	www.vssut.ac.in Internet Source	<1 %

112	"Springer Handbook of Geographic Information", Springer Science and Business Media LLC, 2012 Publication	<1 %
113	Submitted to De Montfort University Student Paper	<1 %
114	Roelof Vos, Saeed Farokhi. "Introduction to Transonic Aerodynamics", Springer Science and Business Media LLC, 2015 Publication	<1 %
115	Submitted to University of New South Wales Student Paper	<1 %
116	bb.uab.edu Internet Source	<1 %
117	dokumen.site Internet Source	<1 %
118	e-repository.perpus.iainsalatiga.ac.id Internet Source	<1 %
119	link.umsl.edu Internet Source	<1 %
120	myfik.unisza.edu.my Internet Source	<1 %
121	studentsrepo.um.edu.my Internet Source	<1 %

upcommons.upc.edu

122

Internet Source

<1 %

123

www.intentproject.org

Internet Source

<1 %

124

"The geometry of the earth", Physical Geodesy, 2006

Publication

<1 %

125

Angelo Amorosi. "Implicit integration of a mixed isotropic–kinematic hardening plasticity model for structured clays", International Journal for Numerical and Analytical Methods in Geomechanics, 07/2008

Publication

<1 %

126

Arthur P. Smith, Hilton Bateman. "Management of holding patterns: A potential ADS-B application", 2008 IEEE/AIAA 27th Digital Avionics Systems Conference, 2008

Publication

<1 %

127

Greg Snead. "NEO (NextGen 4D TM) Provided by SWIM's Surveillance SOA (SDN ASP for RNP 4D Ops)", 2007 Integrated Communications Navigation and Surveillance Conference, 04/2007

Publication

<1 %

128

J. Tadema, E. Theunissen, R.M. Rademaker, M. Uijt de Haag. "Evaluating the impact of sensor data uncertainty and maneuver uncertainty in

<1 %

a conflict probe", 29th Digital Avionics
Systems Conference, 2010

Publication

- 129 John Marksteiner. "Prototype ADS-B system in the Midwest: Description and lessons learned", 2008 Integrated Communications Navigation and Surveillance Conference, 05/2008 $<1\%$
- Publication
-

- 130 Savio Sciancalepore, Roberto Di Pietro. "SOS: Standard-Compliant and Packet Loss Tolerant Security Framework for ADS-B Communications", IEEE Transactions on Dependable and Secure Computing, 2019 $<1\%$
- Publication
-

- 131 T. Cheng, J. Liu, S. Chen. "Floquet study of ionization and high-order harmonic generation for a hydrogen atom in high-frequency laser fields", The European Physical Journal D - Atomic, Molecular and Optical Physics, 2002 $<1\%$
- Publication
-

- 132 Teh-Kuang Lung, Daniel Finkelsztein, Robert Vivona, John Bunnell, Doug Mielke, William Chung. "Airspace and Traffic Operations Simulation for Distributed ATM Research and Development", AIAA Modeling and Simulation Technologies Conference and Exhibit, 2005 $<1\%$
- Publication

133	Xuhang Ying, Joanna Mazer, Giuseppe Bernieri, Mauro Conti, Linda Bushnell, Radha Poovendran. "Detecting ADS-B Spoofing Attacks Using Deep Neural Networks", 2019 IEEE Conference on Communications and Network Security (CNS), 2019 Publication	<1 %
134	creativecommons.org Internet Source	<1 %
135	digitalcommons.calpoly.edu Internet Source	<1 %
136	digitalcommons.wpi.edu Internet Source	<1 %
137	doku.pub Internet Source	<1 %
138	dokumen.pub Internet Source	<1 %
139	epdf.pub Internet Source	<1 %
140	export.arxiv.org Internet Source	<1 %
141	library.wmo.int Internet Source	<1 %
142	tel.archives-ouvertes.fr Internet Source	<1 %

143	usermanual.wiki Internet Source	<1 %
144	www.4emme.it Internet Source	<1 %
145	www.control.isy.liu.se Internet Source	<1 %
146	Yong He Xie, Wei Wang, Gang Qiang Li. "Temperature Stress Field Distribution Study of Asphalt Carrier'S Based on Rockwool Damaged", Advanced Materials Research, 2011 Publication	<1 %
147	etd.adm.unipi.it Internet Source	<1 %
148	"GNSS — Global Navigation Satellite Systems", Springer Science and Business Media LLC, 2008 Publication	<1 %
149	Guochang Xu. "Coordinate and Time Systems", Orbits, 2008 Publication	<1 %
150	J. Zambrano, R. Landry, O. A. Yeste-Ojeda. "Simulation/Optimization Modeling for Robust Satellite Data Unit for Airborne Network", Journal of Air Transportation, 2019 Publication	<1 %

151 Joonsang Baek, Eman Hableel, Young-Ji Byon, Duncan S. Wong, Kitae Jang, Hwasoo Yeo. "How to Protect ADS-B: Confidentiality Framework and Efficient Realization Based on Staged Identity-Based Encryption", IEEE Transactions on Intelligent Transportation Systems, 2017

Publication

<1 %

152 Pengfei Duan. "ADS-B feasibility study for commercial space flight operations", 29th Digital Avionics Systems Conference, 2010

Publication

<1 %

153 Pia Kotiranta, Ilkka Kelder, Markku Rouvala, Jussi Takaneva. "Characterization of flexible interconnects in mobile devices", 2007 IEEE Workshop on Signal Propagation on Interconnects, 2007

Publication

<1 %

154 Yao Yevenyo Ziggah, Hu Youjian, Xianyu Yu, Laari Prosper Basommi. "Capability of Artificial Neural Network for Forward Conversion of Geodetic Coordinates (ϕ, λ, h) to Cartesian Coordinates (X, Y, Z)", Mathematical Geosciences, 2016

Publication

<1 %

155 citeseerx.ist.psu.edu

Internet Source

<1 %

Curriculum Vitae



Basic Information	
Name	Ezra Favian
Place of Birth	DKI Jakarta, Indonesia
Date of Birth	19 September 1995
Address	Mess Sukisno, No.c-5, 007/012, Halim PK, Kec. Makasar, Jakarta Timur.
Year	Education
2017 - 2021	International University Liaison Indonesia
2010 - 2013	SMA Angkasa 1 Halim PK
Year	Courses
2021	Basic L ^A T _E X
2019	Solidedge
2017	Basic Python
2017	Basic Programming
2017	IELTS
2014	Hartnackschule Berlin
2013	Euro Management Indonesia
Year	Internship
2018	PT. GMF AeroAsia Tbk, Maintenance for A320
Year	Work Experiences
2020 - Now	Dini Hari Angkringan as the Owner
2017 - Now	PT. Primajasa Perdanarayautama as The head of Operation, TJ. Priok
2015	Bayerische Motoren Werke AG (BMW) as janitor, Leipzig, Germany

PREDICTION OF AIRCRAFT CRASH LANDING SITE FROM ADS-B DATA USING
MONTE CARLO METHOD

Year	Organizational Experience
2019 - 2020	Vise President of Aviation Engineering Student Organization
2018 - 2019	Public Relations of Aviation Engineering Student Organization
2019	Quality of Octoberfest
2019	The head of Internal Cup VIII of Sport Event
2018	The head of Internal Cup VII of Sport Event
2018 - 2019	The head of Sport Division of Student Organization (BEM)
2018	The head of Security of Octoberfest